

THE ROLE OF RECOMBINATION SIGNAL BINDING PROTEIN-J κ
IN DECIDUALIZATION AND POSTPARTUM REPAIR

By

Michael Robert Strug

A DISSERTATION

Submitted to
Michigan State University
in partial fulfillment of the requirements
for the degree of

Pharmacology and Toxicology – Doctor of Philosophy

2016

ABSTRACT

THE ROLE OF RECOMBINATION SIGNAL BINDING PROTEIN-Jk IN DECIDUALIZATION AND POSTPARTUM REPAIR

By

Michael Robert Strug

Recurrent Pregnancy Loss (RPL) is defined as the loss of 2 or more consecutive clinical pregnancies. RPL is estimated to occur in up to 5% of women and can be attributed to clinically identifiable causes in only 50% of cases. Dysregulated immune function remains one of the most widely hypothesized, yet least understood, mechanisms contributing to RPL. Women with idiopathic RPL display elevated serum levels of cytotoxic cytokines. Further, decidualization of endometrial stromal cells, a process critical for successful embryo implantation, is dysregulated in the setting of RPL, associated with enhanced expression of inflammatory markers and reduced capacity to discriminate embryo quality. My work is focused on understanding the mechanisms driving embryo implantation and how they can be dysregulated in the setting of infertility. We have identified the evolutionarily conserved Notch signaling pathway as a critical mediator of decidualization in mice, non-human primates, and women. Notch signaling drives many developmental mechanisms along with regulation of the immune response and repair following tissue injury. In order to study the function of all Notch pathway signaling, I generated a uterine-specific conditional knockout mouse (*Pgr-cre*) for the canonical Notch receptor transcription factor, Recombination Signal Binding Protein-Jk (*Rbpj*; *Pgr^{cre/+}Rbpj^{ff}*; *Rbpj c-KO*). Initially, these mice display significant sub-fertility due, in part, due to impaired decidualization. Subsequently, *Rbpj c-KO* mice develop secondary infertility after pregnancy due to dysfunctional postpartum

uterine repair. The objective of my dissertation work was to understand the mechanisms contributing to failed decidualization and postpartum repair in *Rbpj* c-KO mice.

Additionally, I identified decreased RBPJ expression in the endometrium of women with RPL. Repeated embryo loss and endometrial repair are particularly relevant in the setting of RPL. Therefore, I used the *Rbpj* c-KO mouse as a model for RPL to determine the impact of *Rbpj* loss in the setting of dysfunctional postpartum repair to understand the effect on future pregnancy potential.

I dedicate my dissertation to my family that I wish I could share this accomplishment with but are no longer around today: Eric, Uncle Albert, and Mom Hilda

ACKNOWLEDGEMENTS

I can remember the days when I entered graduate school and the thought of completing a dissertation seemed like an impossible feat that would never actually come true even though I was supposedly on the right track. Yet here I am almost at the top of the mountain. However, looking back on my experience as a graduate student, I realize how important the people in my life were in getting me through this. First and foremost, I want to thank my family for believing in me. You have always been my biggest supporters, especially when others do not see eye to eye with your unwavering beliefs about my qualifications to obtain any goal I set. Also, thank you for understanding how important achieving my career goals are to me, even if it involved moving 12 hours away for 7 years.

At first it was not an easy transition spending all of my time with my family and friends to only twice per year, but I have found a very happy home in Michigan and had the opportunity to meet the person who has been my biggest supporter, Kelley Brinsky. We fit so well together because we were both the “odd men out” in the first years of medical school not knowing anyone in Michigan, and moving here was somewhat of a culture shock for my “fast-paced East coast mentality” and “your laid back California mentality” or is it the other way around? However, I can never repay you for putting up with the stress I brought home every night after working days on end and making my life a lot brighter.

I would like to acknowledge my mentor Asgi Fazleabas. Your drive, strong work ethic, and commitment to producing high quality research is an inspiration to me, and I

am truly grateful to have had the opportunity to learn from you. I would like to thank you for repeatedly putting my mind at ease when the stress of balancing medical and graduate school became almost too much to bear. Also, thank you for believing in my potential as a future clinical scientist in the field of Reproductive Medicine.

I would be remiss not to mention the people who were the most important in actually allowing me to complete this work and making coming to lab not feel like a job but rather a great time (especially when we snuck away for a nice lunch out at Founders): my lab family (Renwei Su, Mark Olson, Sammantha Bond, Sharra Poncil, Ariadna Ochoa, Alyssa Fedorko). Certainly, successfully juggling medical and graduate training at the same time is truly impossible in my opinion unless you have a strong support system in our lab. Renwei, you are essentially my second mentor, and I appreciate having the opportunity to learn all of the skills you taught me, and I enjoyed our lengthy conversations about science despite how the other lab members felt about them. Samantha Bond and more recently, Sharra Poncil, you worked your butts off to make sure I was able to get everything done I needed in order to write this dissertation, and I will be forever grateful for your commitment to my success.

I would like to acknowledge the other mentors who have ensured that I was able to stay on the right track during my time as a graduate student at MSU and always made themselves available to provide their input as to where I stood and where I was going: Anne, Keith and JaeWook. Lastly, I want to thank the DO/PhD program for allowing me to pave my own path and choose the road less traveled in coming to Grand Rapids for my research training.

TABLE OF CONTENTS

LIST OF TABLES	ix
LIST OF FIGURES	x
KEY TO ABBREVIATIONS	xii
INTRODUCTION	1
SECTION 1: Embryo Implantation and Decidualization	1
SECTION 2: Notch Signaling and Pregnancy	8
SECTION 3: Physiology of Uterine Repair	12
SECTION 4: Notch Signaling and Repair of Injury	20
SECTION 5: Recurrent Pregnancy Loss	25
CHAPTER 1: Modulation of glucose transporter and ovarian steroid hormone receptor expression by the Notch family transcription factor, RBPJ, is essential for decidualization	28
INTRODUCTION	28
RESULTS	31
Rbpj is essential for decidualization in the mouse and drives Pgr signaling	31
Endometrial loss of Rbpj reduces Slc2a1 induction during decidualization	35
<i>RBPJ</i> is indispensable for decidualization of HuF cells and its loss phenocopies the mouse	37
Pyruvate supplementation rescues decidualization failure with <i>RBPJ</i> loss in HuF cells	39
DISCUSSION	41
METHODS	45
Mice	45
<i>In Vivo</i> artificial decidualization model	45
Histological analysis and immunohistochemistry	46
Isolation and culture of HuF cells	47
Transfection of <i>RBPJ</i> small interfering RNA (siRNA) in HuF cells	47
<i>In Vitro</i> decidualization of HuF cells	48
RNA isolation and Real Time-Quantitative PCR (RT-qPCR)	48
Statistical analysis	49
ACKNOWLEDGEMENTS	49
APPENDIX	50
CHAPTER 2: RBPJ mediates top Notch postpartum repair for future pregnancy potential and is reduced in recurrent pregnancy loss	53
INTRODUCTION	53

RESULTS	55
Uterine ablation of <i>Rbpj</i> in mice results in developed infertility following pregnancy and decidualization failure	55
<i>Rbpj</i> mediates uterine parenchymal regeneration during postpartum repair through controlling Luminal epithelium (LE) over-proliferation and promoting apoptosis of epithelial-mesenchymal double-positive cells	60
<i>Rbpj</i> mediates postpartum uterine repair through suppression of immune activation and recruitment	67
Endometrial epithelial and stromal <i>Rbpj</i> regulates the immune microenvironment during postpartum repair through suppression of complement and interferon signaling	71
Failed postpartum uterine repair due to <i>Rbpj</i> loss causes secondary infertility ...	75
RBPJ expression is reduced in RPL patients	78
DISCUSSION	80
METHODS	85
Mouse Work	85
Generation of <i>Rbpj</i> c-KO mice and Fertility Testing	85
Induction of <i>in vivo</i> artificial decidualization (AD)	85
Postpartum repair time course	86
Unilateral tubal ligation and embryo transfer	87
Human Subjects	88
Recurrent pregnancy loss patient selection	88
Endometrial tissue collection	88
Molecular Biology and Histological Techniques	89
Prussian blue staining	89
Immunohistochemistry	89
Immunofluorescence	90
RNA isolation and Real Time-Quantitative PCR (RT-qPCR)	91
cDNA library preparation and RNA-sequencing	91
Bioinformatics workflow	92
Statistical Analysis	93
ACKNOWLEDGEMENTS	93
APPENDIX	95
CONCLUSIONS AND FUTURE AIMS	104
SECTION 1: RBPJ and Decidualization	104
SECTION 2: RBPJ and Postpartum Repair	108
REFERENCES	116

LIST OF TABLES

Table S1-1. Primer sequences used for this study	52
Table S2-1. Significantly affected pathways by Process Network enrichment of PPD3 RNA-seq up regulated genes	100
Table S2-2. Significantly affected pathways by Process Network enrichment of PPD3 RNA-seq down regulated genes	100
Table S2-3. Antibodies used in the study	101
Table S2-4. Primer sequences used for core pathways tested for the study.....	102
Table S2-5. Primer sequences used for Process Network Enrichment validation from PPD3 RNA-seq results.....	103

LIST OF FIGURES

Figure 1-1. Decreased <i>in vivo</i> artificial decidualization response in <i>Rbpj</i> c-KO mice	32
Figure 1-2. Down regulation of Pgr signaling and up regulation of Esr1 signaling in <i>Rbpj</i> c-KO mice during <i>in vivo</i> artificial decidualization	34
Figure 1-3. Reduced glucose transporter, Slc2a1, expression associated with <i>Rbpj</i> loss during <i>in vivo</i> artificial decidualization.....	36
Figure 1-4. Loss of HuF Cell <i>RBPJ</i> phenocopies the mouse during decidualization	38
Figure 1-5. Pyruvate supplementation rescues decidual marker gene and <i>PGR</i> expression in the setting of <i>RBPJ</i> loss	40
Figure S1-1. Confirmation of <i>RBPJ</i> loss in <i>Rbpj</i> c-KO mice and siRNA knockdown HuF cells.....	51
Figure 2-1. Loss of <i>Rbpj</i> results in developed infertility with evidence of failed postpartum repair associated with reduced decidualization	56
Figure 2-2. Infertility and impaired decidualization with loss of <i>Rbpj</i> is associated with enhanced immune recruitment and estrogen signaling	57
Figure 2-3. Loss of <i>Rbpj</i> results in dysfunctional postpartum uterine	61
Figure 2-4. Dysfunctional postpartum uterine repair with loss of <i>Rbpj</i> is associated with an altered proliferation and apoptotic profile.....	62
Figure 2-5. Loss of <i>Rbpj</i> is associated with accumulations of cytokeratin-vimentin double-positive cells during postpartum uterine repair	64
Figure 2-6. <i>Rbpj</i> regulates epithelial regeneration through inducing apoptosis of cytokeratin-vimentin double positive cells during postpartum uterine repair	65
Figure 2-7. <i>Rbpj</i> is essential for global uterine immune suppression and developmental pathways on PPD3	68
Figure 2-8. <i>Rbpj</i> suppresses neutrophil and lymphocyte recruitment during postpartum uterine repair.....	70
Figure 2-9. <i>Rbpj</i> suppresses endometrial Complement C3 postpartum repair	73

Figure 2-10. Rbpj suppresses endometrial M1 macrophage induction through IFN γ during postpartum repair.....	74
Figure 2-11. Dysfunctional postpartum repair with <i>Rbpj</i> loss impairs future embryo implantation	77
Figure 2-12. RBPJ is reduced in women with uRPL.....	79
Figure S2-1. Generation of <i>Rbpj</i> c-KO mice and fertility testing results	96
Figure S2-2. Graphical representation with statistical significance for staining intensity and cell counts.....	97
Figure S2-3. Validation of Enriched Process Network Pathways by RT-qPCR.....	98
Figure S2-4. Principal Component Analysis (PCA) for PPD 3 RNA-Sequencing.....	99
Figure 3. Summary of the role of RBPJ during the establishment of pregnancy and postpartum repair.....	114

KEY TO ABBREVIATIONS

2-NBDG = 2-(*N*-(7-Nitrobenz-2-oxa-1,3-diazol-4-yl)Amino)-2-Deoxyglucose

Arg1 = Arginase 1

AD = Artificial Decidualization

BSA = Bovine Serum Albumin

BMDC = Bone Marrow Derived/Stem Cells

BMP = Bone Morphogenetic Protein

cAMP = Cyclic Adenosine Monophosphate

CDS-FBS = Charcoal:Dextran Stripped Fetal Bovine Serum

COX2 = Cyclooxygenase-2

CSF1 = Macrophage Colony Stimulating Factor-1

CSF2 = Granulocyte-Macrophage Colony Stimulating Factor 2 (Csf2)

dbcAMP = di-butryl-cyclic adenosine monophosphate

dNK = Decidual Natural Killer

D-HSCORE = Digital HSCORE

DPC = Days Post Conception

E2 = Estradiol

EPS = Epithelial Progenitor/Stem

ESR1 = Estrogen Receptor Alpha

GE = Glandular Epithelium

GSI = Gamma Secretase Inhibitors

H&E = Hematoxylin and Eosin

HESC = Human Endometrial Stromal Cells
HuF = Human Uterine Fibroblasts
hCG = human Chorionic Gonadotropin
ICAM = Intercellular Adhesion Molecule
IFN γ = Interferon γ
IGFBP1 = Insulin-like Growth Factor Binding Protein-1
IP-10 = Interferon- γ -inducible protein 10
I/R = Ischemia/Reperfusion
LE = Luminal Epithelium
LRP6 = low-density lipoprotein receptor-related protein 6
LTF = Lactoferrin
MCP = monocyte chemotactic protein
MET = Mesenchymal to Epithelial Transition
MPA = medroxyprogesterone acetate
MRC1 = Mannose Receptor 1
MSC = Mesenchymal Stem Cells
NICD = Notch Intra-Cellular Domain
P4 =Progesterone
PBS = Phosphate Buffered Saline
PCA = Principal Component Analysis
PFA = Paraformaldehyde
PGR = Progesterone Receptor
Pgr-cre = progesterone receptor driven cre-recombinase

PPD = Postpartum Day

PRL = Prolactin

RBPJ = Recombination Signal Binding Protein-Jk

RIN = RNA Integrity Number

ROS = Reactive Oxygen Species

RPL = Recurrent Pregnancy Loss

RT-qPCR = Real Time-Quantitative Polymerase Chain Reaction

St = Stroma

siRNA = small interfering RNA

TCF/LEF = T cell factor/lymphoid enhancer factor

TGF β = Transforming Growth Factor β

TNF α = Tumor Necrosis Factor- α

Tregs = Regulatory T Cells

T_H = T Helper

WNT = Wingless-type MMTV integration site family

INTRODUCTION

SECTION 1: Embryo Implantation and Decidualization

Successful pregnancy in mammals relies on a series of highly coordinated events including embryo implantation, decidualization, placentation and ultimately parturition¹. Following parturition, postpartum repair occurs, regenerating an essentially scar-free endometrium, and allows pregnancy to occur again in a continuous cycle¹. Simplistically, two key components are necessary for the initiation of successful implantation: a competent blastocyst and a receptive uterus^{1,2}. Receptivity of the uterus to a developing embryo is initiated through both hormonal regulation by the corpus luteum and embryonic signals, both of which favor embryo attachment and trophoblast invasion³⁻⁵. The process of invasion and embryonic cues trigger transformation of the endometrial stromal fibroblasts into secretory, epithelioid-like decidual cells, termed decidualization⁶⁻⁸. Decidualized stromal cells migrate towards and encapsulate the implanting embryo, where they simultaneously support and control trophoblast invasion⁹⁻¹². The decidua also functions to modulate the maternal immune response^{13,14}, promote vascular remodeling^{15,16} and acts as a gatekeeper during implantation, ensuring proper embryo quality¹⁷. Clinical consequences of impaired decidualization include recurrent pregnancy loss, preeclampsia, preterm labor, and intra-uterine growth restriction (IUGR)^{17,18}. Furthermore, patients with gynecological pathologies contributing to infertility, such as endometriosis, display markedly reduced decidualization responses as a result of the disease¹⁹.

Decidua, derived from the Latin word *decidere* meaning *to die or detach*, was so named to describe the maternal endometrial component that detaches with the fetal placenta during parturition. This is required so that the uterus can subsequently regenerate itself^{9,20}. Decidualization occurs strictly in mammals and, more precisely, in species where the placenta invades the endometrial luminal epithelial layer. This includes rodents and primates, where hemochorial placentation occurs, which enables the embryonic trophoblast to directly communicate with the maternal blood supply²¹. In primates, including women, spontaneous decidualization occurs during the mid-luteal phase of each menstrual cycle. The first signs of decidualization occur on approximately cycle day 23 and is characterized with the enlargement of the stromal cells surrounding the endometrial spiral arterioles, which eventually spreads to involve the entire stromal compartment forming the predecidua by day 27²². In the absence of an embryo and withdrawal of progesterone due to corpus luteum regression, resolution of the predecidua results in menstruation with sloughing of the functional endometrial layer. Otherwise, in the presence of an embryo and with corpus luteal rescue, ovarian progesterone secretion, along with a variety of embryonic signals and factors secreted by the endometrium itself, maintains the decidua^{9,23}. Known factors that promote decidualization in the primate include embryo-derived human Chorionic Gonadotropin (hCG)^{3,5,24-26}, cyclic adenosine monophosphate (cAMP) and molecules that increase it (i.e., relaxin, prostaglandin E2)²⁷⁻³⁰, IL-11^{31,32}, and IL-1 β ^{33,34}. Specific molecules secreted by decidualized human endometrial stromal cells (HESC) have been described extensively and serve to support the early stages of embryo implantation. Endometrial prolactin (PRL) production during the mid-luteal phase of the menstrual cycle coincides

with the initiation of decidualization and continues during pregnancy^{35,36}. PRL functions during embryo implantation include support of trophoblast invasion, angiogenesis and immune modulation to prevent fetal rejection³⁷⁻³⁹. Insulin-like growth factor binding protein-1 (IGFBP1) represents another well-characterized decidual product that supports trophoblast invasion⁴⁰. Based on our knowledge of molecules critical for initiating decidualization, we can recapitulate differentiation of HESC to decidual cells *in vitro* and use the secretion of PRL and IGFBP1 as markers of this process⁴¹.

Although many similarities exist between decidualization in primates and rodents, there are distinct differences. Among these differences, one of the most significant is the trigger responsible for initiating decidualization^{1,9,42}. Unlike in women, decidualization in rodents will not occur in the absence of an embryo, and more specifically, the physical contact of the embryo with a receptive endometrium^{9,42-44}. As a result, mechanical stimulation of the hormone-primed mouse uterus can be used to experimentally induce a decidual response, which has been used extensively for determining critical pathways for decidualization^{9,42-45}. Additional features unique to rodent decidualization include decidual cell polyploidy and independence from cAMP for initiation⁹. Overall, the shared features of hemochorial placentation and decidualization with primates along with the ability to genetically manipulate the mouse genome has made them useful for dissecting important pathways during embryo implantation. In particular, the advent of the progesterone receptor driven cre-recombinase (*Pgr-cre*) expressing mouse allows for tissue-specific ablation of a gene to determine its function in reproduction⁴⁶⁻⁵⁰. An advantage of this model is the ability to study specific molecules where a completely null genetic mutation results in embryonic lethality, which includes

many important signaling pathways essential for development⁴⁶. The tissue-specific expression of *Pgr-cre* is limited to the uterus, ovary, oviduct, pituitary gland and mammary gland, and although one copy of the *Pgr* gene is non-functional, these mice are essentially indistinguishable, phenotypically, from wild type mice⁵⁰. Further, immune cells, including lymphocytes and macrophages, do not expression nuclear *Pgr*, thereby limiting target gene ablation to the reproductive tissue parenchyma^{51,52}. Identification and dissection of novel pathways important for promoting implantation in mouse models can further our understanding of the dysregulation witnessed in human infertility and gynecological diseases contributing to infertility.

Endometrial steroid hormone receptor signaling, particularly PGR, is essential for decidualization in both primates and the mouse^{9,53,54}. During the period of uterine receptivity in mice, an epithelial-to-stromal proliferation shift occurs, which is largely driven by *Pgr* signaling⁵³. This proliferation shift allows the embryo to infiltrate the endometrial luminal epithelium and initiate differentiation of the underlying proliferating stromal cells towards a decidual phenotype to support the implantation¹. Further, stromal *Pgr* expression is essential to inhibit estrogen-induced epithelial proliferation⁵⁵. During decidualization, *Pgr* signaling promotes expression of mediators that enhance stromal cell proliferation, survival and differentiation [*Ihh*^{48,49}, *Hoxa10*⁵⁶, *Bone Morphogenetic Protein 2 (Bmp2)*^{48,49,57-59}, *Wingless-type MMTV integration site family, member 4 (Wnt4)*^{60,61}, *Cdk6*⁶²] along with vascular permeability (*Cox2*^{56,63}).

Bmp2 and *Wnt4* signaling regulate the endometrial stromal *Pgr*-mediated response for decidualization in both the mouse and human, and as a result serve as excellent decidual markers^{58,59}. *Bmp2*, a member of the Transforming Growth Factor- β

(TGF- β) superfamily of growth factors, is induced during decidualization and its expression is inhibited with administration of Pgr antagonist RU486⁵⁹. In canonical TGF- β /BMP2-Smad signaling, BMP ligands bind to TGF- β type II receptors, which recruits type I receptors to form a ternary complex⁶⁴. Next, the type II receptor phosphorylates the type I receptor in the complex, thereby activating its kinase activity for subsequent phosphorylation of receptor-regulated Smads (R-Smads; 1, 5 and 8 for BMP signaling)⁶⁵⁻⁶⁷. R-Smads coordinate downstream activation of target gene expression through interaction with Smad4, which is a shared central regulator of multiple TGF- β superfamily pathways. Selective ablation of *Bmp2* in the *Pgr*^{cre/+} mouse and in isolated mouse or human endometrial stromal cells impairs decidualization in part through downregulation of Wnt4^{58,59}.

Wnt/ β -Catenin signaling is crucial for many developmental processes through controlling cell fate and differentiation⁶⁸. In the absence of Wnt ligand, β -Catenin is maintained within the cytoplasm, recognized for ubiquitination due to N-terminal phosphorylation by casein kinase 1 and glycogen synthase kinase 3, and subsequently degraded by the proteasome⁶⁸. Degradation of β -Catenin allows the T cell factor/lymphoid enhancer factor (TCF/LEF) to bind and repress Wnt/ β -Catenin target gene expression. In canonical Wnt/ β -Catenin signaling, Wnt ligand binding to its receptor Frizzled and co-receptor low-density lipoprotein receptor-related protein 6 (LRP6) results in LRP6 phosphorylation and downstream stabilization of β -Catenin. Accumulation of β -Catenin and its translocation to the nucleus allows for interaction with the TCF/LEF and resulting in target gene transcription. Loss of Wnt4 in the mouse is associated with subfertility due to reduced adenogenesis, defective embryo implantation

and impaired decidualization⁶⁰. Loss of Wnt4 in mouse endometrial stromal cells was associated with diminished cell survival and P4-responsiveness⁶⁰. Further studies have confirmed that Bmp2 acts upstream of Wnt4 during decidualization in HESC, and Wnt4 coordinates canonical Wnt/ β -Catenin signaling with nuclear translocation of β -Catenin⁶¹. Altogether, these studies described Bmp2 and Wnt4 as effectors of P4 action during decidualization and identified evolutionarily conserved pathways critical for the decidual response.

Growing evidence describes a role for endometrial glucose metabolism in supporting the events of early pregnancy including embryo implantation and decidualization⁶⁹⁻⁷³. The family of facilitative glucose transporters (known as the GLUT or SLC2 family) regulates uptake of glucose and have distinct temporal and tissue-specific expression patterns⁷⁴. SLC2A1 (GLUT1) is one of most well characterized glucose transporter in the uterus and is ubiquitously expressed throughout the whole uterus in women and rodents⁶⁹. Additionally, its expression is further induced during early gestation⁷⁵ and with *in vivo* and *in vitro* decidualization in the mouse and in HESC⁷¹. Progesterone signaling increases *SLC2A1* expression in both women⁷⁰ and mice^{71,72}. Administration of P4 induces *Slc2a1* expression in endometrial epithelial cells of non-pregnant mice and in isolated murine stromal cells^{71,72}. Additionally, P4 influences *Slc2a1* localization, where P4 increases the fraction of *Slc2a1* present on the plasma membrane compared to that found intracellularly^{71,72}. Interestingly, SLC2A1 expression is significantly decreased in HESC isolated from women with idiopathic infertility compared to patients with identifiable causes of infertility⁷⁰.

Among the many important functions coordinated by the decidua during the establishment of pregnancy, modulation of the maternal immune environment is a critical component. The specific cytokine milieu produced by the decidua, and strict regulation of this process, are essential for protecting the implanting fetal allograft which also express paternal antigens from immune attack¹⁴. In addition to preventing fetal rejection, stromal recruitment of specialized immune cells drives uterine spiral artery remodeling for establishment of the placental vasculature^{76,77}. During decidualization, endometrial stromal cells are initially pro-inflammatory with expression of specific cytokines followed by transition to anti-inflammatory phenotype accompanied by downregulation of many chemokines⁷⁸. The decidua recruits distinct immune cells, largely uterine natural killer (uNK) cells and decidual macrophages, while maintaining a population scarce in cytotoxic T cells and B cells⁷⁹. Selective immune recruitment occurs in endometrial stromal cells, in part, through epigenetic modification of the promoter region of several chemokine genes responsible for attracting cytotoxic T cells, thereby reducing their response to Tumor Necrosis Factor- α (TNF α) and Interferon γ (IFN γ)¹³.

Clearly, elevated levels of cytotoxic cytokines have detrimental effects on embryo implantation. IFN γ inhibits stromal cell differentiation during decidualization and its expression in lymphoid aggregates is believed to regulate location and timing of spontaneous decidualization in women⁸⁰⁻⁸². Elevated levels of TNF α drastically inhibit decidualization and promote the secretion of pro-inflammatory cytokines^{83,84}. Additionally, TNF α impacts trophoblast cell adhesion and impairs migration⁸⁵. Therefore, the decidua regulates the immune microenvironment to prevent production of

cytotoxic cytokines¹⁴. Endometrial macrophage populations are maintained at lower levels during decidualization in the mouse, in part, due to the decreased levels of Csf1 in the decidua, resulting in limited macrophage proliferation and recruitment⁸⁶⁻⁸⁹. However, myometrial Csf1 is not suppressed, contributing to uterine compartment-specific differences in immune populations⁸⁹. Further, decidual macrophages are characterized by an M2-like phenotype, associated with immunosuppression and tissue remodeling, rather than the M1 phenotype that drives the cytotoxic effects under the influence of IFN γ with TNF α production^{77,90-92}. Macrophage polarization will be discussed in greater detail in the following section. As mentioned previously, the decidua reduces recruitment of cytotoxic T cells populations (i.e. Th1 type) through down regulation of their chemoattractants¹³. Overall, the decidua drives many critical functions during the establishment of pregnancy, particularly by serving as a gatekeeper to permit successful embryo implantation. The decidual gatekeeper role is maintained through suppressing the immune response to prevent fetal rejection and allowing for remodeling of the uterine ultrastructure and vasculature. While these decidual functions are well characterized, the mechanisms underlying these responses remain elusive suggesting a need to further understand and identify novel pathways involved.

SECTION 2: Notch Signaling and Pregnancy

The evolutionarily conserved Notch signaling pathway was first identified over 100 years ago as a genetic mutation resulting in a “nicked wing phenotype” in *Drosophila melanogaster*⁸⁴. Upon cloning of the gene and its identification as a membrane receptor, it was so-named Notch⁹³⁻⁹⁵. Notch signaling consists of four

heterodimeric transmembrane receptors (Notch1-4) whose five ligands (Delta-like1, Delta-like3, Delta-like4, Jagged1, and Jagged2) are expressed on the surface of neighboring cells, thereby inducing receptor-ligand interactions through a juxtacrine mechanism. Upon ligand binding, activated Notch receptors undergo a cleavage cascade, mediated by ADAM protease and gamma-secretase, producing the Notch intracellular domain (NICD)⁹⁶⁻⁹⁹. In canonical Notch signaling, the NICD acts as a co-activator of transcription by binding to the transcription factor shared by all four Notch receptors Recombination Signal Binding Protein-Jk (RBPJ) to promote transcription of Notch target genes, such as the 'Hairy enhancer of split' (Hes) and Hes-related (Hey) transcription factor families¹⁰⁰⁻¹⁰³. All four Notch receptors share the evolutionarily conserved transcription factor RBPJ, which binds to the DNA sequence motif CGTGGGAA¹⁰⁴. Basally, RBPJ forms a repression complex by recruiting co-repressors, which are displaced upon NICD binding with subsequent activator complex formation enhancing Notch target gene expression¹⁰³. Additionally, RBPJ binds to other non-canonical genes irrespective of Notch receptor regulation¹⁰⁵.

Notch signaling controls important developmental and homeostatic functions including embryogenesis, organ self-renewal^{96,98}, and immune cell development^{106,107}. Control of these diverse functions occurs through regulation of cell survival, proliferation, cell-cycle progression, differentiation and apoptosis^{108,109}, processes identified as critical for successful decidualization and implantation. During the implantation window, protein expression of NOTCH1 is induced in endometrial stromal cells of the non-human primate and in women in response to hCG, an embryonic signal which promotes uterine receptivity and decidualization^{3,110-113}. Notch1 protein is induced

upon initiation of implantation in the mouse, initially, in the stromal cells of the primary decidual zone and subsequently in the secondary decidual zone¹¹⁴. **Our work demonstrated the critical role of Notch signaling in the initiation of decidualization during early pregnancy** through the generation of a uterine-specific *Notch1* genetically ablated mouse (*Pgr^{cre/+} Notch1^{ff}; Notch1 c-KO*)^{114,115}. Use of the Cre-LoxP system to develop a tissue-specific knockout mouse proved necessary for functional studies in the reproductive tract as a total *Notch1* knockout results in embryonic lethality¹¹⁶. In *Notch1 c-KO* mice, LoxP sites flank the signal peptide coding exon for the *Notch1* gene, resulting in selective ablation in Pgr-positive tissues^{46-50,115}. *Notch1 c-KO* mice display a significantly impaired decidualization response from Day 3 to Day 5 post-mechanical stimulation using a well-established *in vivo* artificial decidualization protocol, and these findings were corroborated in mice treated with gamma secretase inhibitors (GSI), preventing cleavage of Notch receptors to their active form^{114,117}.

There is a relationship between Notch and ovarian steroid hormone receptor signaling during decidualization and the implantation window. Antagonism of PGR in the baboon simulated pregnancy model resulted in a drastic reduction in the expression of NOTCH1¹¹². Additionally, progesterone appears to favor γ -secretase mediated cleavage of the full length NOTCH1 receptor to its transcriptionally active form in the presence of hCG¹¹². Decidualization failure in *Notch1 c-KO* mice was associated with broad down-regulation of genes crucial for P4-induced stromal decidualization and pathways related to cell proliferation, cell cycle progression, and *Esr1* signaling¹¹⁴. Furthermore, in uteri of *Notch1 c-KO* mice the apoptotic signaling cascade was up regulated at a time when

uterine stromal cell survival and differentiation to a secretory decidual phenotype is essential for successful decidualization¹¹⁴.

Notch signaling has been implicated in immune modulation and maternal-fetal vessel formation during the establishment of pregnancy. Specifically, *in vitro* activation of uNK cell Notch receptors by ligand enhances IFN γ secretion, a uNK cell cytokine important for vascular development^{118,119}. *Rbpj* has been shown to modulate function of regulatory T cells (Tregs), an immunosuppressive CD4+ T cell subtype present in early pregnancy that promotes maternal-fetal tolerance¹²⁰. T cell specific *Rbpj* ablation in an acute allograft rejection model, displayed enhanced immunoreactivity against donor heart and skin allografts along with reduced Treg ability to suppress T cell proliferation¹²¹. Interestingly, *Rbpj* regulates memory CD4+ T cell survival through Glut expression¹²². These findings suggest a critical role of the Notch pathway in immune signaling that may potentiate a controlled immune environment for enhancing embryo implantation.

Notch1 c-KO mice produce reduced litter sizes in the first litter but, otherwise, exhibited normal fecundity¹¹⁴ suggesting that compensation by one of the other three Notch receptors may have rescued fertility in *Notch1* c-KO mice. Other Notch receptors have been implicated in decidualization¹²³. In order to gauge the role of Notch signaling during pregnancy, disruption of all Notch signaling through selective ablation of *Rbpj* was necessary and is therefore the focus of this dissertation. *Rbpj* expression mirrors *Notch1* in the mouse uterus during embryo implantation, with initial induction in the primary decidual zone and subsequently in the secondary decidual zone^{114,124}. Similar to *Notch1*, total ablation of *Rbpj* results in embryonic lethality prior to gestational day

10.5¹²⁵, therefore, use of the Cre-LoxP system in *Rbpj*^{ff} mice is essential for tissue-specific functional studies. *Rbpj*^{ff} mice contain LoxP sites flanking the sixth and seventh exons, corresponding to the DNA binding domain¹²⁶. For the studies described in this dissertation, we generated mice with reproductive-tract specific knockout of *Rbpj* (*Pgr*^{cre/+}*Rbpj*^{ff}; *Rbpj* c-KO). Other initial studies in *Rbpj* c-KO mice described subfertility with embryo loss at mid-gestation, in part, due to abnormal embryonic-uterine honing for implantation and defective luminal closure¹²⁴. Defective decidual remodeling was associated with enhanced uterine estrogen receptor signaling and down-regulated expression of matrix metalloproteinases (MMP) 2 and 9¹²⁴ in *Rbpj* c-KO mice. Further, ovarian function and steroid hormone levels (E2, P4) were not altered in the *Rbpj* c-KO mice¹²⁴. However, the mechanisms contributing to the decidualization defects in *Rbpj* c-KO mice and the relevance of RBPJ in human decidualization remain unknown. Furthermore, the fertility phenotype of *Rbpj* c-KO mice beyond the first litter was not investigated in the previous study¹²⁴. These unanswered questions were addressed as part of the studies described in this dissertation.

SECTION 3: Physiology of Uterine Repair

The female reproductive tract has the unique ability to repair and regenerate itself without evidence of overt scarring^{127,128}. Physiologic repair of the uterus occurs during two instances in women: after menstruation and during the postpartum period. Menstruation is a process shared by all species that undergo spontaneous decidualization and represents resolution of the predecidua in the absence of pregnancy^{9,129}. Current hypotheses predict that menstruation with subsequent repair

serves to precondition the uterus for a successful future pregnancy¹³⁰. Since rodents do not spontaneously decidualize in the absence of implantation, they do not menstruate. Rather, continuous proliferation and apoptosis of the endometrium occurs during the estrous cycle^{131,132}. However, induced mouse menstruation models do exist, which have shed light on the repair processes in the endometrium¹³³⁻¹³⁶, which are otherwise difficult to study in women. Because menstruation in primates represents breakdown of the predecidual tissue associated with declining P4 levels at the end of the luteal phase, these models utilize this principle in their design. In the mouse menstruation model, the mice are ovariectomized, hormonally primed and mechanically decidualized as described previously^{9,42-45}. Subsequently, removal of P4 or PGR antagonist administration induces decidual breakdown, sloughing of the endometrium followed by endometrial repair¹³³⁻¹³⁶. Interestingly, decidual senescence is hypothesized to initiate both menstruation and parturition along with a “functional” P4 withdrawal, since there is no decline in P4 levels until after parturition in humans^{137,138}. Therefore, the decidua likely plays an important role in coordinating the events leading up to physiologic endometrial injury and prepares the endometrium for subsequent repair.

Parturition and placental detachment corresponds to an ischemia/reperfusion injury with subsequent wound healing. Similar to other organ systems, repair of the uterus can be divided into two components: 1) immune activation and 2) parenchymal regeneration¹³⁹. Initially, the injury results in activation of the coagulation cascade along with the innate inflammatory response (i.e., complement)¹³⁹, which acts to stop bleeding and prevent infection. Subsequently, neutrophils are recruited to the site of injury in response to complement activation and products of platelet breakdown¹⁴⁰. Neutrophils

are recruited by upregulation of endothelial adhesion molecules for diapedesis and tissue extravasation, including E- and P-selectins and intercellular adhesion molecules (ICAM), which interact with integrins expressed on neutrophils¹⁴¹. Also, specific chemokine expression attracts neutrophils to the site of injury, such as IL-8 and monocyte chemoattractant protein-1 (MCP-1)¹⁴². Neutrophil-specific roles in the initial stages of the inflammatory response include phagocytosis of dead cells, release of reactive oxygen species (ROS) and other anti-microbials to prevent bacterial infection¹⁴³, and stimulate macrophage repair functions¹⁴⁴.

After the acute neutrophil-driven phase of the inflammatory response, a chronic, macrophage-dominant response predominates^{139,145,146}. Upon extravasation from the vasculature, blood monocytes transform to mature tissue macrophages in response to various factors, including cytokines, chemokines, and growth factors¹⁴⁷⁻¹⁵⁰. Macrophage colony stimulating factor 1 (Csf1) and granulocyte-macrophage colony stimulating factor 2 (Csf2) represent cytokines secreted in response to injury and are responsible for macrophage proliferation and recruitment for repair¹⁵¹⁻¹⁵⁶. Further, decidual Csf2 levels increase following parturition in the mouse¹⁴⁰. IFN γ and its downstream mediators dictate the recruitment and activation of both macrophages and neutrophils during wound healing^{157,158}. Constitutive activation of IFN γ -inducible protein 10 (IP-10) results in impaired wound healing due to a pronounced inflammatory response with abnormal re-vascularization, and granulation tissue formation¹⁵⁷. Alternatively, knockout of IFN γ results in improved wound repair due to reduced inflammatory infiltrate coupled with enhanced angiogenesis and granulation tissue formation¹⁵⁸. In addition to recruitment and activation of immune cells, IFN γ expression at the site of injury shifts macrophages

towards a cytotoxic M1 functional phenotype producing TNF α , which will be described in greater depth in the following paragraph^{159,160}. Altogether, these findings suggest that tight regulation of IFN γ is necessary for controlling inflammation and preventing further damage during injury, which appears to be the case during uterine repair^{136,140}. TNF α levels, although elevated from gestational levels, do not change between parturition and 2-6 hours postpartum in the mouse, suggesting a similar pattern for IFN γ ¹⁴⁰. Additionally, in a mouse menstruation model, IFN γ levels do not significantly change at the heaviest point of bleeding or during the repair process¹³⁶.

The cytokine and chemokine milieu at the site of injury skews, or polarizes, macrophages towards a specific functional phenotype, which will dictate their actions upon arrival¹⁵⁹. Macrophages are polarized towards an M1 or M2 phenotype but most display features of both along a broad spectrum depending on functional necessity¹⁵⁹. IFNs (β and γ) and TLR signaling via STAT1 induce macrophages towards an M1 phenotype, and they produce cytotoxic metabolites (ROS via iNOS) and cytokines, such as IL-12, IL-23 and TNF α ¹⁶⁰. M1 macrophages are pro-inflammatory and result in tissue damage, which is ideal in the setting of bacterial infections particularly by intracellular pathogens^{159,161}. On the other hand, macrophages are skewed towards an M2 phenotype by factors including IL-4, IL-10 and IL-13¹⁶². Stat6 induces expression of anti-inflammatory and wound healing genes, such as IL-10, TGF β 1, Mannose Receptor 1 (MRC1), and Arginase 1 (ARG1), in M2 macrophages while inhibiting M1 genes^{159,161,163}. Based on these described functions, initially, an M1 response may be beneficial to recruit further immune support after tissue injury, but ultimately, an M2 driven response is important for proper repair¹⁶⁴. M2 macrophage numbers predominate

during postpartum repair in the uterus, and their numbers peak at Postpartum Day (PPD) 3 and gradually decrease over time¹⁶⁵. Further, continued maintenance of M1 macrophages worsens tissue damage and inhibits repair¹⁶⁶. Interestingly, in instances of iron overload as in patients with chronic venous ulcers with blood extravasation into tissue, macrophages are maintained in the M1 phenotype leading to further damage due to ROS production and fibroblast cellular senescence. These findings indicate that iron metabolism impacts macrophage polarization and subsequently the repair process, which is particularly relevant to macrophages responsible for postpartum uterine repair in the mouse^{145,166,167}.

In rodents, the repair site of placental detachment forms a distinct structure, termed a postpartum nodule¹⁴⁶. A component of nodules are mesometrial hemosiderin-laden macrophages, referred to as “nodule cells”, usually found at the endometrial-myometrial interface or between the layers of myometrium initially and then regress over time¹⁴⁵. Nodule cells stain positive for macrophage markers F4/80 and CD68 during the postpartum uterine repair process¹⁴⁵. Hemosiderin can be identified by Perls Prussian Blue staining and its presence within macrophages indicates phagocytosis and subsequent oxidation of iron, typically from phagocytosis of erythrocytes during the repair of tissue injury¹⁶⁸. Hemosiderin-laden macrophages are often found in disease states associated with chronic vascular hemorrhage of smaller vessels or capillaries, such as in Pulmonary Veno-Occlusive Disease¹⁶⁹. Evidence of postpartum nodules, specifically nodule cells, can persist for up to 3 months after parturition and presumably beyond^{145,170}. Further, embryo implantation in subsequent pregnancies does not occur

in the areas of postpartum nodules, which are associated with a reduced decidualization response¹⁷¹.

The second component of repair, parenchymal regeneration, refers to the processes necessary for reforming the uterine ultrastructure, including the endometrial epithelium and stroma, myometrium, and vasculature^{9,127,146}. After shedding of the placenta during parturition or menstruation, the endometrial epithelium is the first uterine compartment to regenerate^{9,127}. In the case of intestinal wounds, which represent repair of a mucosal surface similar to the endometrium, the epithelial cells at the edge of the injury migrate to repair the defect, and this process is dependent on the presence of a layer of dead cells mixed with mucus and fibrin¹⁷²⁻¹⁷⁴. Multiple studies have shown that epithelial cells from endometrial glands contribute to the re-epithelialization process^{135,175,176}. On the other hand, mounting evidence supports a role for stromal cells in regenerating the luminal epithelium^{177,178}. Specifically, a mesenchymal to epithelial transition in endometrial stromal cells aids in repopulating the luminal epithelium, as evidenced by the presence of cells staining for both vimentin and pan-cytokeratin, stromal and epithelial markers respectively, early during repair¹⁷⁸. Stromal expansion follows re-epithelialization during repair after menstruation. Evidence supporting delayed stromal proliferation includes the presence of mitotic spindles in stromal cells after the epithelium has reformed^{175,179,180}. In the mouse, the luminal epithelium reforms by PPD 5, and the postpartum nodule is fully formed by PPD 8¹⁴⁵. The postpartum nodule represents a distinct anatomical structure, consisting of extracellular matrix and immune infiltrate isolated within the two layers of myometrium. Ultimately, the nodule

regresses as the extracellular matrix degrades and the vasculature entering through the mesometrium reforms, only leaving evidence of few nodule cells¹⁴⁵.

For quite some time, many have believed progenitor, or stem, cells contribute to endometrial regeneration and exist in the basal layer of the endometrium^{9,181-183}. More recently, two types of endometrial progenitor/stem cell populations have been identified: epithelial progenitor/stem (EPS) cells and mesenchymal stem cells (MSC)¹⁸⁴⁻¹⁸⁶. These cells likely contribute to the regeneration of their respective endometrial compartments, which is supported by the presence of monoclonal cells within the endometrial glands likely developing from a single source⁹. Additionally, MSCs appear to play a role in the previously described mesenchymal to epithelial transition that contributes to postpartum regeneration of the endometrial luminal epithelium^{177,178}. Bone marrow derived/stem cells (BMDC) represent another source for repopulating endometrial cells, which been described extensively¹⁸⁷⁻¹⁹³. In response to uterine ischemia/reperfusion injury, BMDC are recruited to regenerate the endometrium¹⁹⁴. A majority of bone marrow stem cells transform into endometrial stromal cells, but other reports have described their differentiation into endometrial epithelial (glandular and luminal) and endothelial cells^{187,190,191}.

As mentioned earlier, P4 withdrawal initiates menstruation, and decidual senescence with delayed P4 withdrawal contributes to parturition¹³³⁻¹³⁸. Since repair occurs in the absence of hormonal signaling, this suggests that mechanisms responsible for normal wound repair in other systems are conserved within the endometrium, at least in the earliest stages. ESR1 and PGR are present in the deeper endometrial glandular epithelium 3 days following menstruation in the rhesus

monkey¹⁹⁵. Subsequently, after re-epithelialization has occurred by day 5, ESR1 and PGR are present throughout the endometrium, which is consistent with studies supporting a role for the epithelium in stromal hormonal responsiveness^{55,195,196}. Therefore, besides an obvious barrier function during repair, re-epithelialization is necessary for the return of normal endometrial function.

Ovarian steroid hormone signaling, although not essential for endometrial repair, modulates the inflammatory environment, and contributes to structural remodeling^{127,197,198}. According to many, absence of ovarian hormone receptor expression in both peripheral and endometrial leukocytes precludes a direct effect of hormones on their recruitment and function^{199,200}. Some more recent studies have described both nuclear and membrane-bound ESR and PGR present with direct effects on leukocytes, including neutrophils, macrophages and lymphocytes²⁰¹⁻²⁰⁵; however, mounting evidence suggests that hormonal effects on leukocytes occur indirectly through endometrial parenchymal inflammatory signaling^{200,206,207}. Both endometrial epithelial and stromal cells express various cytokines, which vary during the menstrual cycle in response to fluctuating levels of E2 and P4 and subsequently affects recruitment of specific immune cell types^{208,209}. For instance, endometrial expression of neutrophil chemoattractant IL-8 is suppressed by P4 and rises in response to P4 withdrawal with implications for immune infiltration upon menstruation and after parturition²⁰⁷. As discussed earlier, endometrial stromal cells secrete various pro-inflammatory and anti-inflammatory mediators during their transformation into decidual cells to modulate the immune environment during decidualization and embryo implantation^{14,76-78}. Clearly, the endometrial parenchyma itself regulates the immune

environment, and the work presented in this dissertation supports a role for endometrial Notch signaling in regulating the inflammatory events during postpartum repair.

SECTION 4: Notch Signaling and Repair of Injury

Tissue response to injury initiates a cascade of evolutionarily conserved defense mechanisms. The initial response is driven by a necessity to minimize blood loss and prevent infection through activation of the coagulation cascade and the innate immune response, respectively¹³⁹. However, recovery from injury depends largely on the tissue's ability to regenerate itself and regulate the inflammatory response to avoid further damage. Preventing immune-mediated injury is particularly necessary in the case of ischemia/reperfusion (I/R) injuries, such as placental detachment²¹⁰. I/R leads to hypoxia with subsequent influx of neutrophils, and both result in ROS production which can further exacerbate injury²¹¹. Myocardial infarction represents one of the most prevalent examples of I/R injury, which follows percutaneous intervention to restore coronary artery blood flow^{212,213}. If a patient survives the initial ischemic event, long term heart failure often results due to exaggerated inflammatory events^{212,213}. Hence, current successful strategies for post-myocardial infarction therapeutics are directed towards preventing acute inflammation^{212,214}. Each organ responds differently to I/R injury, where those with more terminally differentiated cells without the capacity to regenerate are more susceptible, such as the brain and cardiomyocytes²¹⁵. Mucosal organs, such as the intestines and uterus, have the most regenerative capacity and are somewhat more resistant to this injury²¹⁵. Since placental detachment represents a physiological I/R event, certain evolutionarily adapted processes must protect from injury and allow

for rapid repair, but if these mechanisms are disrupted there is potential for long-term negative effects.

The role of Notch signaling has never been investigated in the context of uterine repair; therefore, insight into potential roles in the uterus has been gauged from other systems. The Notch signaling pathway controls many developmental processes and determines cell fate in different organ systems^{96,216}. Among its many roles, Notch mediates key homeostatic functions, including organ self-renewal^{96,98} and immune development^{106,107}. The importance of regulating these two functions in response to injury has been mentioned previously. Recent evidence supports a role for apoptosis in promoting tissue regeneration through activation of stem and progenitor cells²¹⁷. Specifically, signals are transmitted from dying cells during injury, which stimulate proliferation of stem cells²¹⁸. Executioner proteins that mediate cell death, such as caspases-3 and -7, are essential for wound healing and regeneration in the liver post-hepatectomy^{218,219}. Interestingly, caspases are required early during repair, where depletion after 24 hours in a study of *Xenopus* tail regeneration had no negative impact²¹⁹.

The role of Notch signaling in apoptosis has been described extensively but is far from well understood²²⁰. There are many tissue-specific roles determining whether Notch pathway activation promotes or inhibits apoptosis²²⁰. One contributor to our lack of clarity within this issue is the complexity of Notch signaling²¹⁶. The four Notch receptors and five ligands have differential tissue expression profiles and are not necessarily specific for one another^{216,221}. Also, the “dose” of Notch activation determines response, where high Notch activation causes growth arrest while lower

activation results in hyperproliferation²²². Additionally, RBPJ, has a dual role in promoting transcriptional repression and activation, so RBPJ knockout models can display features of Notch signaling activation and suppression^{103,223}. Therefore, RBPJ appears to have accessory roles independent of those performed solely upon NICD binding induced-transcription. RBPJ expression is often reduced in cancer cells, and its loss inhibits apoptosis and promotes cell survival in part through activation of MYC and NF- κ B²²³. Additionally, RBPJ mediates an anti-apoptotic effect in endothelial cells by inhibition of JNK²²⁴.

In the setting of tissue I/R injury, loss of Notch signaling and Rbpj causes enhanced apoptosis and impaired regeneration. Many studies have described the role of Notch signaling in cardiac repair²²⁵. Inhibition of Notch signaling during induced myocardial infarction resulted in production of fewer cardiac progenitor cells and reduced cardiomyogenesis²²⁶. In the same study, NICD elicited Rbpj-dependent transcription of a novel Notch target gene, *Nkx2.5*, a transcription factor associated with cardiac cell fate decisions in progenitors²²⁶. Also, ablation of Rbpj results in liver congestion with abnormal liver sinusoidal endothelial cell functioning and iron deposition²²⁷. These mice also displayed impaired regeneration after partial hepatectomy associated with increased apoptosis and decreased proliferation at 2 and 5 days following surgery²²⁷. In response to I/R injury in the liver, Rbpj loss resulted in enhanced tissue damage with decreased liver function coupled with increased apoptosis and inflammation. These studies identified a role for Rbpj in coordinating repair through STAT3 activation, which reduces production of reactive oxygen species limiting damage²²⁸. Although increased apoptosis may seem to contradict studies

describing an anti-apoptotic effect of Rbpj loss^{223,224}, some degree of apoptosis is crucial for repair in a temporal manner, as mentioned previously^{218,219}. This concept is supported by the requirement of a layer of dead cells for re-epithelialization to occur in intestinal wounds¹⁷²⁻¹⁷⁴. Therefore, if apoptosis is inhibited initially after the insult or injury, delayed repair and regeneration may occur allowing greater damage from the insult causing injury with enhanced apoptosis. Further, altered immune signaling in the absence of Rbpj may exacerbate tissue injury and apoptosis.

Notch signaling plays a central role in coordinating development of the immune system^{106,107,229}. Notch1 and Rbpj are essential for determining cellular fate of lymphoid cells specifically during their differentiation towards T versus B cells, and their ablation skews lymphocytes towards T cell development^{106,126,230}. Differentiation of CD4+ T cells, or T helper cells (T_H cells), towards the T_H1 or T_H2 phenotype upon antigen presentation depends on either Delta-like or Jagged Notch ligand expression by antigen presenting cells, respectively²³¹. Also, Rbpj mediates glucose transporter expression through Akt phosphorylation in memory CD4+ T cells, which is essential for their survival¹²². As mentioned previously, Rbpj promotes signaling of Tregs, which are present in the endometrium during early pregnancy to promote maternal-fetal tolerance, and the absence of Rbpj reduces Treg's ability to suppress T cell proliferation in an acute allograft model^{120,121}. Specifically, NICD, Rbpj and Smad3 (a TGF β mediator) interact to coordinate expression of the major Treg transcription factor Foxp3^{232,233}. Lastly, Notch signaling has also been implicated in controlling myeloid lineage cell fate decisions, including polarization in determining M1 versus M2 phenotypes of macrophages²³⁴.

Rbpj regulates immune cell signaling indirectly through tissue stromal cell control of the cytokine and chemokine environment. Specifically, targeted deletion of Rbpj in bone marrow stromal cells results in an enhanced immune response to an acute graft versus host disease model, largely due to reduced secretion of immunosuppressive molecules IL-6 and PGE2²³⁵. IL-6 levels rise dramatically after parturition and likely regulates the immune response¹⁴⁰. In addition, IL-6 deficiency is associated with delayed wound healing²³⁶. IL-6 has been shown to mediate the switch from acute neutrophil driven to chronic macrophage-dominant inflammation²³⁷. IL-6 plays a critical role in implantation, where IL-6 null mice exhibit impairments in implantation with embryo loss during mid-gestation and delayed labor onset^{238,239}. Women with low endometrial IL-6 levels are at greater risk for recurrent miscarriage²⁴⁰. Further, an Rbpj binding domain has been identified at the *Il6* promoter, where Rbpj coordinates NFκB activation of *Il6* gene transcription²⁴¹. Other studies have also described a repressive function of Rbpj in reducing IL-6 expression²³⁷. IL-6 binding to its receptor consisting of gp130, results in activation of signal transducer and activator of transcription-3 (Stat3) signaling²⁴². Interestingly, Notch signaling through Rbpj has been shown to activate Jak2/Stat3 signaling, and phosphorylation of Stat3 specifically by Notch/Rbpj target gene *Hes5*²²⁸. Cyclooxygenase-2 (Cox2) is responsible for the production of prostaglandins such as PGE2 which promotes decidualization and has been implicated in embryo implantation^{243,244}, and NICD/Rbpj-coordinated transcription of Cox2 through an Rbpj binding domain has also been reported²⁴⁵.

The necessity for tight regulation of IFN γ expression during implantation and uterine repair were discussed at length in the previous sections. Overactive IFN γ

signaling impairs decidualization and skews macrophages towards the cytotoxic M1 phenotype delaying wound repair^{80-82,136,140,158}. Notch has important roles in modifying expression of many immune pathways and directly regulates polarization within macrophages²³⁴. However, the role of Notch signaling in coordinating parenchymal expression of IFN γ and, therefore, indirectly controlling macrophage polarization has not been investigated. Previous studies have reported that Notch signaling acts upstream of IFN γ ^{246,247}. Specifically, inhibition of Notch receptor activation, which subsequently enhances Rbpj repression of target genes, results in reduced IFN γ production^{246,247}. GATA3, a direct transcriptional target of Notch signaling, has been shown to increase expression of IFN γ production in NK cells^{248,249}. Interestingly, GATA3 levels decline after initiation of decidualization in HESC, which corresponds to the decline in NOTCH1 expression at the completion of decidualization¹¹² and is coupled with undetectable levels of IFN γ ²⁵⁰. Therefore, RBPJ may act to suppress GATA3 expression with downstream effects on reducing IFN γ expression during decidualization and injury. Overall, RBPJ controls many dynamic processes important for cellular differentiation and modulation of the immune system after injury, and its potential for regulating these processes in the setting of decidualization and postpartum uterine repair will be investigated in this dissertation.

SECTION 5: Recurrent Pregnancy Loss

Recurrent pregnancy loss (RPL) is defined as the loss of 2 or more consecutive clinical pregnancies²⁵¹. While 15% of clinically-recognized pregnancies result in miscarriage, RPL is estimated to occur in up to 5% of women²⁵². RPL can be attributed

to clinically identifiable causes, including embryo aneuploidy or uterine anatomic abnormalities in only 50% of cases^{253,254}. Dysregulated immune functioning remains one of the most widely hypothesized, yet least understood, mechanisms contributing to RPL. Women with idiopathic RPL display elevated serum levels of cytotoxic cytokines, such as IFN γ , and globally upregulated endometrial immune signaling responses²⁵⁵⁻²⁵⁹.

During embryo implantation, endometrial stromal cells coordinate specific immune recruitment and maintain the immune microenvironment through a unique step-wise cellular transformation as part of the decidualization process⁹. Initially, endometrial stromal cells convert from a structural fibroblast to a pro-inflammatory phenotype, and ultimately differentiate to a secretory anti-inflammatory decidual cell^{9,78}. However, endometrial stromal cells isolated from women with RPL fail to switch to an anti-inflammatory phenotype and are associated with reduced decidual marker gene expression and diminished discriminatory capability in determining low versus high-quality embryos^{17,78,260}.

Repeated embryo loss and endometrial repair are particularly relevant in the setting of RPL. The human endometrium has the unique property of regenerating itself with scar-less wound healing following menstruation and during the postpartum period¹²⁷. Menstruation and subsequent endometrial repair is hypothesized to precondition the uterus for future pregnancy¹³⁰. Given the importance of Notch signaling in both decidualization and during repair of injury, we hypothesize that reduced expression of RBPJ may occur in women with RPL contributing to their infertility and enhanced immune signaling²⁵⁵⁻²⁵⁹. Additionally, we will use the *Rbpj* c-KO mouse as a model for testing the impact of dysfunctional postpartum uterine repair on future embryo

implantation to correlate with RPL. This experiment will highlight the potential translational role for RBPJ in the setting of RPL and address the central hypothesis of my work: RBPJ ensures proper postpartum repair, which is essential for future pregnancy potential.

CHAPTER 1: Modulation of glucose transporter and ovarian steroid hormone receptor expression by the Notch family transcription factor, RBPJ, is essential for decidualization

INTRODUCTION

Receptivity of the uterus to a developing embryo is initiated through both hormonal regulation of the corpus luteum and embryonic signals, altogether favoring embryo attachment and trophoblast invasion³⁻⁵. The process of invasion and embryonic cues trigger transformation of the endometrial stromal fibroblasts into secretory, epithelioid-like decidual cells, termed decidualization⁶⁻⁸. Decidualized stromal cells migrate towards and encapsulate the implanting embryo, where they simultaneously support and control trophoblast invasion⁹⁻¹². Clinical consequences of decidualization defects include recurrent pregnancy loss, preeclampsia, preterm labor, and intra-uterine growth restriction^{17,18}. Implantation defects contribute to ~75% of failed pregnancies, suggesting a need to identify mechanisms regulating the early events, including decidualization, during the establishment of successful pregnancy¹.

The evolutionarily conserved Notch signaling pathway mediates key developmental and homeostatic functions, including cellular differentiation, survival and apoptosis^{96,98}. Notch signaling consists of four heterodimeric transmembrane receptors (NOTCH1-4) whose five ligands (Delta-like1, 3, 4; Jagged1, 2) are expressed on the cell membrane of adjacent cells, thereby initiating receptor-ligand interactions through a juxtacrine mechanism. Upon ligand binding, activated Notch receptors undergo an ADAM protease and gamma-secretase-mediated cleavage cascade which results in the

intracellular release of the Notch intracellular domain (NICD), which is the active form of Notch⁹⁹. In canonical Notch signaling, the NICD translocates to the nucleus and binds to the Notch family transcription factor Recombination Signal Binding Protein-Jk (RBPJ), converting it from a basal transcriptional repressor to an activator of downstream target genes, such as the 'Hairy enhancer of split' (HES) and Hes-related (HEY) transcription factor families¹⁰⁰⁻¹⁰³.

During the implantation window, NOTCH1 expression is induced in endometrial stromal cells of the non-human primate and in women in response to the embryonic signal human Chorionic Gonadotropin (hCG), which promotes uterine receptivity and decidualization^{3,110-113}. We have shown that Notch signaling, specifically NOTCH1, is indispensable for the initiation of decidualization in both the mouse and women^{112,114}. Further, Notch receptors, ligands and target genes are all reduced in eutopic endometrium of baboons and women with endometriosis, contributing to their disease-specific decidualization failure¹⁹. In mice, during implantation, Notch1 expression is initially induced in the stromal cells of the primary decidual zone then subsequently increases in the secondary decidual zone¹¹⁴. Ablation of Notch1 in the mouse uterus using a progesterone receptor (Pgr) driven cre-expressing (*Pgr^{cre/+}Notch1^{ff}*; *Notch1* c-KO) drastically inhibited their response to the *in vivo* artificial decidualization stimulus¹¹⁴. Decidualization failure in *Notch1* c-KO mice was associated with the down-regulation of genes crucial for progesterone-induced stromal cell differentiation and pathways related to cell proliferation, cell cycle progression, and estrogen receptor α (*Esr1*) signaling¹¹⁴. Additionally, apoptotic signaling was upregulated in the uteri of these mice¹¹⁴. *Notch1* c-KO mice produce reduced litter sizes in the first litter but, otherwise, exhibited normal

fecundity¹¹⁴, suggesting compensation by one of the other three Notch receptors may have rescued fertility in these mice, since other Notch receptors have been implicated in decidualization¹²³. Disruption of all potential Notch receptor signaling through ablation of the shared transcription factor, Rbpj, in the mouse uterus (*Pgr^{cre/+}Rbpj^{ff}*; *Rbpj* c-KO) resulted in subfertility due to abnormal embryonic-uterine axis and impaired decidual remodeling¹²⁴. However, the role that RBPJ plays in decidual function beyond initial implantation was not determined in this report nor was its relevance in the setting of human decidualization.

Growing evidence supports the importance of endometrial glucose transporters during decidualization and their dysregulation results in infertility⁶⁹⁻⁷³. Facilitative glucose transporters (known as the GLUT or SLC2 family) regulate cellular glucose uptake and have distinct tissue-specific and temporal expression patterns⁷⁴. SLC2A1 (GLUT1) is ubiquitously expressed through the uterus in both women and rodents⁶⁹. Additionally, GLUT1 is further induced during early gestation and decidualization of mouse and in human endometrial stromal cells^{71,75}. Progesterone administration increases SLC2A1 expression in the stromal cells in both women and mice⁷⁰⁻⁷². Further, Rbpj-induced SLC2A1 expression is essential for memory CD4+ T cell survival in the mouse through control of *Slca1* expression¹²², suggesting that this mechanism may be important for decidualization.

We hypothesized that Notch signaling, through RBPJ, mediates differentiation of endometrial stromal cells during decidualization. In the current study, we induced *in vivo* artificial decidualization in *Rbpj* c-KO and control mice (*Pgr^{+/+}Rbpj^{ff}*). *Rbpj* c-KO mice displayed reduced decidualization associated with altered ovarian steroid hormone

receptor signaling and downregulation of glucose transporter Slc2a1 during decidualization. Our mouse studies were performed in parallel with *in vitro* decidualization of Human Uterine Fibroblast (HuF) cells after knockdown of *RBPJ*. Similar to the *Rbpj* c-KO mice, decidualization was impaired in the absence of *RBPJ*, which was associated with reduced progesterone receptor and *SLC2A1* expression. Lastly, supplementation of pyruvate, bypassing the necessity for glucose, restored decidualization in *RBPJ* knockdown HuF cells. Through translational studies, we have determined that *RBPJ* is essential for decidualization in both the mouse and HuF cells, in part, through regulating progesterone signaling and glucose transporter expression.

RESULTS

***Rbpj* is essential for decidualization in the mouse and drives *Pgr* signaling**

We generated uterine-specific *Rbpj* c-KO mice and confirmed that uterine expression of *Rbpj* was significantly suppressed (**Fig S1-1A-C**). *Rbpj* c-KO and control mice were ovariectomized, hormonally primed to mimic early gestation and induced to decidualize via a mechanical scratch¹¹⁴. Following the scratch, mice were supplemented with estradiol and progesterone daily and sacrificed 3 or 5 days later. Decidualization was significantly reduced in *Rbpj* c-KO mice on both day 3 and day 5 of artificial decidualization (AD) based on uterine decidual to control horn weight ratio (**Fig 1-1A**). We chose to focus on AD5 because this time point corresponded to day 9.5 post-conception in natural mouse gestation, when initial embryo loss begins in *Rbpj* c-KO mice potentially contributing to their subfertility¹²⁴. Impaired decidualization in *Rbpj* c-KO

A *In Vivo* Artificial Decidualization Response

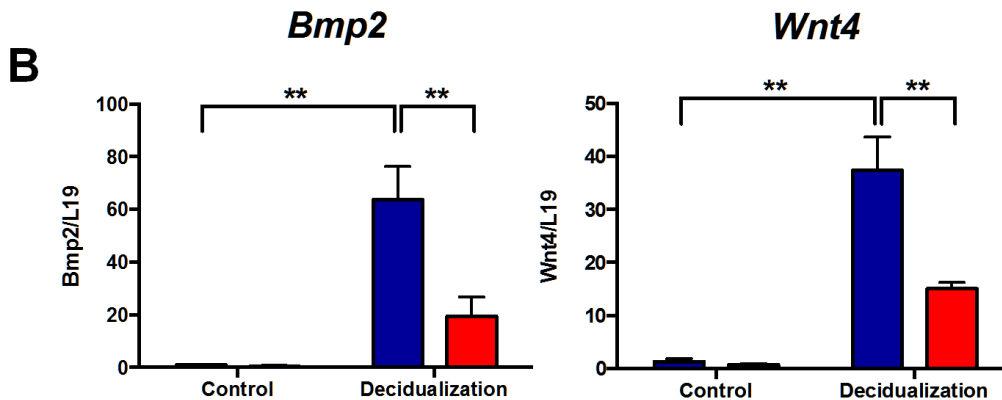
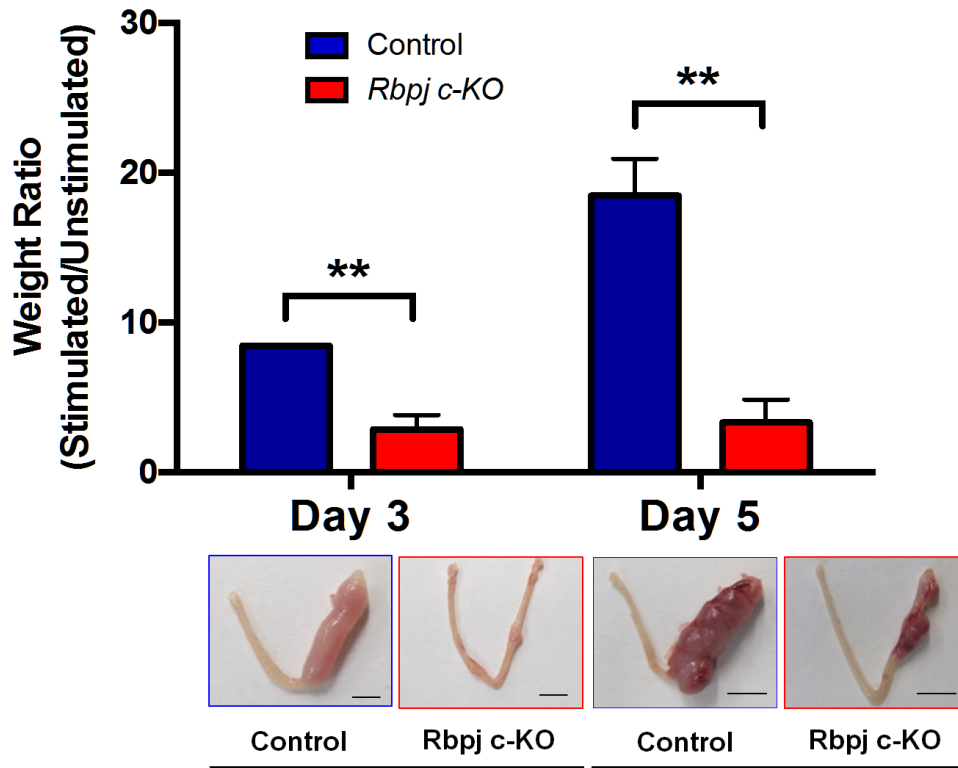


Figure 1-1. Decreased *in vivo* artificial decidualization response in *Rbpj* c-KO mice. Control and *Rbpj* c-KO mice (n=3-5/group) were ovariectomized, hormonally primed and then mechanically induced to decidualize. **(A)** Decreased decidual response in *Rbpj* c-KO mice was present both 3 and 5 days following mechanical decidualization based on stimulated to unstimulated uterine horn weight. **(B)** Impaired decidualization was associated with reduced mRNA expression of decidual marker genes, *Bmp2* and *Wnt4*, in *Rbpj* c-KO mice. Data represented as Mean \pm SEM. **p<0.01; Scale Bar = 0.5 cm.

mice on AD5 was associated with reduced mRNA expression of decidual markers *Bmp2* and *Wnt4* (**Fig 1-1B**). Orchestrated ovarian steroid hormone receptor expression is necessary for promoting stromal survival and, ultimately, mediating the epithelial to stromal proliferation shift that occurs during implantation and decidualization⁵³. Thus, expression patterns of *Esr1* and *Pgr* were investigated in the uteri of artificially decidualized mice. *Pgr* mRNA expression significantly increased in the decidualized uterine horns of control mice compared to the unstimulated horn, while this was not the case in *Rbpj* c-KO mice (**Fig 1-2A**). Consistent with this finding, decreased expression of *Pgr* downstream effectors *Hoxa10* and its target *Cdk6*, *Areg*, and *Ptgs2* were decreased in the decidual horn of *Rbpj* c-KO mice compared to the control mouse decidual horn (**Fig 1-2A**). *Cdk6* plays an important role in mediating the *Hoxa10*-induced differentiation of stromal cells towards the decidual phenotype⁶². Immunostaining revealed reduced protein level in the *Rbpj* c-KO mouse decidualized horn (**Fig 1-2B**). Both mRNA and protein expression of *Esr1* was significantly increased in the decidual horn of *Rbpj* c-KO mice compared to that of the control mice, which was consistent with upregulation of *Esr* target genes, *Complement C3* and *Lactoferrin (Ltf)* (**Fig 1-2C**). Additionally, *Esr1* targets *Ltf* and *Mucin-1 (Muc1)* were elevated in the control horn of *Rbpj* c-KO mice compared to that of control mice. Enhanced *Esr1* in *Rbpj* c-KO mouse decidual horns was localized to both endometrial luminal epithelial and stromal cells (**Fig 1-2D**). The Notch pathway regulates cell survival and differentiation^{96,98}, and failed initiation of stromal differentiation for decidualization occurs as a consequence of reduced *Pgr* signaling and enhanced endometrial *Esr1* in the absence of Notch signaling through *Rbpj*.

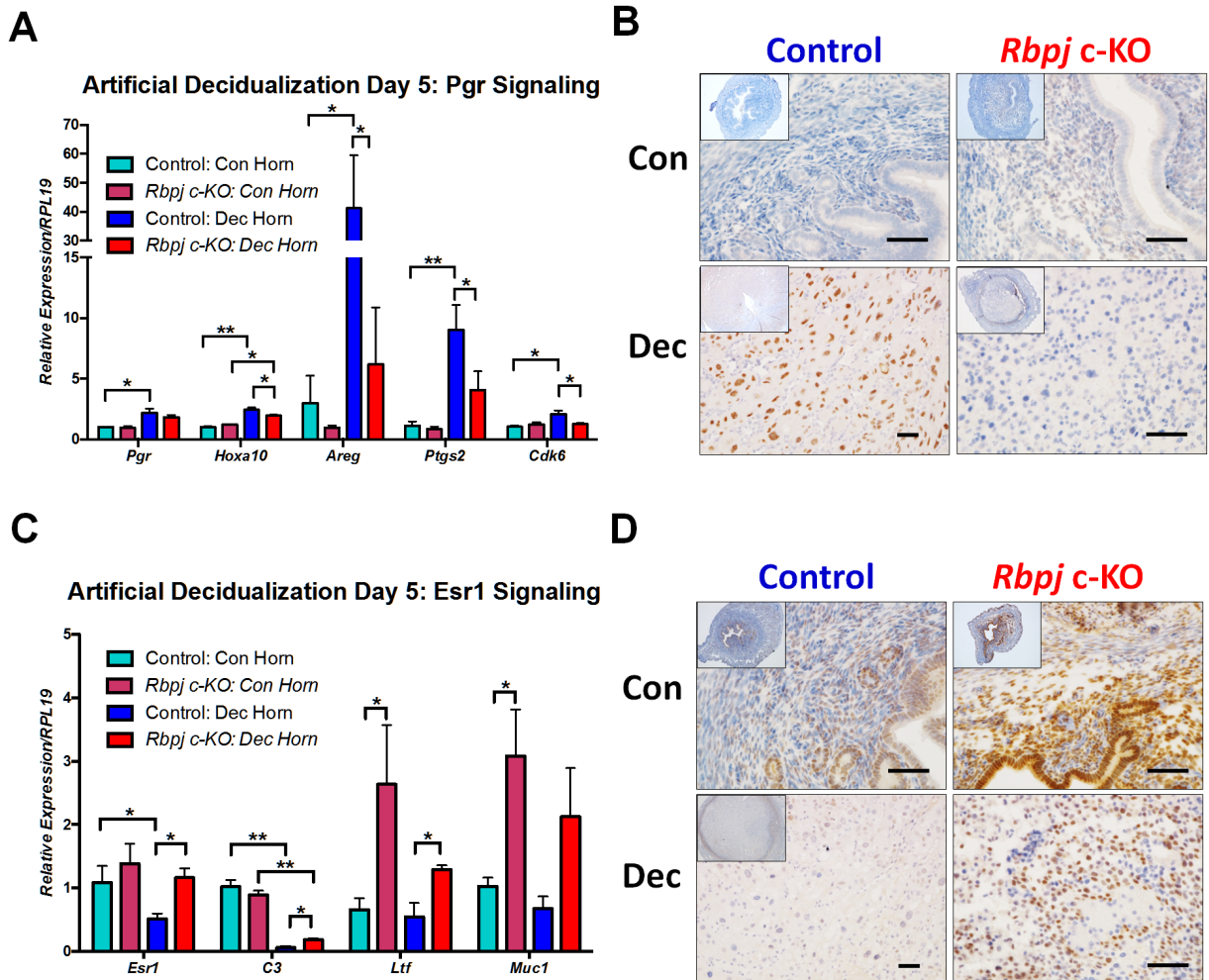
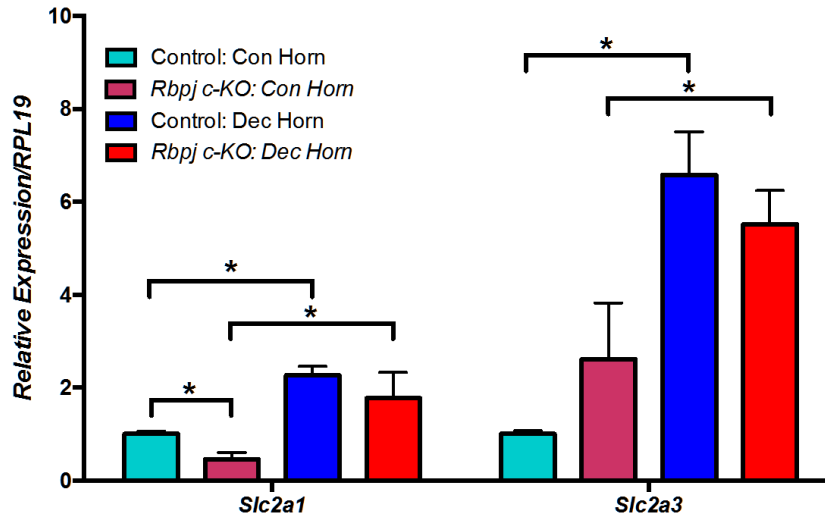


Figure 1-2. Down regulation of Pgr signaling and up regulation of Esr1 signaling in *Rbpj c-KO* mice during *in vivo* artificial decidualization. Ovarian steroid hormone receptor levels were investigated in *Rbpj c-KO* and control mice by RT-qPCR and immunohistochemistry. **(A)** *Pgr* mRNA was significantly induced in the control mouse decidual horn compared to the unstimulated horn, which was not the case in *Rbpj c-KO* mice ($n=3-5/\text{group}$). Additionally, *Pgr* target genes, *Hoxa10*, *Areg*, *Ptgs2* and *Cdk6* were significantly decreased in the decidual horn of *Rbpj c-KO* mice compared to control mice. **(B)** Reduced Pgr expression was localized to the decida of *Rbpj c-KO* mice. **(C)** Up regulation of *Esr1* mRNA levels was present in the *Rbpj c-KO* mouse decidual horn, which was associated with increased target gene expression of *Ltf* and *C3*. **(D)** Esr1 was strongly expressed in the control horn luminal epithelium and stromal cells of *Rbpj c-KO* mice compared to control mice, which persisted in the decidualized uterine horn compared to controls. Data represented as Mean \pm SEM. Comparisons were made using Two-Way ANOVA. * $p<0.05$, ** $p<0.01$; Scale Bar = 50 μm .

Endometrial loss of *Rbpj* reduces *Slc2a1* induction during decidualization

Glucose metabolism plays an important role in rapidly proliferating and differentiating cells, and there is mounting evidence that supports a role of endometrial glucose transporters during decidualization and embryo implantation⁶². We examined the mRNA levels of Glucose transporters *Slc2a1* (*Glut1*) and *Slc2a3* (*Glut3*) on AD5, both of which have been described extensively in the setting of natural pregnancy and *in vitro* decidualization of mouse endometrial stromal cells^{71,261}. However, to our knowledge, their expression has not been investigated in the setting of *in vivo* artificial decidualization. Both *Slc2a1* and *Slc2a3* were up regulated in the decidualized horns of *Rbpj* c-KO and control mice (**Fig 1-3A**). There was no statistically significant difference between decidual horn mRNA levels of either glucose transporter, although there was a trend towards decreased expression in *Rbpj* c-KO mice. Since glucose transporters are often transiently induced in a spatial manner, we performed immunostaining to determine both expression and localization of *Slc2a1* in the mouse decidua on AD5. Consistent with the trend of decreased *Slc2a1* mRNA expression, *Slc2a1* protein levels were reduced in the decidual horn of *Rbpj* c-KO mice compared to control mice (**Fig 1-3B**). Interestingly, staining of *Slc2a1* was concentrated in the cells of the secondary decidual zone of control mice, which did not occur in the *Rbpj* c-KO mice. Overall, these findings suggest *Slc2a1* expression is induced to a greater extent in stromal cells undergoing decidualization rather than upon completion of differentiation, which parallels the increase and the subsequent down regulation of *Notch1* expression during decidualization^{112,114}.

A Artificial Decidualization Day 5: Glucose Transporters



B

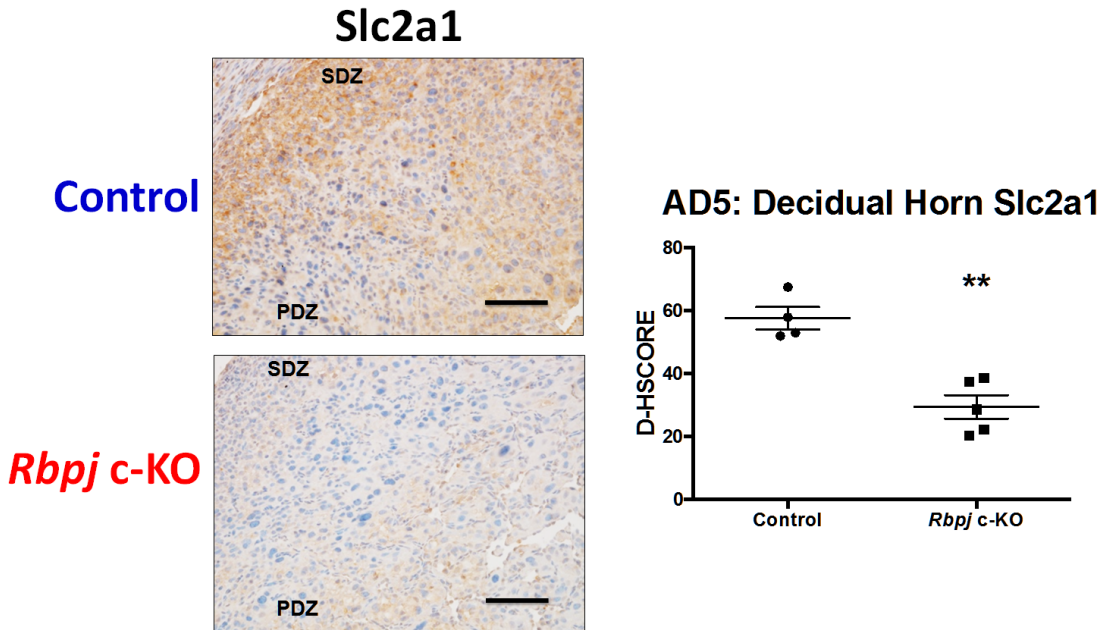


Figure 1-3. Reduced glucose transporter, *Slc2a1*, expression associated with *Rbpj* loss during *in vivo* artificial decidualization. Glucose transporter mRNA and protein levels were investigated by RT-qPCR and immunohistochemistry, respectively, during artificial decidualization. **(A)** Both *Slc2a1* and *Slc2a3* significantly induced in control and *Rbpj* c-KO mouse decidual horns compared to control horns. *Slc2a1* mRNA expression was reduced in the control horn of *Rbpj* c-KO mice compared to control mice (n=3-5/group). **(B)** *Slc2a1* protein localization was significantly reduced in the decidual horn of *Rbpj* c-KO mice, particularly in the secondary decidual zone (n=4-5/group). Data represented as Mean \pm SEM. Comparisons were made using Two-Way ANOVA for more than two groups or using a Student's t-test for two groups. *p<0.05, **p<0.01; Scale Bar = 100 μ m; SDZ = Secondary Decidual Zone, PDZ = Primary Decidual Zone.

***RBPJ* is indispensable for decidualization of HuF cells and its loss phenocopies the mouse**

HuF cells represent a proliferating population of undifferentiated stromal fibroblasts, which can be decidualized *in vitro*^{28,112,262}. To determine the role of *RBPJ* in human decidualization and the translational relevance of our work in the *Rbpj*-ablated mouse, HuF cells were decidualized (EPC) *in vitro* for five days following siRNA-mediated knockdown of *RBPJ*¹¹². We confirmed that *RBPJ* expression was reduced following *RBPJ* knockdown HuF cells (**Fig S1-1D**). Expression of human decidual markers *PRL* and *IGFBP1* were also significantly reduced following *RBPJ* knockdown (**Fig 1-4A**). Similar to the *Rbpj* c-KO mouse, impaired decidualization was coupled with decreased *PGR* expression (**Fig 1-4B**). *ESR1* levels were increased in decidualized cells versus vehicle-treated controls in both siRNA groups, which we hypothesize is due to the presence of only stromal cells rather than whole tissue, where epithelial *ESR1* decreases during implantation but stromal *ESR1* is likely necessary for decidualization²⁶³. Additionally, there was no difference in *ESR1* expression of EPC-treated HuF cells between siRNA treatment groups (**Fig 1-4B**). We investigated levels of glucose transporter *SLC2A1*, which was reduced in *Rbpj* c-KO mice. As expected, *RBPJ* siRNA knockdown in decidualized HuF cells resulted in decreased mRNA expression of *SLC2A1* compared to control siRNA treatment (**Fig 1-4C**). Our findings indicate that similar to the mouse, *RBPJ* expression coordinates both *Pgr* and glucose transporter expression, which are essential for decidualization of human endometrial fibroblasts.

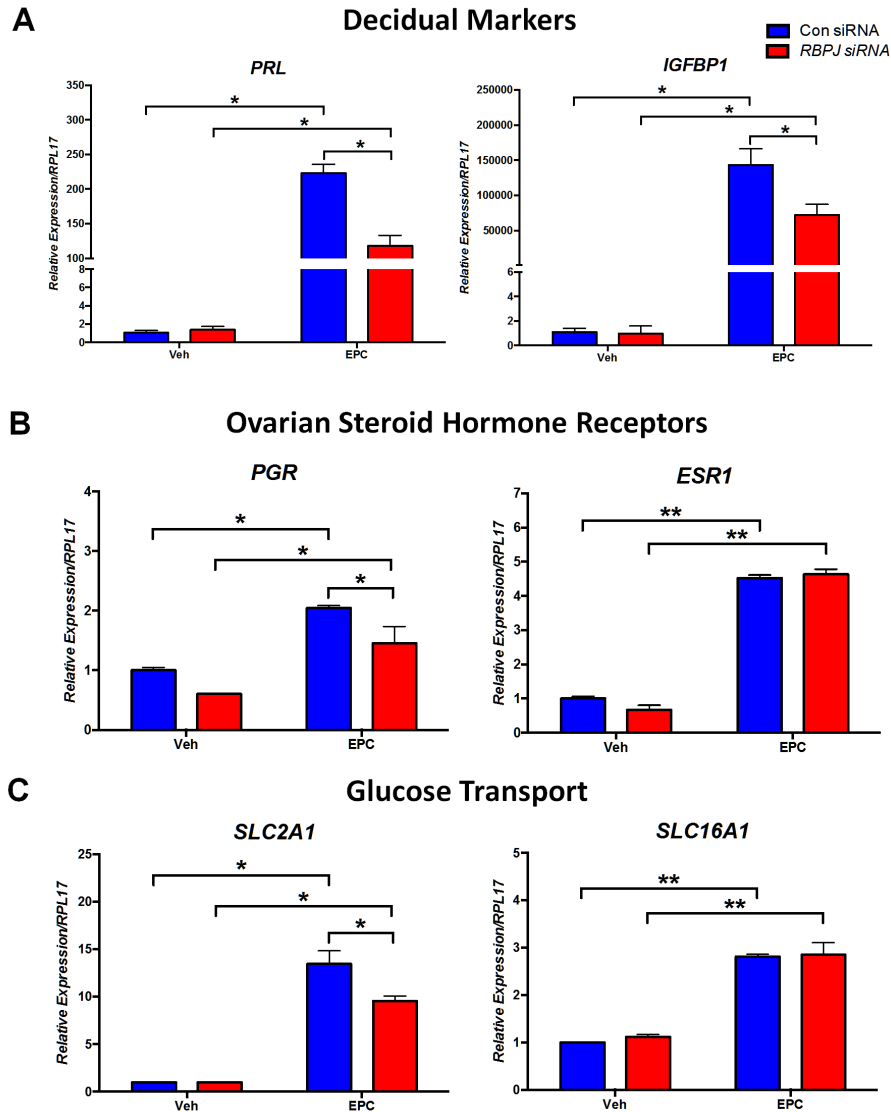


Figure 1-4. Loss of HuF Cell *RBPJ* phenocopies the mouse during decidualization. HuF cells were transfected with either control or *RBPJ* siRNA and subsequently treated with either vehicle or EPC to induce *in vitro* decidualization. Decidual markers, ovarian steroid hormone receptors and glucose transport molecules were investigated by RT-qPCR. **(A)** In response to EPC, *mRNA* expression of human decidual markers PRL and IGFBP1 were significantly reduced with *RBPJ* siRNA knockdown compared to control siRNA cells. **(B)** Similar to the *Rbpj* c-KO mouse, *Pgr* expression was significantly reduced with loss of *RBPJ* during decidualization. However, unlike the mouse, *RBPJ* loss in HuF cells did not affect *ESR1* levels, suggesting an epithelial effect in mouse whole uterine decidual tissue. **(C)** Glucose transporter, *SLC2A1*, *mRNA* expression was reduced in EPC-treated HuF cells with *RBPJ* knockdown. However, pyruvate transporter *SLC16A1* was unaffected by *RBPJ* loss with EPC treatment. Data represented as Mean \pm SEM (n=3-4 HuF cell lines performed in triplicates); comparisons were made using Two-Way ANOVA. *p<0.05.

Pyruvate supplementation rescues decidualization failure with *RBPJ* loss in HuF cells

Both in *Rbpj* c-KO mouse endometrium and isolated HuF cells where *RBPJ* was suppressed, decidualization was dramatically altered and was associated with decreased expression of glucose transporter *SLC2A1*. Therefore, we hypothesized that supplementation of additional glucose or pyruvate, which bypasses the necessity for glucose, might restore decidualization associated with loss of *RBPJ* in HuF cells. First, we confirmed that pyruvate transporter, *SLC16A1*, expression was unaffected by *RBPJ* loss (**Fig 1-4C**). Next, we supplemented the control and *RBPJ* knockdown HuF cells with additional glucose or pyruvate during *in vitro* decidualization of HuF cells. Dosages of glucose and pyruvate (8 mM and 16 mM, respectively) selected for this experiment were determined based on physiological dose-response experiments conducted previously in our laboratory, and were ultimately chosen based on their ability to favor decidualization without negatively affecting cellular osmotic pressure. Remarkably, administration of pyruvate but not glucose restored expression of decidual marker *PRL* in *RBPJ* knockdown HuF cells during decidualization (**Fig 1-5A**). While a statistically significant increase in *IGFBP1* expression did not result from pyruvate and EPC treatment in *RBPJ* knockdown cells, the pyruvate-treated group *IGFBP1* expression was also not significantly reduced compared to the no glucose or pyruvate control siRNA group treated with EPC. Further, pyruvate treatment increased *PGR* expression in decidualized *RBPJ* knockdown HuF cells compared to no glucose or pyruvate cells (**Fig 1-5B**).

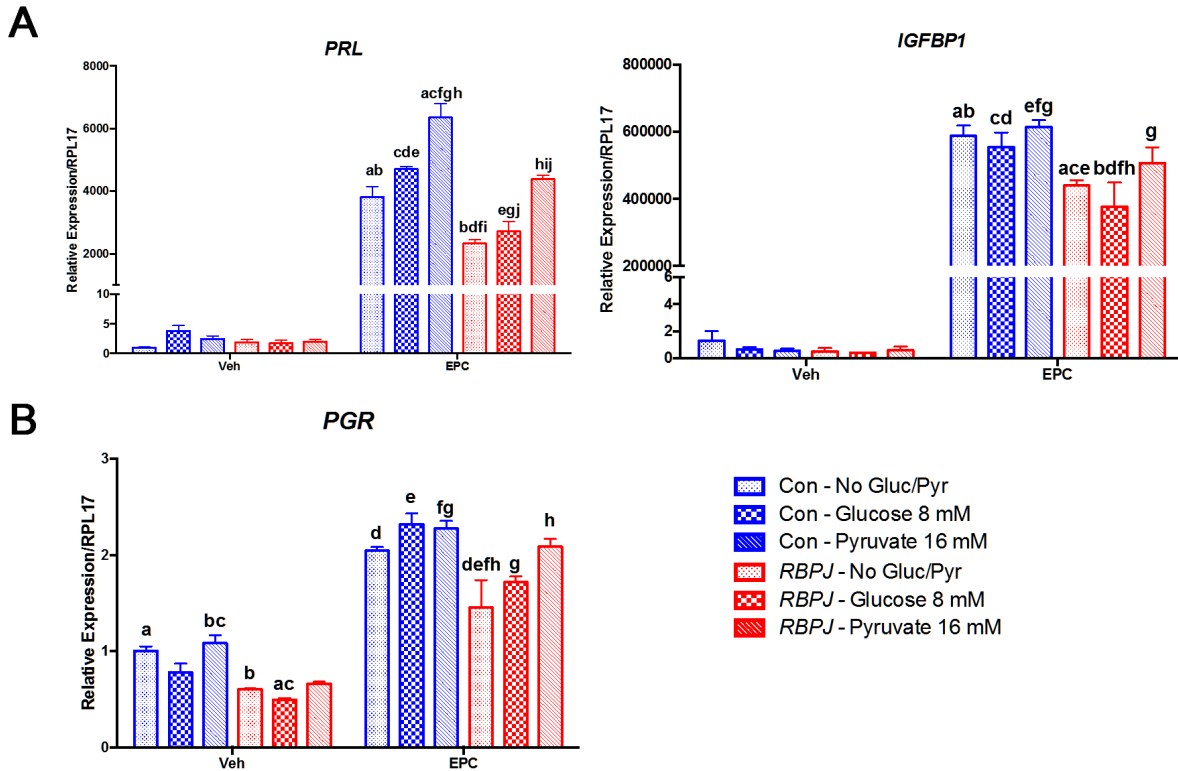


Figure 1-5. Pyruvate supplementation rescues decidual marker gene and *PGR* expression in the setting of *RBPJ* loss. HuF cells were transfected with either control or *RBPJ* siRNA and subsequently treated with either vehicle or EPC to induce *in vitro* decidualization with cell culture media supplementation of 8 mM Glucose, 16 mM Pyruvate, or neither. **(A)** Administration of pyruvate but not glucose restored expression of decidual marker *PRL* in EPC-treated *RBPJ* knockdown HuF cells. While a statistically significant increase in *IGFBP1* expression did not result from pyruvate and EPC treatment in *RBPJ* knockdown cells, the pyruvate-treated group *IGFBP1* expression was also not significantly reduced compared to the no glucose or pyruvate control siRNA group treated with EPC. **(B)** Pyruvate supplementation increased *PGR* expression in decidualized *RBPJ* knockdown HuF cells compared to no glucose or pyruvate cells. Data represented as Mean \pm SEM (n=3-4 HuF cell lines performed in triplicates). Comparisons were made using Two-Way ANOVA. Significantly changed mRNA levels between two groups are represented by matching letters, where p<0.05.

DISCUSSION

Notch is an arbiter of cell fate and, based on our previous work, its expression regulates endometrial transformation during embryo implantation and more specifically, decidualization^{19,112}. In the current study, we demonstrate that ablation of RBPJ in both the mouse uterus and in HuF cells reduces their capacity to differentiate towards their decidual phenotype. Contributors to impaired decidualization in both models included dysregulated ovarian steroid hormone receptor expression and reduced glucose transporter SLC2A1 expression. Additionally, supplemental pyruvate partially restores the expression of decidual markers in Huf Cells in which *RBPJ* was silenced during decidualization. Our findings support a previously undescribed contributor to subfertility in *Rbpj* c-KO mice, where implantation failure is hypothesized to result from abnormal embryonic-uterine axis¹²⁴. However, in the current study, we determined that *Rbpj* c-KO mice display a reduced *in vivo* response to artificial decidualization based on decidual horn wet weight and differentiation marker expression, which is independent of the presence of an embryo. Additionally, we determined a translational role for RBPJ during *in vitro* decidualization of HuF cells.

Similar to *Notch1*, *Rbpj* is dynamically expressed in a temporospatial manner in the mouse uterus during the establishment of pregnancy. Embryonic signals induce *Notch1* expression, which include hCG in primates or physical contact in mice^{112,114}. During implantation in mice, *Notch1* and *Rbpj* are initially expressed in the sub-epithelial stromal cells of the primary decidua and as pregnancy progresses there is a shift of expression to the secondary decidua^{114,124}. Consistent with the mouse, NOTCH1 initially increases in decidualizing HuF cells and subsequently becomes downregulated for

completion of decidualization¹¹². Expression of *Notch1* is tightly regulated, where over-activation of Notch1 signaling impairs decidualization and causes infertility²⁶⁴. Similar to Notch1, *Rbpj* is initially induced in the primary decidual zone in the mouse and subsequently downregulated, at which point its expression is localized within the secondary decidual zone¹²⁴.

During implantation, Pgr drives stromal proliferation and promotes transformation of endometrial fibroblasts towards a secretory phenotype while suppressing epithelial *Esr1*⁵³. In part, Pgr signaling through *Hoxa10* promotes differentiation of stromal cells through induction of cell cycle regulators, such as *Cdk6*^{62,265}. In the *Rbpj* c-KO mice, broad down regulation of the Pgr signaling pathway was evident along with enhanced *Esr1* signaling. Additionally, *Pgr* expression was decreased with *RBPJ* knockdown during decidualization of HuF cells, while *Esr1* expression was not affected. Based on our prior and present work, a close relationship between Pgr and Notch signaling exists. P4-targets were decreased in *Notch1* c-KO mice during decidualization, including *Cdk6*, and Pgr mediates cleavage of Notch1 to its active form^{112,114}. Further, over activation of Notch signaling indirectly suppresses Pgr expression via recruitment of DNA methyltransferases and hypermethylation of its promoter in an *Rbpj*-dependent manner²⁶⁴. Since *Rbpj* basally suppresses Notch target expression, its loss can mimic either down regulation or up regulation of Notch signaling²²³. Therefore, *RBPJ* mediates Notch receptor-independent functions, which may include regulation of Pgr signaling.

Ablation of *Rbpj* in the mouse uterus resulted in enhanced *Esr1* and its target gene expression. Since *ESR1* expression was unaffected in isolated decidualizing human stromal cells in the absence *RBPJ*, it would appear that epithelial *Esr1* is more

likely affected by *Rbpj* loss. Since stromal-to-epithelial cross-talk occurs during implantation, largely driven by *Pgr*, reduced stromal *Pgr* expression may contribute to enhanced epithelial *Esr1* activity in *Rbpj* c-KO mice^{53,266}. Additionally, it was shown that *Rbpj* interacts with *Esr1* in mouse stromal cells and Ishikawa cells, where enhanced phosphorylation occurs in the absence of *Rbpj*¹²⁴. In breast cancer epithelial cells, *Notch1* promotes *ESR1* signaling, but basally, *RBPJ* may act to suppress epithelial estrogen target gene expression in the absence of *Notch* activation since *RBPJ* binding sites have been identified in close proximity to estrogen-responsive elements in both the mouse and human²⁶⁷. Altogether, these findings indicate that *Rbpj* coordinates stromal *Pgr* activation while suppressing epithelial *Esr1* expression during decidualization.

Glucose transporter *SLC2A1* expression was down regulated during *in vivo* and *in vitro* decidualization in the absence of *RBPJ*. In women, stromal *SLC2A1* expression is low in the proliferative phase and increases during the mid-secretory phase, corresponding to the period of uterine receptivity and increased *P4* levels⁷⁰. Further, inhibition of glucose transporters drastically reduced *PRL* secretion during *in vitro* decidualization of human endometrial stromal cells⁷⁰. In the rat, endometrial stromal *Slc2a1* expression pattern during early pregnancy mirrors that of *Rbpj*^{124,261}. Initially, they are induced in the stromal cells of the primary decidual zone and as implantation progresses, expression shifts to the secondary decidual zone²⁶¹. In the current study, *Slc2a1* staining was more concentrated in the stromal cells of the secondary decidual zone on AD5 in control mice, which was reduced in the *Rbpj* c-KO mouse decidual horn. We confirmed decreased *Slc2a1* expression in the mouse with loss of *Rbpj* occurs with *RBPJ* knockdown during decidualization in HUF cells. Based on our findings, we

hypothesize that Rbpj acts upstream of Slc2a1 and that both are early mediators of proliferation and differentiation of stromal fibroblasts into decidual cells. After completion of differentiation during decidualization, both Notch1 and Rbpj are reduced in the primary decidual zone, which may subsequently reduce Slc2a1 expression in the primary decidual zone^{112,114}.

In CD4+ memory T cells, Rbpj mediates survival through regulation of Slc2a1 expression and loss of Rbpj could be overcome by administration of pyruvate, which bypasses the requirement of glucose¹²². In the current study, we found that supplementation of pyruvate rescued expression of *PGR* and decidual marker *PRL* associated with RBPJ knockdown in decidualizing HuF cells. Dysregulated glucose transporter expression represents an understudied contributor to infertility despite reduced levels of SLC2A1 in mid-secretory biopsies of patients with idiopathic versus clear anatomical causes for infertility⁷⁰. A positive impact of pyruvate supplementation in embryo culture media used for IVF patients has been previously reported²⁶⁸. However, to our knowledge, the effect of supplementing extra glucose or pyruvate in IVF culture media during embryo transfer on uterine implantation rates in the setting of impaired uterine receptivity has not been determined. We have shown that impaired decidualization can be restored with supplementation of low levels of pyruvate, through potentially bypassing the necessity for glucose. Future studies are indicated to determine whether endometrial receptivity can be restored in the setting of infertility through supplementation of pyruvate.

METHODS

Mice

All studies performed using animals were approved by the Institutional Animal Care and Use Committee of Michigan State University, East Lansing, MI, USA in compliance with the Guide for Care and Use of Laboratory Animals (2011, National Academy of Sciences). To avoid the embryonic lethality of a complete *Rbpj* knockout¹²⁵, we generated a uterine-specific, conditional *Rbpj* knockout mouse. *Rbpj^{ff}* mice contain LoxP sites flanking the sixth and seventh exons, corresponding to the DNA binding domain¹²⁶. We crossed *Pgr^{cre/+}* mice, containing a knock-in of Cre recombinase in one copy of the Progesterone Receptor (*Pgr*) gene while maintaining normal fecundity and *Pgr* function^{49,50}, with *Rbpj^{ff}* (control) mice to generate *Pgr^{cre/+}Rbpj^{ff}* (*Rbpj* c-KO) mice, in order to ablate *Rbpj* in *Pgr*-positive tissues.

***In Vivo* Artificial Decidualization Model**

Induction of artificial decidualization was performed on 6-week old *Rbpj* c-KO and control mice as previously described¹¹⁴. Mice were ovariectomized and then primed to mimic the hormonal milieu of early pregnancy with daily E2 (100 ng, Sigma-Aldrich, St. Louis, MO, USA) for three days followed by two days of rest and then daily P4 (1 mg) plus E2 (6.7 ng). Six hours following the third day of E2 and P4 injection, a mechanical scratch of the anti-mesometrial luminal epithelium of the left uterine horn (Dec) was performed to induce decidualization. The unscratched right horn served as the unstimulated hormonal control (Con). Subsequently, daily injections of E2 and P4 were provided with sacrifice 3 or 5 days post-scratch (n=3-5 mice/group). Uterine tissues

were collected, weighed and either snap frozen in liquid nitrogen or fixed in 4% paraformaldehyde for paraffin embedding. Decidual response was calculated based on the ratio of Dec to Con horn weight.

Histological Analysis and Immunohistochemistry

Paraformaldehyde fixed-paraffin embedded tissues were sectioned to 6 µm thickness and placed onto microscope slides (Thermo Fisher Scientific, Waltham, MA, USA). For immunohistochemistry, each tissue section was dewaxed, rehydrated with a graded alcohol series, followed by heat-mediated antigen retrieval in citrate buffer (Antigen unmasking solution, Vector Laboratories, Burlingame, CA) and then hydrogen peroxide treatment. Sections were blocked for 1 hour in 10% Normal Horse Serum (Vector Laboratories, Burlingame, CA) in Phosphate Buffered Saline (PBS) incubated overnight at 4°C in one of the following primary antibodies: mouse anti-ESR1 (1:40; Vector Laboratories, Burlingame, CA), rabbit anti-PGR (1:500, DAKO, Carpinteria, CA), mouse anti-GLUT1 (1:100; Santa Cruz Biotechnology). Next, sections were incubated in respective biotinylated secondary antibodies for anti-mouse IgG or anti-rabbit IgG (Vector Laboratories, Burlingame, CA) followed by HRP conjugated streptavidin. Detection for immunoreactivity was achieved using the DAB Substrate Kit (Vector Laboratories, Burlingame, CA) followed by hematoxylin counterstaining. Staining intensity of each section was quantified by image analysis software *ImageJ* (NIH) resulting in a Digital HSCORE (D-HSCORE) of staining intensity as previously reported²⁶⁹.

Isolation and Culture of HuF Cells

HuF cells are isolated from the decidua parietalis from term placentas^{28,112}. Tissues were procured after patient informed consent was obtained under a protocol approved by the Institutional Review Board at Michigan State University. After trypsinization, cells were propagated in phenol-red-free RPMI 1640 (Thermo Fisher Scientific, Waltham, MA, USA) supplemented with 10% Charcoal:Dextran Stripped-Fetal Bovine Serum (CDS-FBS). Each cell line obtained from a single placenta is considered a single sample for statistical analysis; therefore at least three HuF cell lines plated in triplicate were used for each experiment. Further, only cells between passages 3–6 were used for experiments.

Transfection of *RBPJ* small interfering RNA (siRNA) in HuF cells

HuF cells were seeded in six-well dishes at 1.5×10^5 cells per well in 10% CDS-FBS in RPMI. Once confluence reached ~30-50%, cells were washed with sterile PBS then acclimated to serum and antibiotic-free Opti-MEM media (Thermo Fisher Scientific, Waltham, MA, USA) for at least 30 minutes prior to transfection. Subsequently, non-targeting (Control; ON-TARGETplus Non-targeting pool; GE Dharmacon, Lafayette, CO, USA) and *RBPJ* siRNAs (SMARTpool ON-TARGETplus *RBPJ* siRNA; GE Dharmacon, Lafayette, CO, USA) were dissolved in Lipofectamine RNAiMAX (Thermo Fisher Scientific, Waltham, MA, USA) diluted in Opti-MEM. This mixture was added to the cells to achieve a final concentration of 50 nM of either control or *RBPJ* siRNA, and cells were incubated with the siRNA mixture for 5 hours. Finally, cells were washed with PBS

and then incubated overnight in fresh RPMI with 10% CDS-FBS and antibiotics prior to any future experiments.

***In Vitro* Decidualization of HuF Cells**

In vitro decidualization of HuF cells was performed through administration of an EPC cocktail [a combination of 36 nM estradiol-17 β , 1 μ M medroxyprogesterone acetate (MPA) and 0.5 mM di-butyryl-cyclic adenosine monophosphate (dbcAMP; Sigma, St. Louis, MO, USA)] in 2% CDS-FBS in RPMI^{28,112,262}. HuF cells were treated with EPC or vehicle (Veh) for 5 days with replacement of treatment/media every 2 days. For *in vitro* decidualization studies with glucose and pyruvate supplementation, 8 mM D-Glucose or 16 mM Sodium Pyruvate (Sigma, St. Louis, MO, USA) in RPMI, respectively, were used for dilution of EPC or vehicle.

RNA isolation and Real Time-Quantitative PCR (RT-qPCR)

Total RNA was isolated from snap frozen mouse tissues or cultured cells using TRIzol reagent (Invitrogen, Carlsbad, CA, USA) followed by reverse transcription to produce cDNA using the High Capacity cDNA Reverse Transcription Kit (Applied Biosystems, Foster City, CA, USA). Differential gene expression was determined using RT-qPCR performed with either TaqMan Universal Master Mix II (Applied Biosystems, Foster City, CA, USA) or SYBR Green PCR Master Mix (Applied Biosystems, Foster City, CA, USA) using the ViiA 7 qPCR System (Applied Biosystems, Foster City, CA, USA). *RPL17* and *Rpl19* were used for normalization of cDNA from human and mouse samples, respectively. Primer sequences used for RT-qPCR are provided (**Table S1-1**).

Statistical Analysis

Variation between groups was determined using two-way analysis of variance with repeated measures followed by a Holm-Sidak post-hoc test to determine group-specific differences. Statistical significance was defined as $p < 0.05$. All statistical analyses were performed by GraphPad Prism 6.0 (GraphPad Software, San Diego, CA, USA).

ACKNOWLEDGEMENTS

The authors thank Dr. Francesco DeMayo (NIH National Institute of Environmental Health Sciences) for kindly providing the *Pgr*^{cre/+} mice and Dr. Nadia Carlesso (Indiana University) for kindly providing the *Rbpj*^{flox/flox} mice. The authors also thank Ms. Samantha Bond, Ms. Sharra Poncil, Ms. Ariadna Ochoa, and Mr. Mark Olson for their excellent technical assistance. Funding for this study was provided by NICHD R01 HD042280 (ATF) and NICHD F30 HD082951 (MS).

APPENDIX

Gene Symbol	Application	Accession ID	Species	Forward	Reverse
<i>Rpl19</i>	Taqman	NM_001159483	Mouse	Mm01606037_g1	
<i>Rbpj</i>	Taqman	NM_001080927	Mouse	Mm01217627_g1	
<i>Bmp2</i>	SYBR Green	NM_007553	Mouse	CGCAGCTTCCATCACGAA	GCTTCCTGTATCTGTCCCG
<i>Wnt4</i>	SYBR Green	NM_009523	Mouse	AGTGCCAATACCAGTTCCG	CACACTTCTCCAGTTCTCCAC
<i>Pgr</i>	SYBR Green	NM_008829	Mouse	TGAGCCTGATGGTGTTTGG	ACAGCGAGTAGAATGACAGC
<i>Hoxa10</i>	SYBR Green	NM_008263	Mouse	GAAAACAGTAAAGCTTCGCCG	GAAACTCCTTCTCCAGCTCC
<i>Areg</i>	SYBR Green	NM_009704	Mouse	AGATACATCGAGAACCTGGAGG	AGAGACAAGATAGTGACAGCTAC
<i>Ptgs2</i>	SYBR Green	NM_011198	Mouse	CCAGCACTTCACCCATCAG	GTCCAGAGTTTCACCATAAATGTG
<i>Cdk6</i>	SYBR Green	NM_009873	Mouse	GTTCCAGACGTGGATCAACTAGG	TGTCACAAACTTCTCGATGGG
<i>Esr1</i>	SYBR Green	NM_007956	Mouse	AACCGCCCATGATCTATTCTG	AGATTCAAGTCCCAAAGCC
<i>C3</i>	SYBR Green	NM_009778	Mouse	AGACTGCCTGACCTTCAAAG	CATCCCATCGTCTTCTCTG
<i>Ltf</i>	SYBR Green	NM_008522	Mouse	ATCTCTGTGCCCTGTGTATTG	ACATTTCTGCCTTCTCAGC
<i>Muc1</i>	SYBR Green	NM_013605	Mouse	TTCCAACCCAGGACACCTAC	ATTACCTGCCGAAACCTCCT
<i>Slc2a1</i>	SYBR Green	NM_011400	Mouse	TGTATCCTGTTGCCCTTCTG	GACCCTCTTCTTTCATCTCCTG
<i>Slc2a3</i>	SYBR Green	NM_011401	Mouse	CGCTTCTCATCTCCATTGTCC	TGAAGATAGTATTGACCACGCC
<i>RPL17</i>	SYBR Green	NM_000985	Human	ACGAAAAGCCACGAAGTATCTG	GACCTTGTGTCAGCCCAT
<i>RBPJ</i>	SYBR Green	NM_203284.2	Human	CCGAGAAGGTTGGAGATGGG	GTTTGATTGTTAGGGGCA
<i>PRL</i>	SYBR Green	NM_001163558	Human	ACCCTGTCTGGTCGGGACTT	TGTTGTGGATGATTCGGCAC
<i>IGFBP1</i>	SYBR Green	NM_000596	Human	CCTGCCAAACTGCAACAAGA	TCCCATTCCAAGGGTAGACG
<i>PGR</i>	SYBR Green	NM_000926	Human	TGTATTTGTGCGTGTGGGTG	TACAGCCATTCCAGGAAG
<i>ESR1</i>	SYBR Green	NM_000125	Human	GCCCTGGAGACCACAATCA	AGGCAATGGCGAAAAGAAAC
<i>SLC2A1</i>	SYBR Green	NM_006516	Human	TCATCGTGGCTGAACTCTTC	GATGAAGACGTAGGGACCAC
<i>SLC16A1</i>	SYBR Green	NM_003051	Human	AGGTCCAGTTGGATACACCCC	GCATAAGAGAAGCCGATGAAAT

Table S1-1. Primer sequences used for this study

CHAPTER 2: RBPJ mediates top Notch postpartum repair for future pregnancy potential and is reduced in recurrent pregnancy loss

INTRODUCTION

Recurrent pregnancy loss (RPL) is defined as the loss of 2 or more consecutive clinical pregnancies²⁵¹. While 15% of clinically-recognized pregnancies result in miscarriage, RPL is estimated to occur in up to 5% of women²⁵². RPL can be attributed to clinically identifiable causes in only 50% of cases, and identified causes include embryo aneuploidy or uterine anatomic abnormalities^{253,254}. Dysregulated immune function remains one of the most widely hypothesized, yet least understood, mechanisms contributing to RPL. Women with idiopathic RPL display elevated serum levels of cytotoxic cytokines, such as IFN γ , and globally upregulated endometrial immune response signaling²⁵⁵⁻²⁵⁹. During embryo implantation, endometrial stromal cells coordinate specific immune recruitment and maintain the immune microenvironment through a unique step-wise cellular transformation as part of the decidualization process⁹. Initially, endometrial stromal cells convert from a structural fibroblast to a pro-inflammatory phenotype, and ultimately differentiate to a secretory anti-inflammatory decidual cell^{9,78}. However, endometrial stromal cells isolated from women with RPL fail to switch to an anti-inflammatory phenotype and are associated with reduced decidual marker gene expression and diminished discriminatory capability in determining low versus high-quality embryos^{17,78,260}.

Repeated embryo loss and endometrial repair are particularly relevant in the setting of RPL. The human endometrium has the unique property of regenerating itself

with scar-less wound healing following menstruation and during the postpartum period¹²⁷. Menstruation and subsequent endometrial repair is hypothesized to precondition the uterus for future pregnancy¹³⁰. However, the mechanisms regulating endometrial repair, both following menstruation and during the postpartum period, remain poorly understood. Further, the role of dysfunctional endometrial repair as it pertains to future fertility potential has not been well characterized.

The evolutionarily conserved Notch signaling pathway mediates key developmental and homeostatic functions, including organ self-renewal^{96,98} and immune development^{106,107}. In canonical Notch signaling, ligand binding to one of four Notch receptors initiates ADAM protease and gamma-secretase-mediated cleavage cascade of the receptor to its active form⁹⁹. Subsequently, the Notch intracellular domain translocates and binds to Recombination Signal Binding Protein-Jk (RBPJ), which then converts it from a basal transcriptional repressor to an activator of downstream target genes, such as the 'Hairy enhancer of split' (Hes) and Hes-related (Hey) transcription factor families^{102,103}. We have described the role of Notch signaling, specifically Notch1, during decidualization in both the mouse¹¹⁴ and women¹¹². Reduced endometrial Notch signaling occurs in endometriosis and contributes to disease-related decidualization failure¹⁹. Ablation of *Rbpj* in the mouse uterus results in subfertility of the first pregnancy in part due to abnormal coordination of embryo-uterine interaction and decidual remodeling¹²⁴.

While initial studies performed in the uterine-specific *Rbpj* knockout mouse described subfertility, we identified dysfunctional postpartum endometrial repair following pregnancy, which contributes to developed infertility in these mice. Therefore,

the objective of our study was to determine the mechanisms contributing to dysfunctional endometrial repair and its impact on future fertility. Based on our findings, dysregulation of endometrial parenchymal regeneration through altered cell lineage determination contributes to delayed postpartum repair, and developed infertility results from enhanced immune signaling including IFN γ and Complement, features described in RPL patients²⁵⁵⁻²⁵⁹. We identified reduced expression of RBPJ in women with RPL and correlated our findings in the *Rbpj* c-KO mouse. Altogether, our work identifies dysfunctional endometrial repair as a previously undescribed contributor to infertility and presents Notch signaling as a novel pathway dysregulated in the setting of RPL.

RESULTS

Uterine ablation of *Rbpj* in mice results in developed infertility following pregnancy and decidualization failure

We generated uterine-specific *Rbpj* conditional knockout mice (*Pgr^{cre/+}Rbpj^{ff/ff}*; *Rbpj* c-KO) and confirmed uterine expression of *Rbpj* was successfully suppressed (**Fig S2-1A-C**). *Rbpj* c-KO and control (*Rbpj^{ff/ff}*) mice were bred with fertile, control males for six months and monitored for litters and corresponding litter sizes. Consistent with previous work¹²⁴, *Rbpj* c-KO mice are subfertile with significantly reduced litter sizes (**Fig S2-1D**). However, closer scrutiny of the fertility test results revealed declining fertility in *Rbpj* c-KO mice with infertility after one or two litters (**Fig 2-1A**). To determine ovarian versus uterine mechanisms contributing to the developed infertility in *Rbpj* c-KO mice, bilateral salpingo-oophorectomies were performed in infertile *Rbpj* c-KO and control mice at the end of the 6-month fertility test on 0.5 days post conception.

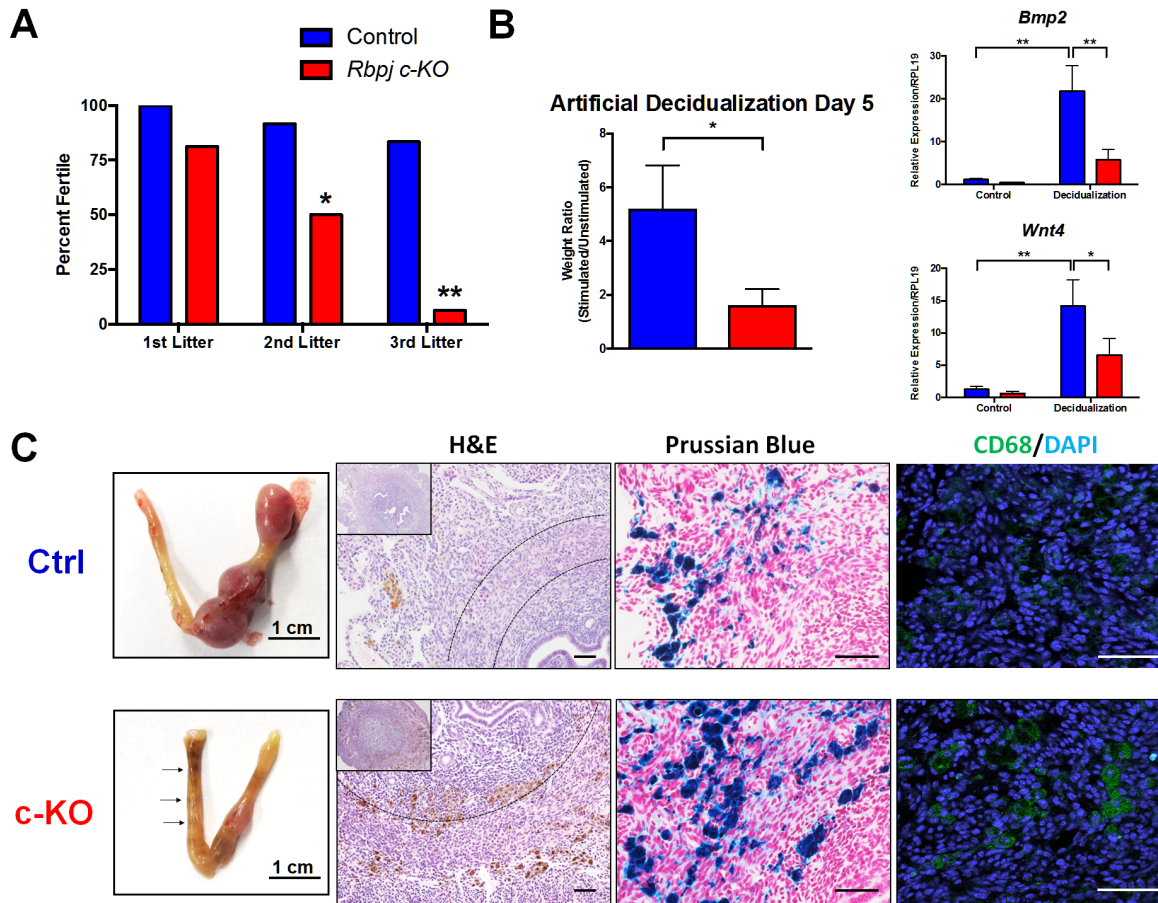
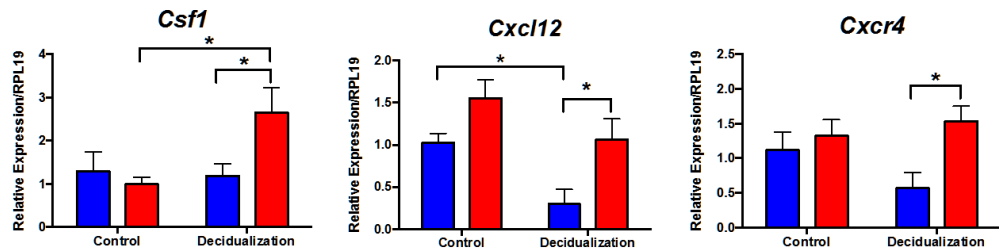
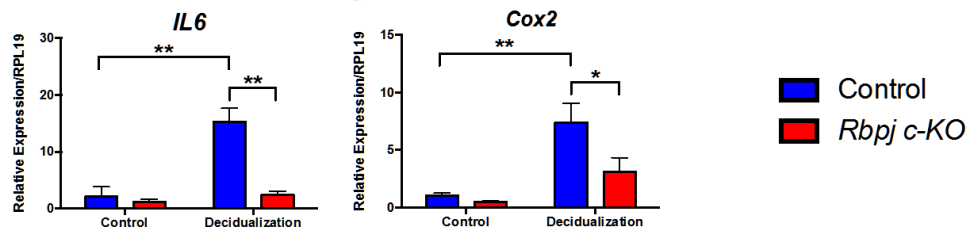


Figure 2-1. Loss of *Rbpj* results in developed infertility with evidence of failed postpartum repair associated with reduced decidualization. Female control and *Rbpj* c-KO mice (n=5-6/group) were set up in mating pairs with control fertile males for a six month breeding test. **(A)** Declining fertility was present in *Rbpj* c-KO mice over the course of the fertility test, with significantly fewer mice having more than one or two litters before becoming infertile for the remainder of the study. After the breeding test completed, mice were set up in mating pairs to induce pregnancy followed by salpingo-oophorectomies. Following 2 weeks of rest, mice were hormonally primed and decidualization was mechanically induced in the left uterine horn with sacrifice 5 days later. **(B)** *Rbpj* c-KO mice displayed reduced response to artificial decidualization (AD) based on uterine stimulated to unstimulated wet weight and down regulation of decidual markers, *Bmp2* and *Wnt4*, by RT-qPCR compared to control mice. **(C)** *Rbpj* c-KO mouse uteri exhibited distinct, evenly spaced brown uterine bands (arrows), which showed accumulations of large brown cells with dark pigmented granules upon H&E staining. These cells were largely located at the interface of the endometrium-myometrium and near the interface of the two myometrial layers (circular myometrium indicated by dashed lines). Identification of the brown cells as nodule cells were performed through Prussian Blue staining, which stains hemosiderin blue and localizes to nodule cells, and macrophage marker CD68. Data represented as Mean \pm SEM. **p<0.01, *p<0.05. Scale Bar = 0.5 cm.

A Immune Chemoattractants:



B Anti-Inflammatory Markers:



C Estrogen Receptor Signaling:

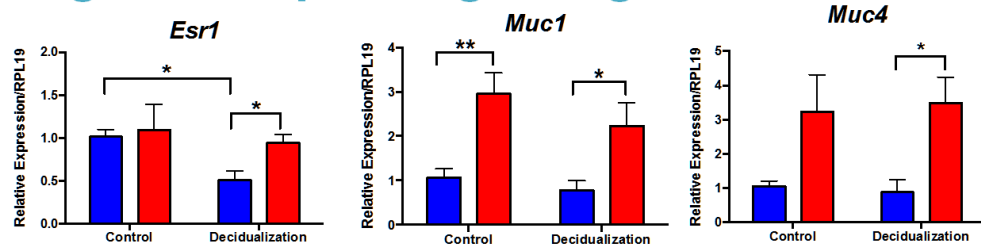


Figure 2-2. Infertility and impaired decidualization with loss of *Rbpj* is associated with enhanced immune recruitment and estrogen signaling. After the 6-month fertility test, ovariectomized female control and *Rbpj* c-KO mice (n=5-6/group) were hormonally primed and decidualization was mechanically induced in the left uterine horn with sacrifice 5 days later. **(A)** Associated with impaired decidualization and infertility, *Rbpj* c-KO mouse decidual horns displayed elevated mRNA levels of macrophage (*Csf1*) and lymphocyte chemoattractant/receptor (*Cxcl12/Cxcr4*) on AD5. **(B)** Additionally, reduced expression of described anti-inflammatory mediators *Il6* and *Cox2* were evident in *Rbpj* c-KO decidual horns. **(C)** Lastly, increased Estrogen receptor alpha (*Esr1*) mRNA levels were present in the decidual horn of *Rbpj* c-KO mice, along with target genes *Muc1* and *Muc4*. Data represented as Mean \pm SEM. **p<0.01, *p<0.05.

Oviduct flushes revealed no difference in the number or morphology of zygotes present suggesting normal ovarian function. Subsequently, these mice were allowed to rest for two weeks after ovariectomy, at which point, hormonal supplementation followed by mechanical induction of *in vivo* artificial decidualization (AD)¹¹⁴ was performed. Similar to their nulliparous counterparts, the infertile *Rbpj* c-KO mice displayed significant decidualization failure associated with reduced expression of decidual marker genes *Bmp2* and *Wnt4* (**Fig 2-1B**). More strikingly, distinct, brown uterine bands were present in the *Rbpj* c-KO mice, which were evenly spaced similar to implantation sites during pregnancy and were absent in control mice (**Fig 2-1C**). Histological analysis of the bands revealed the presence of large, brown-pigmented cells, which were positive for hemosiderin by Prussian Blue staining and stained positive for macrophage marker CD68 (**Fig 2-1C**). These hemosiderin-laden macrophages represent nodule cells, a component of placental detachment repair sites from a previous pregnancy, termed postpartum nodules. Postpartum nodules are distinct anatomical structures which represent resolution of placental detachment sites in rodents¹⁴⁵. They consist of extracellular matrix and immune infiltrate isolated within the longitudinal and circular myometrium¹⁴⁵. Ultimately, the nodule regresses as the extracellular matrix degrades and the vasculature entering through the mesometrium reforms, only leaving remnants of few nodule cells¹⁴⁵.

Typically, small collections of nodule cells persist in the rodent uterine mesometrial attachment site for up to 3 months following parturition, which were present in the control mice; however, in the *Rbpj* c-KO mice, nodule cells were ubiquitously found throughout the uterus, largely near the longitudinal and transverse myometrial

layers and at the endometrial-myometrial interface (**Fig 2-1C**). Further, implantation of embryos in subsequent pregnancies will not occur in the vicinity of nodule cells, which are also associated with a reduced decidualization response¹⁷¹. Therefore, the presence of nodule cell accumulations throughout the *Rbpj* c-KO mouse uterus likely contributes to the developed infertility in these mice. Further, enhanced decidual horn mRNA expression of immune chemoattractants *Csf1* and *Cxcl12* with its receptor *Cxcr4* was associated with impaired decidualization (**Fig 2-2A**) and may represent an exaggerated inflammatory response during the period of uterine receptivity and prevent pregnancy. Additionally, mRNA expression levels of *IL-6* and *Cox2* were significantly decreased in the decidual horn of *Rbpj* c-KO mice (**Fig 2-2B**), which are *Rbpj* transcriptional targets that contribute to immunosuppression by bone marrow stromal cells²³⁵. Estrogen receptor α (*Esr1*) expression was increased in the *Rbpj* c-KO mouse decidual horn along with transcriptional targets *Muc1* and *Muc4* (**Fig 2-2C**), which are associated with impaired uterine receptivity during implantation in mice²⁷⁰. Altogether, *Rbpj* c-KO mice developed infertility with accumulations of nodule cells, a component of postpartum repair. Therefore, we hypothesized that dysfunctional postpartum repair contributes to failed resolution of nodule cells and developed infertility. Additionally, impaired decidualization in these mice was associated with elevated expression of chemoattractants and *Esr1* signaling likely contributing to impaired uterine receptivity and implantation failure.

***Rbpj* mediates uterine parenchymal regeneration during postpartum repair through controlling Luminal Epithelium (LE) over-proliferation and promoting apoptosis of epithelial-mesenchymal double-positive cells**

To identify the role of endometrial RBPJ after parturition, the postpartum repair process was characterized in *Rbpj* c-KO and control mouse uterine tissues at key time points: Postpartum Day (PPD) 1, 3, 5 and 10 (**Fig 2-3**). Based on previous work, the endometrial luminal epithelium (LE) reforms along the mesometrial pole where the placenta detaches by PPD 5, and the postpartum nodule is fully formed by PPD 8¹⁴⁵. Specific endpoints for analysis included: 1) tissue morphological integrity 2) re-epithelialization of the LE, and 3) myometrial regeneration along the circumference of the uterus forming a distinct postpartum nodule. At PPD 1, bleeding at the site of placental detachment was present in both the control and *Rbpj* c-KO uteri (**Fig 2-3A,B**). However, there were clear differences between the *Rbpj* c-KO and control uteri. In the control mice, folds of endometrium including LE and stroma protruded into the uterine lumen, which did not occur in the *Rbpj* c-KO. Also, the LE in the control mice consisted of a monolayer of epithelial cells (**Fig 2-3a**), while there was extensive epithelial hyperplasia forming a “saw-tooth” pattern in the *Rbpj* c-KO mice (**Fig 2-3b**). At PPD 3, active bleeding into the uterine lumen was controlled with the initiation of re-epithelialization in the control mice, where remaining bleeding was walled off by surrounding cells, presumably phagocytes (**Fig 2-3C**). In the *Rbpj* c-KO mice, endometrial bleeding persisted along with evidence of a “saw-tooth” LE (**Fig 2-3D**). As expected, re-epithelialization was complete in the control mice at PPD 5 (**Fig 2-3E**);

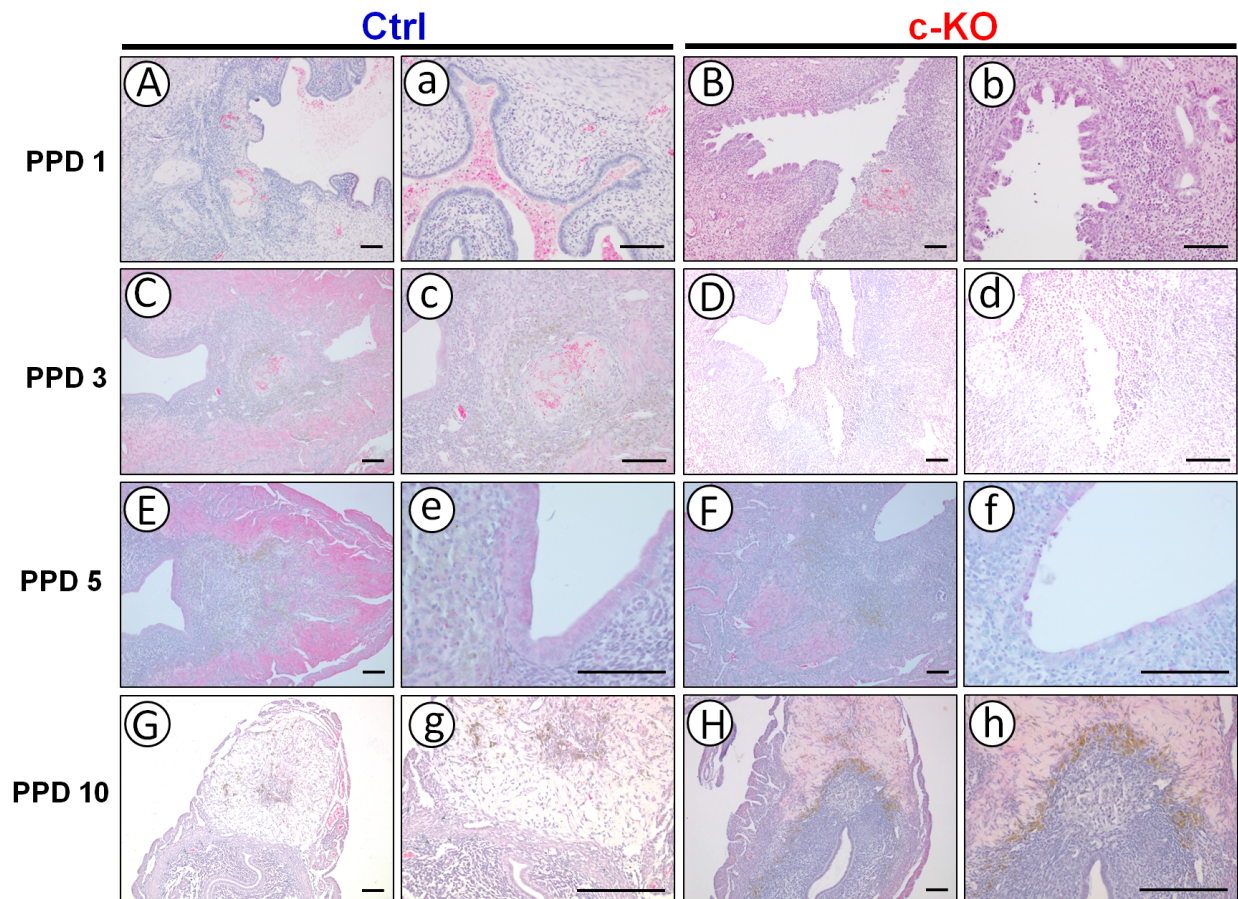


Figure 2-3. Loss of *Rbpj* results in dysfunctional postpartum uterine repair. Female *Rbpj* c-KO and control mice were caged with fertile males to induce pregnancy and sacrificed following parturition during significant time points during the repair process: PPD 1, 3, 5, and 10 (n=3-6/group/time point). H&E staining was performed on placental detachment sites during the various time points collected during the course of postpartum repair. **(A,B)** On PPD1, bleeding from the mesometrial placental detachment site was present in both the control and *Rbpj* c-KO uteri. However, endometrial luminal epithelial (LE) morphology was different between groups, where the control mouse LE appeared as a single layer of cells while a hyperplastic **(a)**, sawtooth pattern was evident in the *Rbpj* c-KO mouse LE **(b)**. **(C)** On PPD 3, mesometrial bleeding was contained in control mice, **(D)** while bleeding into the uterine lumen continued in *Rbpj* c-KO mice along with persistence of a “saw-tooth” LE. **(E)** Re-epithelialization was complete in the control mice at PPD 5; **(F)** however, the *Rbpj* c-KO mouse LE remained incomplete. **(G)** On PPD 10, the control mouse myometrium reformed along the mesometrial uterine aspect, isolating a defined postpartum nodule. **(H)** Alternatively, the *Rbpj* c-KO mouse myometrium was incomplete with extensive nodule cells present at the interface of the myometrium and endometrium, suggesting dysfunctional postpartum repair. Lower case letters denote high magnification of upper case image. Scale Bar = 100 μ m.

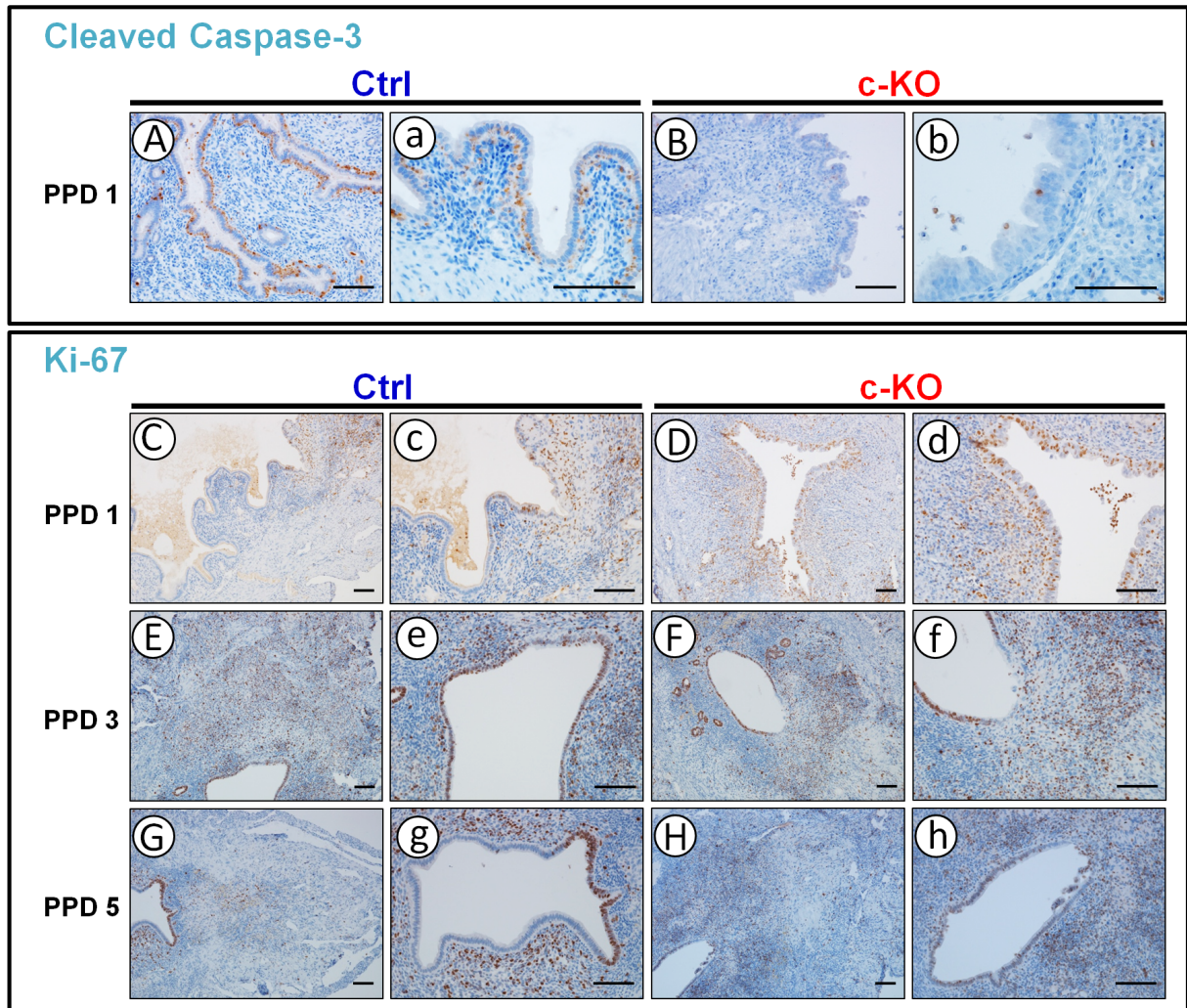


Figure 2-4. Dysfunctional postpartum uterine repair with loss of *Rbpj* is associated with an altered proliferation and apoptotic profile. In order to identify potential contributors to postpartum repair deficits in *Rbpj* c-KO mice, immunostaining for apoptotic (Cleaved Caspase-3; CC-3; Top Panel) and proliferation (Ki-67; Bottom Panel) markers were performed during postpartum uterine repair. **(A)** At PPD 1, CC-3 staining was present along the entire basal LE of control mice, **(B)** which was essentially absent in *Rbpj* c-KO mice. **(C)** In control mice, Ki-67 staining was low in the LE and high in the mesometrial stroma on PPD 1 and then increases within the mesometrial LE to regenerate in the region of placental detachment on **(E)** PPD 3 and **(G)** 5. **(D)** Ki-67 staining revealed enhanced proliferation in *Rbpj* c-KO mouse LE on PPD 1, along the circumference of the LE except for the mesometrial region of the LE and persists through PPD 5. Lower case letters denote high magnification of upper case image. Scale Bar = 100 μ m.

however, the *Rbpj* c-KO mouse LE remained incomplete (**Fig 2-3F**). At PPD 10, the control mouse myometrium reformed along the full circumference of the uterus forming the postpartum nodule (**Fig 2-3G**). On the other hand, the *Rbpj* c-KO mouse myometrium was incomplete with extensive nodule cells present at the interface of the myometrium and endometrium (**Fig 2-3H**), which closely resembled control mice at PPD 5. Altogether, the *Rbpj* c-KO mice display delayed postpartum repair associated with abnormal epithelial regeneration.

In order to determine potential contributors to delayed re-epithelialization, immunostaining was performed in the mouse uteri at PPD 1, 3 and 5 for apoptotic and proliferative markers, Cleaved Caspase-3 (CC-3) and Ki-67, respectively (**Fig 2-4**). *Rbpj* c-KO mice displayed an altered apoptotic and proliferation profile. CC-3 staining was intense within the cells of the basal epithelial region of control mouse uteri on PPD 1 (**Fig 2-4a**), which was absent in the *Rbpj* c-KO mice (**Fig 2-4b**). On PPD 1, epithelial and stromal proliferation was limited to the mesometrial placental detachment region in control mice (**Fig 2-4c**), but in *Rbpj* c-KO mice, both stromal and epithelial proliferation was drastically increased throughout the uterus (**Fig 2-4d**), likely contributing to the “sawtooth” epithelial overgrowth. Ki-67 staining was strongly positive in the LE, glandular epithelium (GE), and mesometrial stroma in both groups on PPD 3 (**Fig 2-4E,F**). Corresponding to the completion of re-epithelialization on PPD 5, epithelial proliferation was confined to the mesometrial LE in control mice (**Fig 2-4g**). Surprisingly, in the *Rbpj* c-KO mouse, endometrial LE cells continued to proliferate except in the mesometrial region on PPD 3 and 5 (**Fig 2-4f,h**), which likely contributes to the delay in re-epithelialization and postpartum repair. Characterization of epithelial (pan-

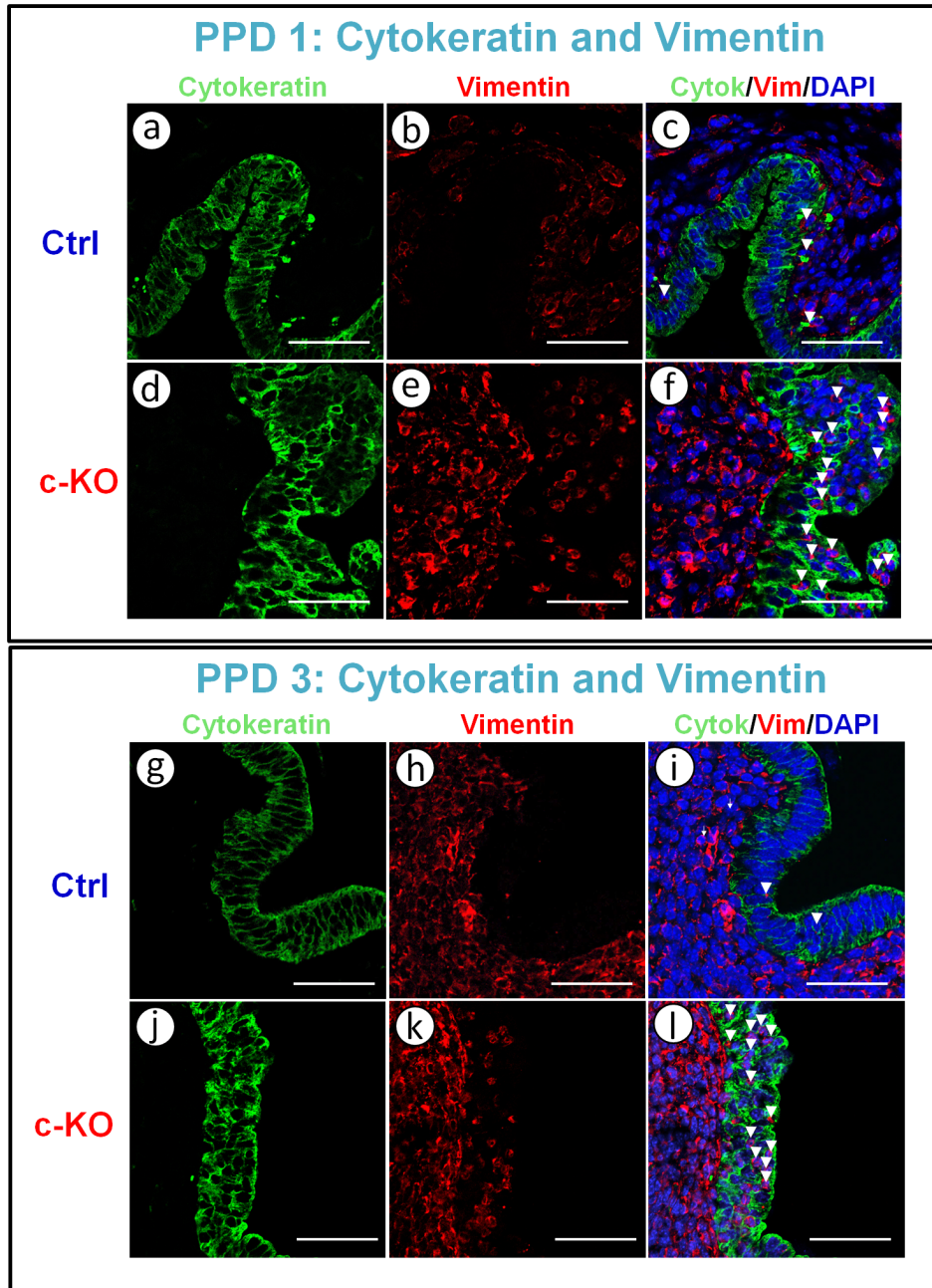


Figure 2-5. Loss of *Rbpj* is associated with accumulations of cytokeratin-vimentin double positive cells during postpartum uterine repair. To identify specific cell types during postpartum repair, dual staining immunofluorescence for epithelial (Cytokeratin) and stromal (Vimentin) cell markers was performed on PPD 1 (Top Panel) and 3 (Bottom Panel). (a-c) On PPD 1, double positive cells were present in the control mouse basal LE on PPD 1. (d-e) The “sawtooth” pattern LE in *Rbpj* c-KO mice on PPD 1 was associated with accumulations of cells double positive for cytokeratin and vimentin throughout the epithelium. (g-i) On PPD 3, many double positive cells persisted in the epithelium of *Rbpj* c-KO mice uteri, (j-l) while these cells were scarce in the control mice at this time point. White arrow heads indicate double positive cells. Scale Bar = 50 μ m.

PPD 1: Cleaved Caspase-3 in Cytokeratin/Vimentin Dual-Positive Cells

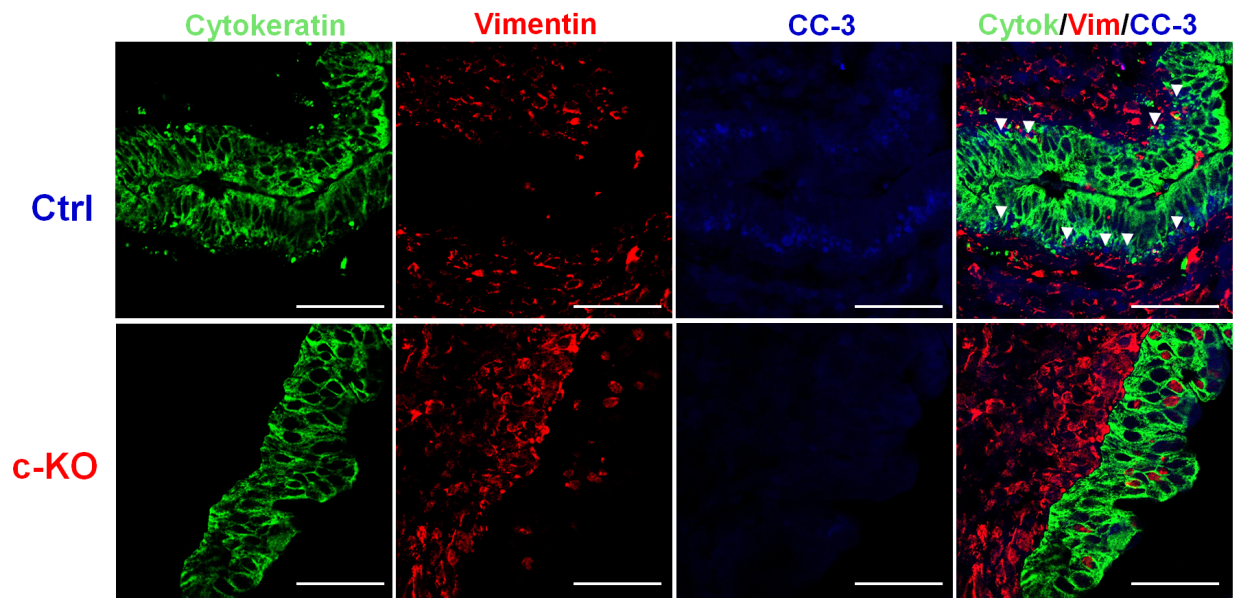


Figure 2-6. *Rbpj* regulates epithelial regeneration through inducing apoptosis of cytokeratin-vimentin double positive cells during postpartum uterine repair. We hypothesized that apoptosis observed in control mice on PPD 1 is necessary to prevent over-proliferation of dual positive epithelial-mesenchymal cells. Therefore, we performed triple immunofluorescent staining with cytokeratin, vimentin, and Cleaved Caspase-3 (CC-3). Consistent with the previous PPD 1 CC-3 immunostaining, apoptosis was essentially absent in the *Rbpj* c-KO mouse endometrium. Many apoptotic cells were present in the control mouse LE (white arrows), and among these most cells were triple positive for all three markers, suggesting that apoptosis of the epithelial-mesenchymal dual-positive cells may represent a physiologic mechanism to prevent their over-proliferation during repair. Scale Bar = 50 μ m.

cytokeratin) and mesenchymal (vimentin) markers was performed to identify cell-type specific differences during endometrial regeneration in the postpartum period between *Rbpj* c-KO and control mice (**Fig 2-5**). Dual-staining immunofluorescence on PPD 1 revealed positive cytokeratin staining within the luminal epithelium with few cytokeratin staining cells also positive for vimentin intercalated within the basal epithelium (**Fig 2-5a-c**). Interestingly, the “saw-tooth” over-proliferative luminal cells in the *Rbpj* c-KO mice stained positive for epithelial marker cytokeratin, but there were a significantly larger percentage of these cells double positive for cytokeratin and vimentin, particularly localized within the protruding areas (**Fig 2-5d-f; Figure S2-2A**). By PPD 3, few dual cytokeratin-vimentin staining cells were present within the LE of control mice, but the augmented presence of these cells persisted within the LE of *Rbpj* c-KO mice (**Fig 2-5g-i; Figure S2-2A**). Previous work has described a mesenchymal to epithelial transition (MET) during endometrial repair, where mesenchymal progenitors contribute to re-epithelialization, and these cells are positive for both epithelial and mesenchymal markers¹⁷⁸. Since the apoptotic marker CC-3 was enhanced in an unknown cell population located within the basal endometrial LE of control mice on PPD 1, we hypothesized that these cells, in part, represented mesenchymal-derived cells responsible for replenishing the LE during repair and that their programmed death was necessary for reducing over-proliferation following injury. Triple staining with CC-3 revealed that cells positive for both vimentin and cytokeratin undergo apoptosis in control mice on PPD 1 along with normal epithelial cells (**Fig 2-6**). Consistent with the immunohistochemistry results, CC-3 expression was absent in the *Rbpj* c-KO mouse uterus on PPD1 and did not overlap with cells dually staining for cytokeratin and

vimentin. This evidence suggests that *Rbpj* regulates the endometrial regeneration process following placental detachment through suppression of epithelial over-proliferation during parenchymal regeneration by inducing apoptosis of dual-staining epithelial-mesenchymal derived cells. Further, these findings indicate a potential role for *Rbpj* in regulating MET during postpartum uterine repair.

***Rbpj* mediates postpartum uterine repair through suppression of immune activation and recruitment**

In order to identify early mechanisms responsible for the delayed postpartum repair in *Rbpj* c-KO mice, RNA-seq was performed on PPD 3 nodules collected from control and *Rbpj* c-KO mice (n=3 pooled nodules/animal/group). 2152 genes were differentially expressed between control and *Rbpj* c-KO mouse nodules on PPD 3. Process Network enrichment of differentially expressed genes was performed on the entire data set of differentially expressed genes between groups using GeneGo (Metacore) GO Processes to identify potential mechanisms responsible for dysfunctional repair in *Rbpj* c-KO mice. The top 50 processes were categorized based on higher order classification provided by GeneGo, and the most significant proportion of the processes affected by *Rbpj* ablation on PPD 3 involved inflammation and immune response (**Fig 2-7A**). Other affected pathways included cell adhesion, apoptosis, proliferation, and development. The differentially expressed genes were divided into 7 clusters to generate a heat map based on Euclidean distance and complete linkage, followed by Process Network enrichment (**Fig 2-7B**). Up regulated gene clusters in the

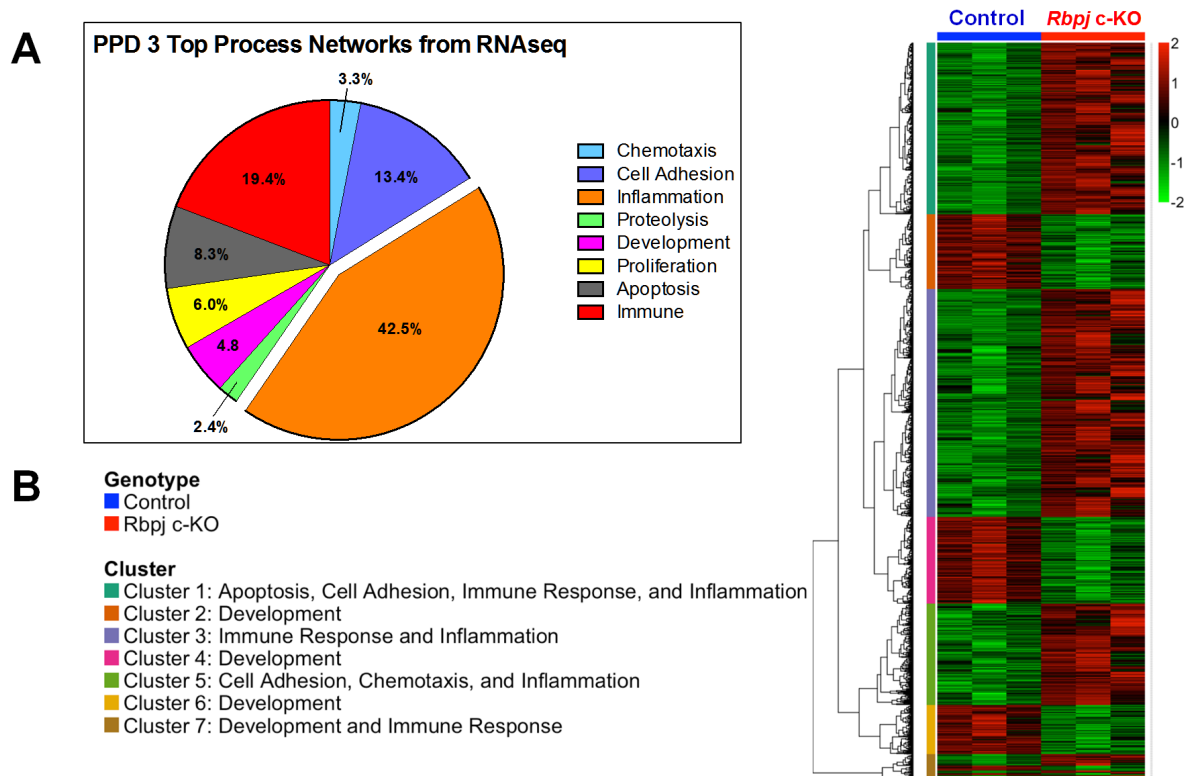


Figure 2-7. *Rbpj* is essential for global uterine immune suppression and developmental pathways on PPD3. RNA-sequencing was performed on PPD 3 nodules (n=3 pooled nodules/animal/group). 2152 genes were differentially expressed between groups. **(A)** The largest proportion of genes differentially expressed were involved in Immune Response or Inflammation. **(B)** Up regulated gene clusters in the *Rbpj* c-KO mice were represented by pathways important for immune signaling, while down regulated gene clusters were involved in development.

Rbpj c-KO mice were largely represented by pathways important for immune response and inflammation while down regulated clusters were responsible for development. Altogether, the RNA-seq findings indicated global up regulation of inflammatory degradation and death domain receptor/caspase-mediated apoptosis. Down regulated pathways in *Rbpj* c-KO mice included actin filaments and Wnt/ β -catenin/Notch Signaling (**Table S2-2**). Since alpha-smooth muscle actin (*Acta2*) is a direct transcriptional target signaling and down regulated pathways for development contribute to dysfunctional postpartum repair in *Rbpj* c-KO mice on PPD 3.

In order to further identify specific pathways altered within the broad categories described, differentially expressed genes from the RNA-seq results were divided into up regulated (1512) and down regulated (640) genes followed by Process Network enrichment. The majority of pathways contributing to dysfunctional postpartum repair in *Rbpj* c-KO mice included up-regulation of both innate and adaptive immune signaling pathways (**Table S2-1**). Select examples of pathways associated with the exaggerated immune response in *Rbpj* c-KO mice included the complement system, neutrophil activation, lymphocyte proliferation, and interferon signaling. In addition to inflammatory signaling, RNA-seq identified other important pathways contributing to dysfunctional uterine repair in *Rbpj* c-KO mice. Up-regulated pathways included connective tissue of Notch/*Rbpj*, failed actin pathway signaling re-confirms reduced Notch pathway signaling and, further, suggests an additional mechanisms contributing to dysfunctional repair²⁷¹. Between nine to ten genes were randomly selected from each pathway described above to validate by RT-qPCR (**Fig S2-3**).

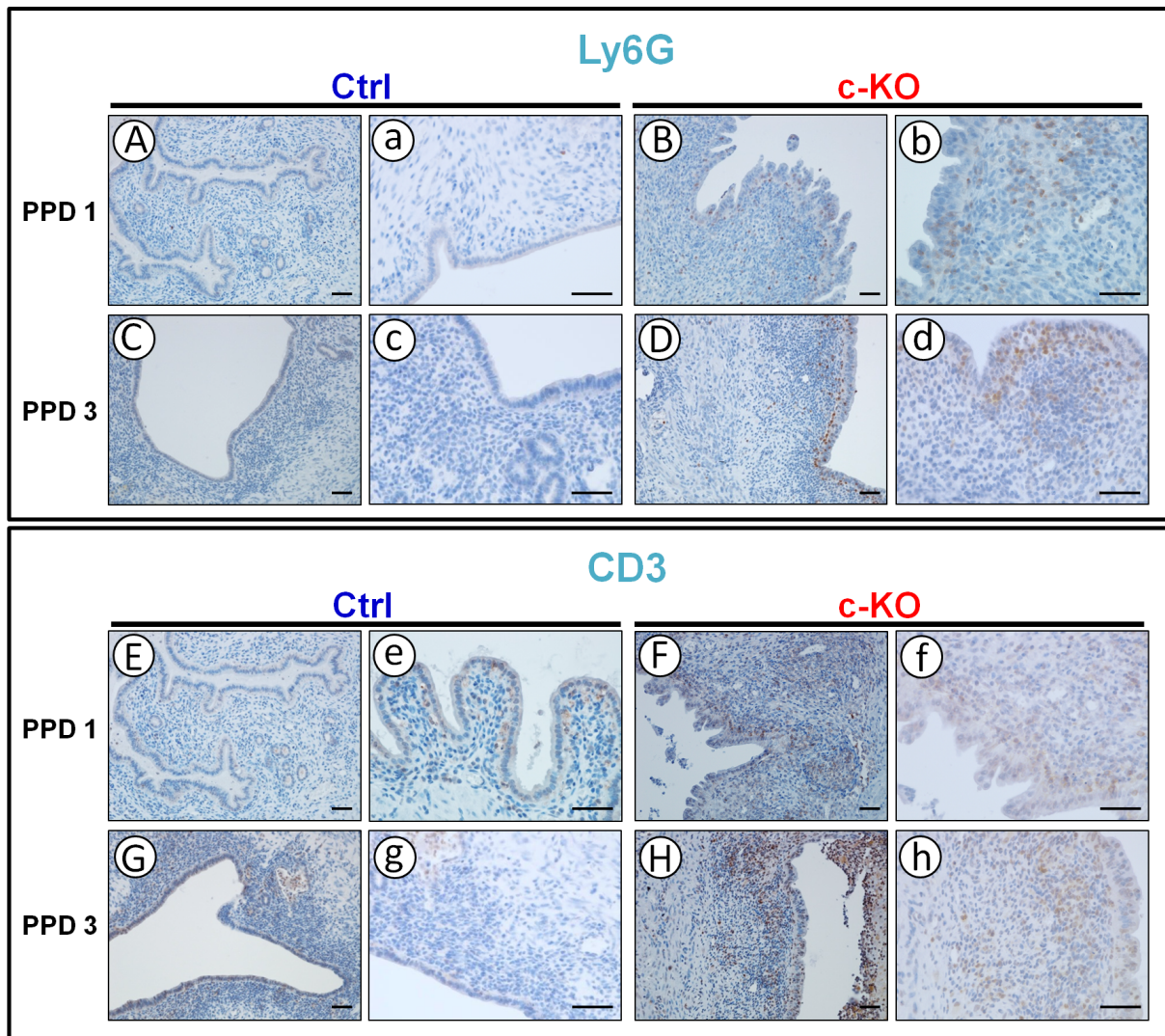


Figure 2-8. *Rbpj* suppresses neutrophil and lymphocyte recruitment during postpartum uterine repair. Pathway enrichment of differentially expressed genes from PPD 3 RNAseq showed upregulation of “Neutrophil Activation” and “Lymphocyte Proliferation”. Therefore, immunostaining for neutrophil (Ly6G) and T cell (CD3) markers was performed on PPD 1 and 3. **(A-D)** Neutrophils were scarce during both time points in the control mice but were highly abundant in the *Rbpj* c-KO mice at both PPD1 and 3, which were localized particularly in the sub-epithelial stroma. **(E-H)** Few CD3⁺ T cells were present in the PPD1 uterus of control mice, and were only present within the proximity of the mesometrial detachment site on PPD3. On the other hand, T cells were ubiquitously found throughout the endometrium in *Rbpj* c-KO mice on PPD 1 and 3. Lower case letters denote high magnification of upper case image. Scale Bar = 50 μ m.

To determine the impact of the dysregulated inflammatory pathways on immune cell populations, we performed immunostaining for T lymphocyte (CD3) and Neutrophil (Ly6G) markers on PPD 1 and 3 (**Fig 2-8**). Consistent with the RNA-seq findings, T cells and Neutrophils were present in greater numbers in the *Rbpj* c-KO mouse endometrium at both time points (**Fig S2-2B**). Neutrophils were essentially absent in the PPD 3 control mouse uterus (**Fig 2-8C**), consistent with the physiologic shift from acute neutrophil-driven to chronic macrophage dominant inflammation in response to injury¹³⁹. However, accumulations of neutrophils were found throughout the endometrium of *Rbpj* c-KO mice, particularly within the mesometrial and sub-epithelial regions (**Fig 2-8D**). These findings indicate an exaggerated immune response with delayed shift from acute to chronic inflammation contributes to dysfunctional postpartum repair in *Rbpj* c-KO mice.

Endometrial epithelial and stromal *Rbpj* regulates the immune microenvironment during postpartum repair through suppression of complement and interferon signaling

The role of Notch signaling in mediating immune cell function has been described extensively, but in our model, Pgr driven-cre recombinase selectively ablates *Rbpj* in the uterine parenchyma rather than immune cells; therefore, the effect of enhanced immune signaling in *Rbpj* c-KO mice was likely driven by the endometrium itself. Therefore, we hypothesized that endometrial expression of chemokines in response to injury associated with placental detachment contributed to immune recruitment and activation. Further, tissue-mediated immune suppression during injury prevents additional insults

from the immune response itself and has been described in other systems in the setting of *Rbpj* loss²³⁵. Based on the RNA-Seq results, complement signaling, which initiates the innate immune response, was increased in PPD 3 *Rbpj* c-KO mouse nodules. *Esr1* increased in the decidualized horn of infertile *Rbpj* c-KO mice and it regulates expression of complement C3²⁷². Since C3 was differentially expressed according to the RNA-Seq, we sought to determine its protein localization and expression. Immunofluorescence confirmed significantly increased C3 expression in *Rbpj* c-KO mouse uteri on PPD3 (**Fig 2-9; Figure S2-2**) and co-localization with cytokeratin-positive epithelial cells.

The cytokine and chemokine milieu at the site of injury skews or polarizes macrophages towards an M1 or M2 functional phenotype, which will dictate their actions¹⁵⁹. M1 macrophages are pro-inflammatory and produce cytotoxic metabolites and cytokines, including Tumor Necrosis Factor- α (TNF α), which are ideal for preventing attack by intracellular pathogens but impedes wound healing^{159,166}. On the other hand, M2 macrophages are anti-inflammatory and facilitate wound healing by expressing genes including IL-10, Transforming Growth Factor β 1 (TGF β 1), and Mannose Receptor 1 (MRC1)^{159,161}. M2 macrophage numbers predominate during postpartum repair in the uterus, and their numbers peak at PPD 3 and gradually decrease over time¹⁶⁵. Developed infertility in *Rbpj* c-KO mice was associated with increased numbers of nodule cells (macrophages) in part due to elevated levels of *Csf1*. Based on the RNA-Seq results, macrophage signaling was enhanced in *Rbpj* c-KO mice, and we confirmed the presence and recruitment of macrophages was increased by RT-qPCR for macrophage marker *Emr1* (*F4/80*) and chemoattractant *Csf1* (**Fig 2-**

PPD 3: Complement C3

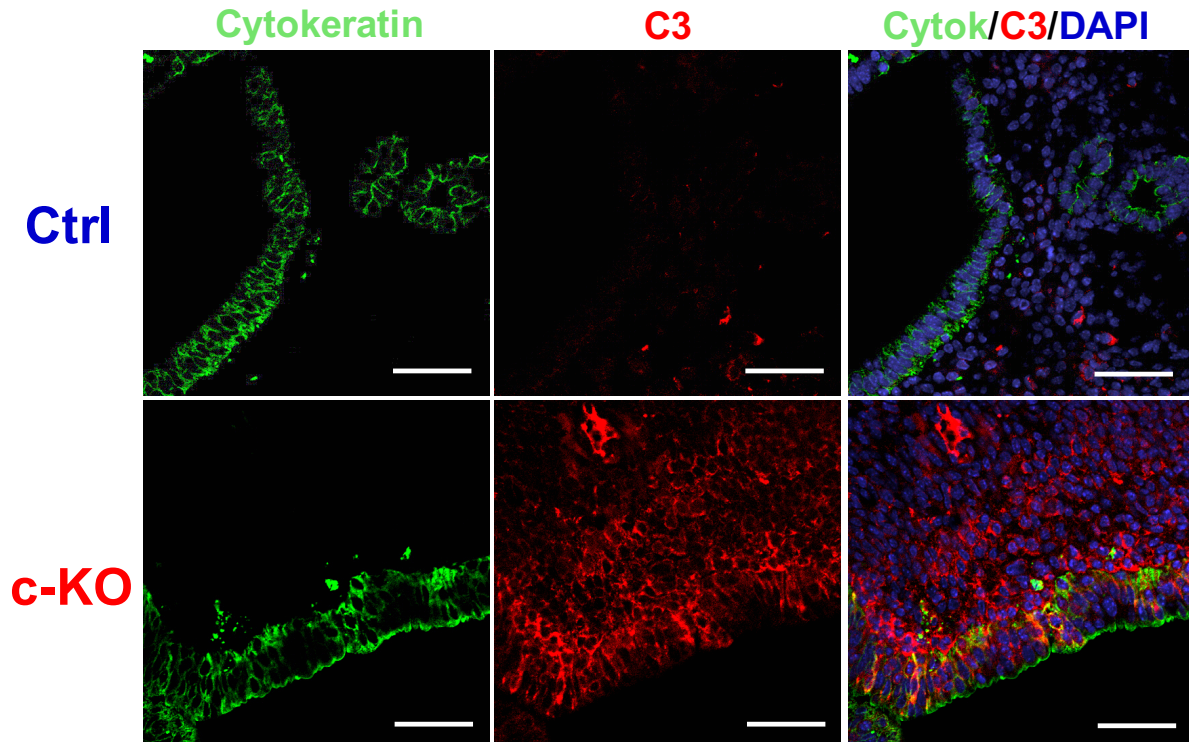


Figure 2-9. *Rbpj* suppresses endometrial Complement C3 during postpartum repair. C3 mRNA levels were elevated in *Rbpj* c-KO mice at PPD 3; therefore, we sought to determine C3 protein expression and localization using immunofluorescence for C3 and cytokeratin. C3 was significantly elevated in both the LE and stroma in *Rbpj* c-KO mice. Scale Bar = 50 μ m.

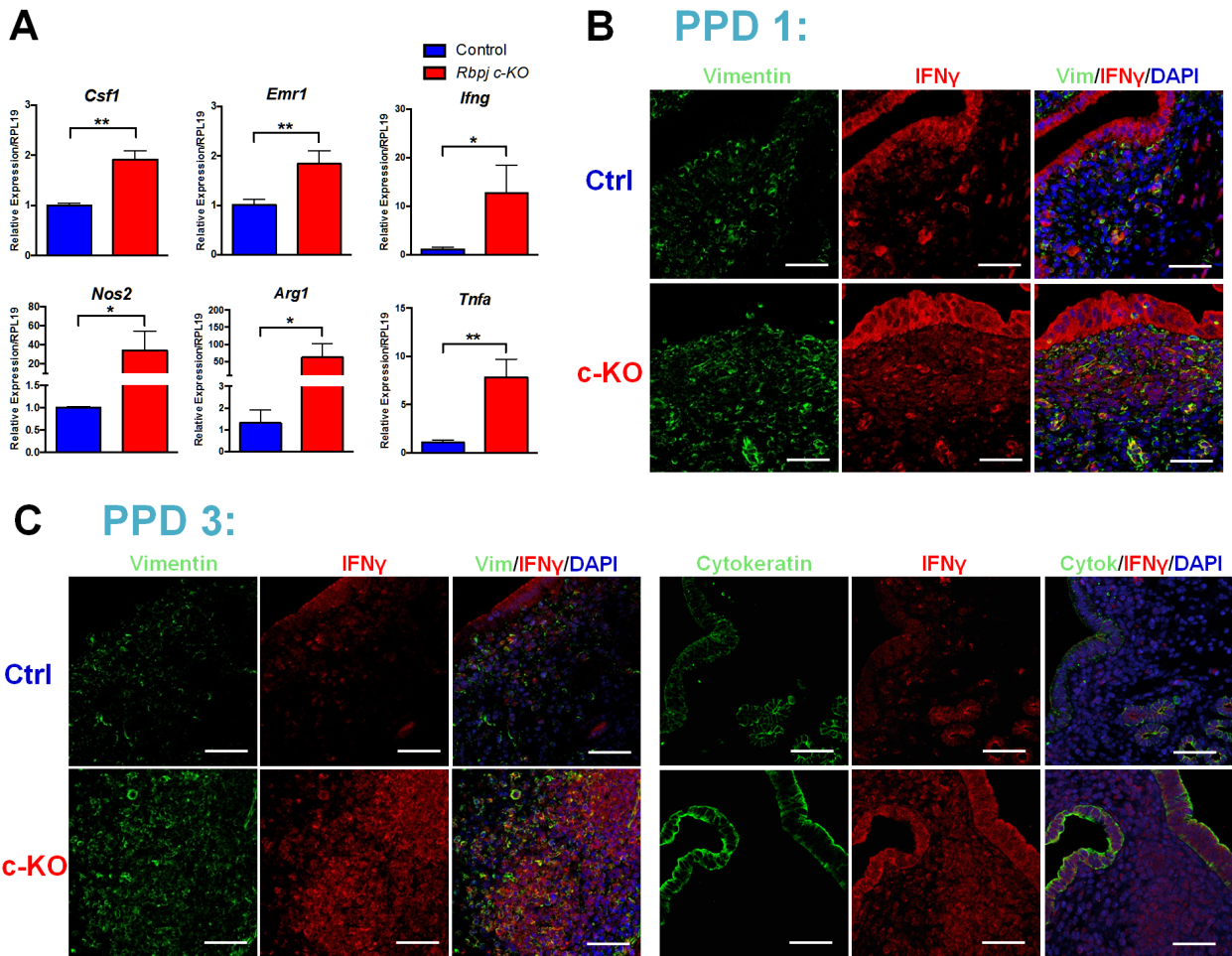


Figure 2-10. Rbpj suppresses endometrial M1 macrophage induction through IFN γ during postpartum repair. (A) mRNA levels of macrophage chemoattractant (*Csf1*) and marker (*Emr1*) were elevated in *Rbpj* c-KO mice on PPD 3. Additionally, IFN γ mRNA levels were elevated with upregulated M1 marker *Nos2* and secreted factor *Tnfa* in *Rbpj* c-KO mice. Additionally, *Arg1*, an M2 marker, was elevated with *Rbpj* loss. **(B)** Expression and localization of IFN γ were determined at PPD1 and PPD3 by immunofluorescence. On PPD1, stromal IFN γ levels were elevated in *Rbpj* c-KO mice and co-localized with vimentin. Interestingly, IFN γ levels were high in the LE of both groups on PPD1 and not significantly different. **(C)** On PPD3, IFN γ levels are lower in control mice and significantly increased in both stromal and epithelial cells of *Rbpj* c-KO mice with strong co-localization. N = 3-5/group. Data represented as Mean \pm SEM. ** $p < 0.01$, * $p < 0.05$. Scale Bar = 50 μ m.

10A). Additionally, interferon signaling and both M1 (*Nos2*, *Tnfa*) and M2 (*Arg1*) macrophage marker expression were associated with dysfunctional postpartum repair based on the RNA-seq, which we validated by RT-qPCR (**Fig 2-10A**). We hypothesized the endometrium represented the source for enhanced endometrial IFN γ expression in *Rbpj* c-KO mice, and increased IFN γ levels may contribute to the increased macrophage presence and numbers of M1 macrophages with the potential to impede postpartum repair. Dual immunofluorescence revealed significantly increased IFN γ expression in *Rbpj* c-KO mouse endometrial stromal cells on PPD 1 and 3 (**Fig 2-10B,C; Fig S2-2C**). Additionally, IFN γ expression was increased in the LE of both control and *Rbpj* c-KO mice on PPD1 but remained high in the endometrial LE on PPD3 in *Rbpj* c-KO mice with the potential for contributing to the enhanced expression of M1 macrophage marker *Nos2*. Additionally, since IFN γ remained elevated in the LE of the *Rbpj* c-KO mice, this may represent a potential response to continuous MET of endometrial mesenchymal progenitor cells, which persisted to PPD 3 in these mice. Altogether, endometrial *Rbpj* expression plays an immunosuppressive role during postpartum repair in regulating the innate immune response via complement and cytotoxic M1-macrophage polarization.

Failed postpartum uterine repair due to *Rbpj* loss causes secondary infertility

While *Rbpj* c-KO mice developed infertility after initial subfertility, we sought to prove that pregnancy with functional postpartum repair is indispensable for future pregnancy potential. First, to demonstrate that the banding pattern and nodule cell accumulations in the infertile *Rbpj* c-KO mice resulted from previous pregnancy, we

performed unilateral tubal ligation to prevent the left uterine horn from establishing a pregnancy upon coitum. After paired mating with two pregnancies, mice were sacrificed at two weeks postpartum and examined for the presence of uterine banding (**Fig 2-11A**). As expected, evidence of either prior pregnancy or existing postpartum nodules were absent in the left uterine horn of *Rbpj* c-KO and control mice. Also, in *Rbpj* c-KO mice, the nodules and brown banding pattern were clearly more extensive in the right uterine horn where pregnancies were established while small, organized mesometrial nodules were present in the control mice. Additionally, clear fluid-filled cystic structures were present in the *Rbpj* c-KO mouse uteri. These findings provided proof of concept for the surgical technique and, more importantly, that prior pregnancy contributes to the abnormal uterine morphology following pregnancy in *Rbpj* c-KO mice.

In order to prove that dysfunctional uterine repair contributed to developed infertility in *Rbpj* c-KO mice, we performed unilateral tubal ligation followed by paired mating of both mouse strains. Following one litter and two weeks of rest, bilateral embryo transfer of 7 blastocysts was performed on day 2.5 of pseudopregnancy with visualization of implantation sites two days later via tail injection of Chicago blue dye (**Fig 2-11B,C**). We hypothesized there would be no difference between implantation in the nulliparous versus multiparous horn of control mice in the setting of normal postpartum repair, and that *Rbpj* c-KO mice would display reduced implantation. There were no significant differences between the numbers of implantation sites present in either uterine horn of control mice (**Fig 2-11B**). Surprisingly, none of the *Rbpj* c-KO mice were pregnant in either uterine horn following embryo transfer. Histological analysis revealed the presence of morphologically normal implantation sites in both uterine horns

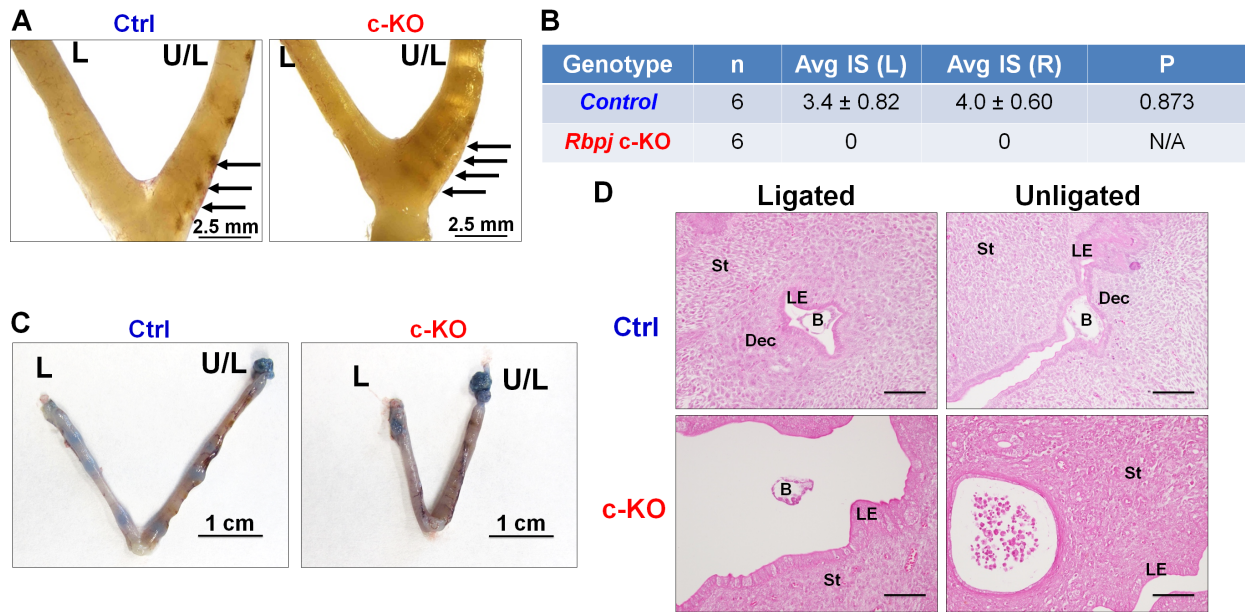


Figure 2-11. Dysfunctional postpartum repair with *Rbpj* loss impairs future embryo implantation. (A) Unilateral oviduct ligation spares the ligated horn from pregnancy. Additionally, the unligated horn in *Rbpj* c-KO mice displayed extensive brown uterine banding (arrows) while small mesometrial nodules (arrows) were identified in the control mice. (B) Unilateral ligation and paired mating for one litter was performed (N=6/group), followed by bilateral embryo transfer. (C) Chicago blue dye injection on 4.5 days post-plug with observation of implantation sites (IS). As expected, there was no significant difference between either uterine horn of control mouse IS numbers. Remarkably, none of the *Rbpj* c-KO mice were pregnant. (D) H&E staining revealed normal IS in both horns of control mice with LE closure present and decidualization in the underlying stromal cells. Floating embryos were present in the ligated uterine horn of *Rbpj* c-KO mice, without LE closure or a decidual response. Surprisingly, no embryos were identified within the unligated uterine horn of *Rbpj* c-KO mice, rather endometrial cysts and mild LE hyperplasia was present. Data represented as Mean ± SEM. Statistical comparisons were determined using Student's t-test. Scale bar = 100 μm; L = Ligated Horn, U/L = Unligated Horn, B = Blastocyst, Dec = Decidua, LE = Luminal Epithelium, St = Stroma.

of control mice with an initial decidual response in the underlying stromal cells surrounding the implanting embryo (**Fig 2-11D**). In the nulliparous horn of *Rbpj* c-KO mice, free floating embryos were present without evidence of closure of the luminal epithelium or stromal decidualization for implantation (**Fig 2-11D**). Surprisingly, no embryos were identified within the multiparous horn of the *Rbpj* c-KO mice. However, many cystic structures and mild hyperplasia of the epithelium were noted. These findings suggest that despite sparing one uterine horn of pregnancy, a global uterine defect from dysfunctional repair occurs, likely in the form of increased immune activation contributing to impaired uterine receptivity.

RBPJ expression is reduced in women with RPL

Dysregulated complement signaling and its role in pregnancy loss have been described extensively in RPL patients, particularly with clinically identifiable causes such as Antiphospholipid Antibody Syndrome^{273,274}. Many phenotypical features of *Rbpj* c-KO mice overlap with aspects of RPL in women including subfertility and enhanced immune signaling through both complement and IFN γ ²⁵⁸. Therefore, we hypothesized that RBPJ expression may be altered in the setting of RPL. Endometrial biopsies from women with clinically defined unexplained RPL (uRPL) were obtained during the mid-secretory phase of the menstrual cycle. Immunostaining revealed significantly reduced RBPJ expression in women with uRPL versus normal fertile control patients (**Fig 2-7**). Both endometrial stromal and glandular epithelial compartments displayed decreased RBPJ expression. Consistent with previous reports in women with RPL, our patient cohort of uRPL displayed elevated IFN γ levels (Fig 2-12). Therefore, loss of *Rbpj* in our mouse

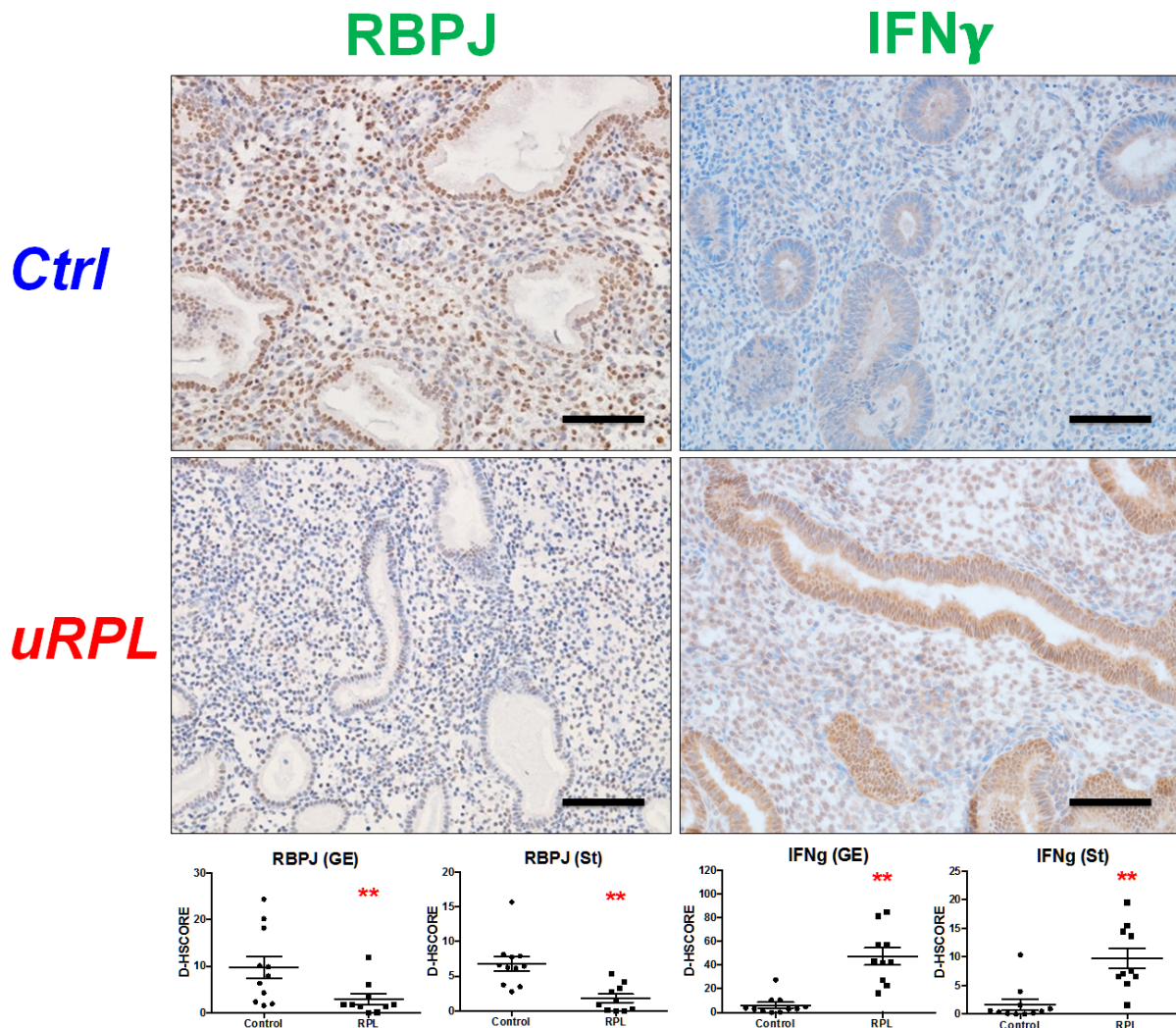


Figure 2-12. RBPJ is reduced in women with uRPL. Many phenotypical features of *Rbpj* c-KO mice mimic clinical aspects of RPL, including infertility and enhanced inflammatory signaling. In order to determine the potential for dysregulated RBPJ expression in women with uRPL, we performed immunostaining for RBPJ in mid-luteal endometrial biopsies from uRPL patients and healthy, fertile controls. Expression of RBPJ was significantly downregulated in both endometrial glands and stroma. Consistent with previous reports, IFN γ expression was increased in the same patient cohort of women with uRPL. Data represented as Mean \pm SEM. ** $p < 0.01$, * $p < 0.05$; Scale bar = 100 μ m; St = Stroma, GE = Glandular Epithelium.

model parallels phenotypic characteristics of women with uRPL, including impaired fertility and enhanced immune signaling. These findings suggest that loss of RBPJ and dysfunctional endometrial repair, as described in the *Rbpj* c-KO mouse, may contribute to fertility defects in women with uRPL.

DISCUSSION

The endometrium has the unique capacity to completely repair and regenerate itself following parturition, as well as following menstruation in primates^{9,127}. The highly coordinated sequence of events during repair require tight regulation over differentiation of uterine progenitor cells along with promoting an immune environment favoring wound healing. Notch signaling is conserved among species and drives both cellular differentiation for repair and immune signaling in many tissues^{96,98,106,107}. The objective of our study was to characterize the postpartum uterine repair process and its dysregulation in the absence of the Notch family transcription factor Rbpj. Two key uterine postpartum repair processes were impacted by loss of Rbpj: 1) parenchymal regeneration and 2) inflammatory signaling. *Rbpj* c-KO mice displayed dysfunctional re-epithelialization and myometrial reformation. Abnormal postpartum epithelial proliferation was associated with delayed re-epithelialization. Further, programmed cell death of dual-staining cytokeratin-vimentin cells does not occur on PPD 1 in the absence of Rbpj, suggesting a potential role for Rbpj in regulating progenitors for MET during uterine repair. Transcriptome analysis displayed global upregulation of many inflammatory pathways with loss of Rbpj. Specifically, Rbpj suppresses endometrial complement signaling to prevent innate immune activation and influx of neutrophils

during repair, and it promotes M2 macrophage predominance for repair through decreasing interferon signaling. To date, the mechanisms regulating repair of the uterus remain largely unknown and, to our knowledge, the impact of failed repair in preventing the establishment of future pregnancy has never been described.

Given the importance of Notch signaling during development and maintenance of organ homeostasis, it is no surprise that dysregulated *Rbpj* expression contributes to dysfunctional endometrial repair^{96,98}. Endometrial re-epithelialization represents the first step in the repair of injured mucosal surfaces and therefore during postpartum uterine repair^{9,127}, which was delayed in *Rbpj* c-KO mice. Multiple sources of cells are responsible for repopulating the luminal epithelium, including epithelial cells from either the injury edges or endometrial glands^{135,172,176}. Recently, mounting evidence supports a role for MET with stromal cells or “mesenchymal progenitors” regenerating the luminal epithelium after injury^{177,178}. Our findings in the current study support previous reports of mesenchymal-derived cells differentiating into epithelial cells, based on the presence of cells double-positive for cytokeratin and vimentin within the endometrium of mice from PPD 1 to 3. Control of MET must be highly regulated in order to prevent over-proliferation. As a result, cytokeratin-vimentin double-positive cells undergo apoptosis on PPD 1. In the absence of *Rbpj*, dual-staining cells did not undergo apoptosis on PPD 1, and their presence was still ubiquitous within the LE on PPD 3. Notch signaling has been described extensively in the setting of Epithelial to Mesenchymal transition (EMT), and over activation of Notch signaling contributes to metastasis of mucosal epithelial cancers^{109,275,276}. However, Notch regulation of the transition of mesenchymal derived cells to regenerate the epithelium after injury has not been reported, nor dysregulation

of this process in the setting of *Rbpj* loss. Loss of *Rbpj* has been shown to increase expression of CXCR4 and promote infiltration of mesenchymal stem cells to the site of injury after liver ischemia/reperfusion injury²⁷⁷, and this protein was elevated in *Rbpj* c-KO mice on PPD3 suggesting a potential mechanism for recruitment of mesenchymal progenitor cells. Further, we have previously shown that endometrial stromal cell differentiation during decidualization is impaired in both the mouse and non-human primate with loss of NOTCH1^{112,114}. Therefore, in this study, we describe another role for Notch signaling, through *Rbpj*, in mediating stromal differentiation for repair of the endometrium.

Abnormal endometrial repair in *Rbpj* c-KO mice was associated with up regulated immune signaling. Initially after injury, a pro-inflammatory tissue response driven largely by innate immune mediators, such as complement, is important to stop bleeding and prevent infection¹³⁹. As a result, during and immediately after parturition, neutrophils are recruited to the endometrium in response to complement activation and products of platelet breakdown¹⁴⁰. However, transition of the endometrium towards an anti-inflammatory environment is necessary to promote wound healing, largely through recruitment of M2 type macrophages¹⁶⁴. Reduced cytotoxic M1 populations during repair occur through suppression of tissue IFN γ production, where continued expression of IFN γ or presence of M1 macrophages inhibits repair^{157,166}. Uterine M2 macrophages predominate during the postpartum period, and their numbers peak on PPD 3 and gradually decrease over time¹⁶⁵. Other studies have shown that IFN γ levels do not significantly change at the heaviest point of bleeding or during the repair process in a mouse menstruation and repair model¹³⁶. Notch signaling has been implicated to control

the immune environment after injury to prevent further damage^{106,107}. Based on our work, endometrial Rbpj mediates suppression of both complement and interferon signaling during the early postpartum period. It is unlikely that Rbpj directly regulates IFN γ expression, as there are no reported Rbpj binding sites within range of the promoter region. However, others have described a role for RBPJ expression in basally suppressing IFN γ secretion, in the absence of Notch activation^{278,279}. Since we did not see a postpartum repair phenotype in *Notch1* c-KO mice, this supports a potential Notch-independent function for Rbpj. GATA3, a transcriptional target of Rbpj, induces IFN γ , and Rbpj may suppress its expression during repair. Specifically, inhibition of Notch receptor activation, which subsequently enhances Rbpj repression of target genes, results in reduced IFN γ production^{246,247}. In the absence of Rbpj expression, numbers of neutrophils and M1-macrophages predominate with the potential for generating a cytotoxic immune environment, which worsens tissue injury, delays repair and may prevent future embryo implantation.

We have shown that decreased RBPJ expression occurs in the setting of uRPL and generated a mouse model, which phenotypically mirrors many features of RPL. Initially, *Rbpj* c-KO mice are sub-fertile with mid-gestation embryo loss¹²⁴ and, subsequently, these mice become infertile due to dysfunctional endometrial repair. Additionally, pregnancy and parturition appear to initiate the events of enhanced immune recruitment and pro-inflammatory signaling resulting in dysfunctional repair and future implantation failure. Additionally, we have determined using RNASeq that many of the previously described pathways altered in women with RPL based on transcriptomic studies are similarly affected with uterine Rbpj ablation in the uterus on

PPD3^{257,258,273,274,280}. These pathways include regulation of immune pathways such as complement and interferon signaling, along with markers of proteolysis, like matrix metalloproteinases^{257,258}. Interestingly, mice with exaggerated complement signaling display features of RPL with neutrophil infiltration contributing to embryo loss^{40,55}. Aberrant decidualization is a key feature of RPL where endometrial stromal cells fail to switch to an anti-inflammatory phenotype and these cells fail to sense embryo quality^{17,78,260}. Both decidualization failure and enhanced immune recruitment were present in the decidua of infertile *Rbpj* c-KO mice. A final important aspect of the work presented is the evidence of dysfunctional repair on future pregnancy potential. This finding is substantially more significant in primates, where significant endometrial repair occurs with menstruation on a monthly basis versus only after pregnancy or induced menstruation in rodents. Since *Rbpj* acts upstream of many dysregulated pathways in RPL, the *Rbpj* c-KO mouse provides an excellent model for studying endometrial repair and its failure in response to different types of endometrial injury. Additionally, these mice may be used for targeting therapeutics to overcome disrupted pathways associated with embryo loss. Lastly, reduced RBPJ expression may serve to identify patients at risk for recurrent pregnancy loss and its expression pattern during disease development will be an important determinant for its use as a potential biomarker.

METHODS

Mouse Work:

Generation of *Rbpj* c-KO mice and Fertility Testing

All studies performed using animals were approved by the Institutional Animal Care and Use Committee of Michigan State University, East Lansing, MI, USA in compliance with the Guide for Care and Use of Laboratory Animals (2011, National Academy of Sciences). We generated a uterine-specific *Rbpj* knockout mouse in order to avoid the embryonic lethality of a complete *Rbpj* knockout¹²⁵. Specifically, we crossed *Pgr*^{cre/+} mice^{49,50} with *Rbpj*^{ff} (control) mice¹²⁶ to produce *Pgr*^{cre/+}*Rbpj*^{ff} (*Rbpj* c-KO) mice, resulting in selective ablation of *Rbpj* in *Pgr*-positive tissues. For fertility testing, fertile female mice were housed with males for six months with daily observation and records were maintained regarding litter date and number of pups. At the end of the fertility test, both control and *Rbpj* c-KO mice were caged with fertile males to induce pregnancy. We designated the day of vaginal plug as 0.5 dpc. The afternoon of the same day, mice were anesthetized with isoflurane and bilateral salpingo-oophorectomies were performed with oviduct flushing. Embryo numbers were recorded to determine whether differences existed between *Rbpj* c-KO and control mice.

Induction of *In Vivo* Artificial Decidualization (AD)

Two weeks following salpingo-oophorectomy after completion of the fertility test, *Rbpj* c-KO and control mice were subjected to an AD protocol as previously described¹¹⁴. Mice were primed to mimic the physiologic hormonal milieu of early pregnancy with daily E2

(100 ng; Sigma-Aldrich, St. Louis, MO, USA) for three days followed by two days rest and then daily P4 (1 mg) plus E2 (6.7 ng). Six hours following the E2 and P4 injection on the third day, a mechanical scratch of the anti-mesometrial luminal epithelium of the left uterine horn (Dec) was performed to induce decidualization using a blunted syringe. The non-scratched right horn served as the unstimulated hormonal control (Con). P4 (1 mg) plus E2 (6.7 ng) were administered daily with sacrifice 5 days post-scratch (AD5; n=5-6 mice/group). Uterine tissues were collected, weighed and snap frozen in liquid N₂ or fixed in 4% paraformaldehyde (PFA) for paraffin embedding. The decidual response was calculated based on the ratio of Dec to Con uterine horn weight.

Postpartum Repair Time Course

Rbpj c-KO and control female mice were caged with fertile males to induce pregnancy. Mice were followed from vaginal plug detection till the date of delivery of a litter, which was considered Postpartum Day (PPD) 0. Mice were sacrificed on significant time points during the repair process: PPD 1, 3, 5, and 10 (n=3-6/group/time point). Placental detachment site (or postpartum nodule) numbers were correlated to litter size and subsequently fixed in 4% PFA for paraffin embedding. Additional tissues were collected and snap frozen in liquid N₂ from PPD 3 *Rbpj* c-KO and control mice for RNA sequencing (n=3 mice/group), where 3 nodules were pooled per mouse to increase RNA yield and reduce variability.

Unilateral Tubal Ligation and Embryo Transfer

In order to prevent pregnancy in one uterine horn, 6-week old *Rbpj* c-KO and control female mice (n=6/group) were anesthetized by isoflurane and left unilateral tubal ligation was performed by cutting the oviduct approximately 3 mm distal to the uterotubal junction followed by electrocautery of both free ends of the oviduct. In order to ensure that pregnancy was spared in the left uterine horn, mice were mated with fertile males two weeks following their procedure and sacrificed after two litters with visualization of the uterine morphology to detect the presence of postpartum remnants from previous pregnancies. We confirmed the left uterine horn was spared of pregnancy and proceeded to determine the impact of pregnancy and its repair on future embryo implantation. Unilateral tubal ligation was repeated, as described above, in *Rbpj* c-KO and control mice (n=6/group) followed by two weeks rest. These mice were set up with fertile males to induce pregnancy and delivery of one litter, at which point they were rested for two weeks to allow substantial time for postpartum uterine repair. Following rest, mice were set up with vasectomized males, whose infertility was confirmed, to induce pseudopregnancy. P4 (1 mg/mouse) was supplemented on day 0.5 and 1.5 of pseudopregnancy, with a single E2 (100 ng) injection on the morning of embryo transfer on day 2.5 of pseudopregnancy. All embryos used for embryo transfer were collected from wild type C57BL/6 females. On the afternoon day 2.5 of pseudopregnancy, seven blastocysts were transferred into the lumen of each uterine horn followed by detection of implantation status two days later (4.5 dpc) by tail vein injection of 0.1% Chicago Sky Blue in Normal Saline (Sigma-Aldrich, St. Louis, MO, USA). Whole uterine horns were fixed in 4% PFA for paraffin embedding.

Human Subjects:

Recurrent Pregnancy Loss Patient Selection

Informed consent was obtained from all participants in this study, which was approved by the Institution Review Board of Greenville Hospital System or University of North Carolina, Chapel Hill. Women with two or more consecutive pregnancy losses without any readily identifiable causes (uRPL) were evaluated in the Division of Reproductive Endocrinology at Greenville Hospital System in Greenville, SC and recruited to this study. Inclusion criteria for this study included patients with regular, ovulatory cycles, at least one patent fallopian tube (without hydrosalpinges) and were 42 years of age or younger. Exclusion criteria included a previous diagnosis of uterine fibroids, septum, a history of pelvic inflammatory disease, polycystic ovarian disease, or a partner with an abnormal semen analysis [by the World Health Organization (WHO) criteria]. Patients with known moderate or severe endometriosis were excluded, although women with a history of mild or minimal were not. Patients with clinical histories associated with explained RPL were excluded including thrombophilia, genetic or immunologic abnormalities, or Müllerian defects. The control group consisted of proven fertile women undergoing tubal ligation through the Department of Obstetrics and Gynecology at University of North Carolina, Chapel Hill.

Endometrial Tissue Collection

Mid-secretory phase endometrial biopsies were obtained from women with (n=8) or without (n=13) RPL. Pipelle suction of endometrial tissue was performed between days 21 and 24 of the menstrual cycle based on urinary LH surge detection (LH plus 7–

10 days). Endometrial tissues collected were formalin fixed and paraffin embedding for histologic analysis.

Molecular Biology and Histological Techniques:

Prussian Blue Staining

PFA fixed/paraffin embedded tissues were sectioned to 6 μm thickness and placed onto microscope slides (Thermo Fisher Scientific, Waltham, MA, USA). To identify nodule cells in uterine tissue sections from fertility test *Rbpj* c-KO and control mice, uterine horns were stained by Prussian Blue using an Iron Stain Kit (Sigma-Aldrich, St. Louis, MO, USA) as per the manufacturer's recommendations. With Prussian Blue stain, hemosiderin appears blue and is prevalent in nodule cells, which represent hemosiderin-laden macrophages^{145,168}.

Immunohistochemistry

PFA fixed/paraffin embedded tissues were sectioned to 6 μm thickness and placed onto microscope slides (Thermo Fisher Scientific, Waltham, MA, USA). For immunohistochemistry, each tissue section was dewaxed, rehydrated with a graded alcohol series, followed by heat-mediated antigen retrieval in citrate buffer (Antigen unmasking solution, Vector Laboratories, Burlingame, CA) and then hydrogen peroxide treatment. Sections were blocked for 1 hour in 10% Normal Horse Serum (Vector Laboratories, Burlingame, CA, USA) in Phosphate Buffered Saline (PBS) incubated overnight at 4°C in primary antibody (**Table S2-3**). Next, sections were incubated in respective biotinylated secondary antibodies for anti-mouse IgG, anti-rabbit IgG, or anti-

rat (Vector Laboratories, Burlingame, CA, USA) followed by HRP conjugated streptavidin (Life Technologies, Rockford, IL, USA). Detection for immunoreactivity was achieved using the DAB Substrate Kit (Vector Laboratories, Burlingame, CA; SK-4100) followed by hematoxylin counterstaining. Positive cell percentages were calculated for immune markers. Staining intensity of each section was quantified by image analysis software *ImageJ* (NIH) resulting in a Digital HSCORE (D-HSCORE) of staining intensity as previously reported²⁶⁹. Graphical representation of quantitative data is shown in **Fig S2-2**.

Immunofluorescence

PFA fixed/paraffin embedded tissues were sectioned, rehydrated with citrate buffer antigen retrieval as described above. Following antigen retrieval, tissue sections were incubated in permeabilizing solution containing 0.5% Triton X-100 (Sigma-Aldrich, St. Louis, MO, USA) in PBS for 30 minutes. Sections were blocked for 1 hour in 10% Normal Horse Serum (Vector Laboratories, Burlingame, CA, USA) and 10% Bovine Serum Albumin (Fisher Scientific, Pittsburgh, PA, USA), in PBS and incubated overnight at 4°C in primary antibodies (**Table S2-3**). Next, sections were incubated in respective species-specific fluorochrome-conjugated secondary antibodies. To reduce autofluorescence, slides were incubated in 0.1% Sudan Black in 70% ethanol for 30 minutes, washed in PBS and then mounted with Vectashield Antifade Mounting Medium with or without DAPI (Vector Laboratories, Burlingame, CA, USA). Tissue fluorescence was visualized using a Nikon Eclipse Ti (Melville, NY, USA) inverted confocal microscope. Staining intensity for each section was quantified by image analysis

software *ImageJ* (NIH) resulting in a Digital HSCORE (D-HSCORE)²⁶⁹. Graphical representation of quantitative data is shown in **Fig S2-2**.

Whole uterine horns from the unilateral tubal ligation and embryo transfer experiments were sectioned in their entirety followed by Hematoxylin and Eosin (H&E) staining to detect the presence of embryos and/or implantation sites.

RNA isolation and Real Time-Quantitative PCR (RT-qPCR)

Total RNA was isolated from snap frozen mouse tissues or cultured cells using TRIzol (Invitrogen, Carlsbad, CA, USA) with cleanup using the RNeasy Mini Kit (Qiagen, Valencia, CA, USA) with DNase digestion using the RNase-Free DNase Set (Qiagen, Valencia, CA, USA). Subsequently, RNA was reverse transcribed to produce cDNA using the High Capacity cDNA Reverse Transcription Kit (Applied Biosystems, Foster City, CA, USA). Differential gene expression was determined using RT-qPCR performed with either TaqMan Universal Master Mix II (Applied Biosystems, Foster City, CA, USA) or SYBR Green PCR Master Mix (Applied Biosystems, Foster City, CA, USA) using the ViiA 7 qPCR System (Applied Biosystems, Foster City, CA, USA). *Rpl19* was used for normalization of cDNA. Primer sequences used for RT-qPCR are listed in (**Table S2-4 and S2-5**).

cDNA Library Preparation and RNA-Sequencing

RNA quality was determined using a 2100 Bioanalyzer (Agilent, Santa Clara, CA, USA), which produced an RNA integrity number (RIN). RIN numbers above 8 were considered acceptable for sequencing and in the instance where a RIN number was not generated,

the bioanalyzer trace was observed for evidence of RNA degradation. Libraries were prepared using the TruSeq Stranded mRNA Library Preparation Kit (Illumina, San Diego, CA, USA). After library validation and quantitation, all libraries were pooled in equimolar amounts. This pool was loaded on two lanes of an Illumina HiSeq 2500 Rapid Run flow cell (v1) and sequenced using TruSeq Rapid SBS Reagents in a 1x50bp single read format. Base calling was done by Illumina Real Time Analysis (RTA) v1.18.64 and output of RTA demultiplexed and converted to FastQ format with Illumina Bcl2fastq v1.8.4.

Bioinformatics Workflow

Gene-level differential expression was performed using a pipeline consisting of subread, featureCounts, and edgeR. Reads were aligned to the reference mouse genome (mm10) with Subread²⁸¹. All 24 files were aligned and then the split lane aligned reads for each sample were merged into a single file using samtools. Quality control was performed on the merged bams via RSeQC. All samples were determined to be of high quality based on the inspection of raw sequence quality, nucleotide composition bias, CG bias, mapped read distributions, and coverage uniformity.

Aligned reads were summarized on the gene and transcript-level using featureCounts²⁸². Principal component analysis was performed with the expected distribution of the two different mouse genotypes clustering apart (**Fig S2-4**). Differential expression was performed on the gene-level counts using the R/Bioconductor package edgeR. Genes with less than one count per million in at least 3 samples were removed prior to differential expression. Differential expression was performed using the

exactTests function. Genes with a p-value < 0.05 were considered to be differentially expressed. Differentially expressed genes were input into MetaCore (Thomson Reuters, New York, NY, USA) for pathway and process enrichment. Significantly enriched pathways were validated by RT-qPCR as described above. To generate a heat map of the differentially expressed genes (**Fig 2-4B**), genes were z-score normalized prior to unsupervised hierarchical clustering. Genes were clustered using euclidean distance and complete linkage. Seven main clusters were identified. Similar to the entire gene list, the genes associated with each cluster were imported into MetaCore (Thomson Reuters, New York, NY, USA) for process network enrichment and top processes are shown.

STATISTICAL ANALYSIS

Significant variation between groups for parametric values were determined using the Student's t-test, one-way analysis of variance followed by Tukey's post hoc multiple-range test, or a two-way analysis of variance with repeated measures followed by a Holm-Sidak post-hoc test to determine group-specific differences. For non-parametric measures, a Fisher's Exact Test was performed. Differences between groups were considered statistically significant if $p < 0.05$. All statistical analyses were performed by GraphPad Prism 6.0 (GraphPad Software, San Diego, CA, USA).

ACKNOWLEDGEMENTS

The authors thank Dr. Francesco DeMayo (NIH National Institute of Environmental Health Sciences) and Dr. Nadia Carlesso (Indiana University) for kindly providing the

Pgr^{cre/+} and *Rbpj*^{flox/flox} mice, respectively. We thank Dr. Bruce Lessey (University of South Carolina School of Medicine) and Dr. Steve Young (University of North Carolina School of Medicine) for generously supplying the endometrial tissues from control women and those with RPL. The authors also thank Ms. Samantha Bond, Ms. Sharra Pencil, Ms. Ariadna Ochoa, and Mr. Mark Olson for their excellent technical assistance. The authors would like to thank the Michigan State University Research Technology Support Facility Genomics Core (East Lansing, MI, USA) for their assistance with library preparation and RNA-sequencing. We would also like to thank the Van Andel Research Institute Bioinformatics and Biostatistics Core (Grand Rapids, MI, USA) for performing data analysis of the RNA-sequencing results. Funding for this study was provided by NICHD R01 HD042280 (ATF) and NICHD F30 HD082951 (MS).

APPENDIX

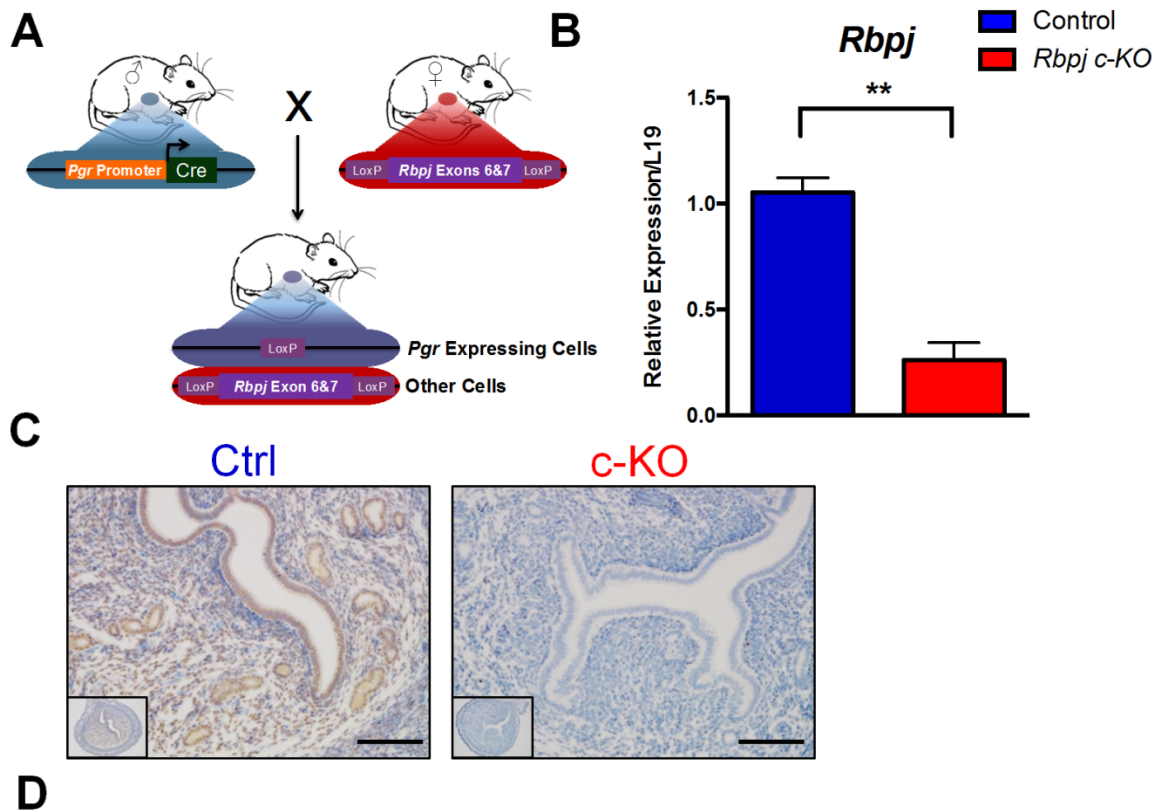


Figure S2-1. Generation of *Rbpj* c-KO mice and fertility testing results (A) *Pgr*^{cre/+} mice were crossed with *Rbpj*^{ff} mice, with LoxP sites flanking *Rbpj* exons 6 and 7, resulting in selective ablation of *Rbpj* in Pgr-positive cells of mice (*Pgr*^{cre/+} *Rbpj*^{ff}; *Rbpj* c-KO). (B,C) Reduced mRNA and protein expression of *Rbpj* was confirmed in 6-week old *Rbpj* c-KO mice by RT-qPCR and immunohistochemistry, respectively. (D) Fertility testing of female *Rbpj* c-KO and control mice was performed by paired mating for six months with daily observation and recording of litters and litter sizes. Data represented as Mean ± SEM. **p<0.01, *p<0.05; Scale Bar = 100 μm.

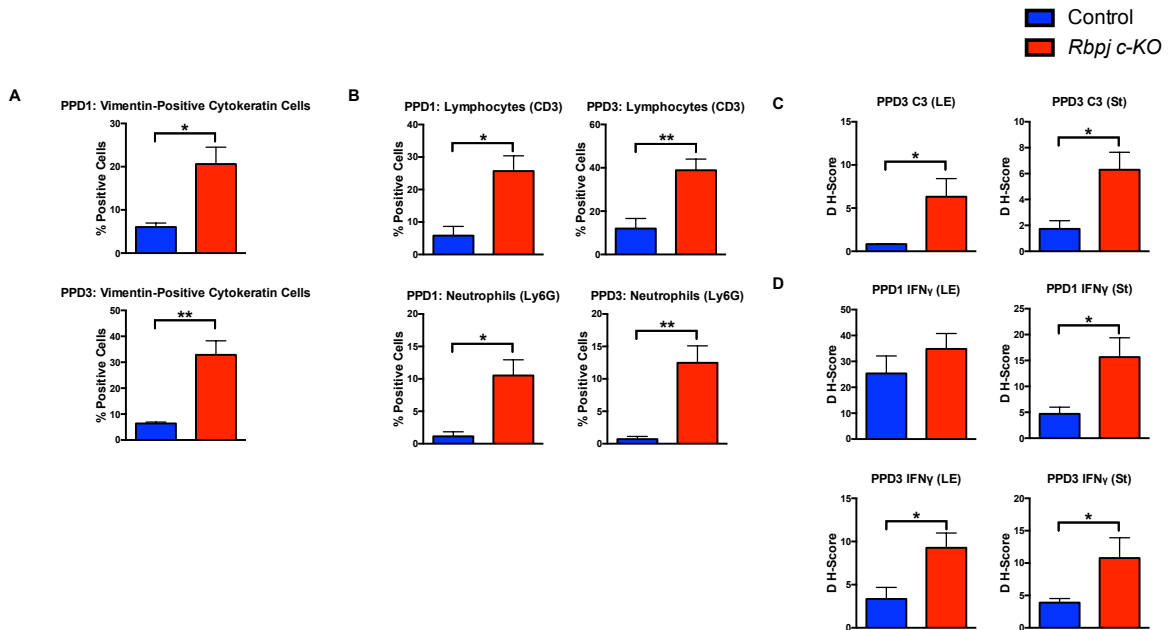


Figure S2-2. Graphical representation with statistical significance for staining intensity and cell counts. Staining intensity and cell counts were determined using *ImageJ* (NIH) software. **A)** Percentage of vimentin positive cells of cyokeratin staining cells on PPD 1 and 3 for **Fig 2-5.** **B)** Percentage of total cells positive for lymphocyte (CD3) and neutrophil (Ly6G) markers on PPD 1 and 3 for **Fig 2-8.** **C)** Staining intensity for Complement C3 on PPD 3 for **Fig 2-9.** **D)** Staining intensity of IFN γ on PPD 1 and 3 for **Fig 2-10.** LE = Luminal Epithelium, St = Stroma; Data represented as mean \pm SEM. **p<0.01, *p<0.05.

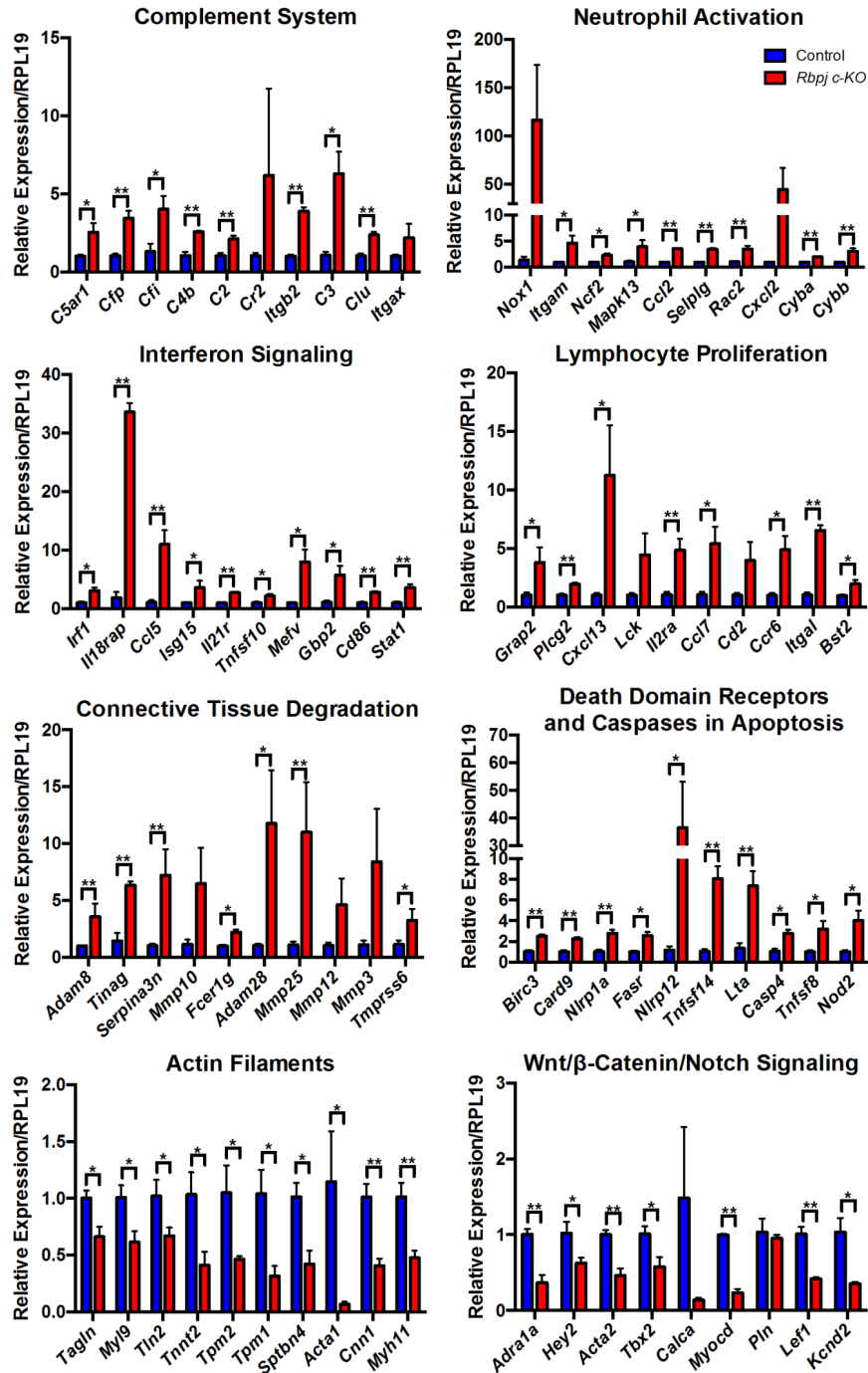


Figure S2-3. Validation of Enriched Process Network Pathways by RT-qPCR. Eight pathways from Process Network enrichment were selected to validate by RT-qPCR. Six of these pathways were based on up regulated genes (Complement System, Neutrophil Activation, Interferon Signaling, Lymphocyte Proliferation, Connective Tissue Degradation, Death Domain Receptors and Caspases in Apoptosis) and two were based on down regulated genes (Actin Filaments, Wnt/ β -Catenin/Notch Signaling). Data represented as Mean \pm SEM. ** $p < 0.01$, * $p < 0.05$.

Principal Component Analysis for PPD 3 RNA-Seq

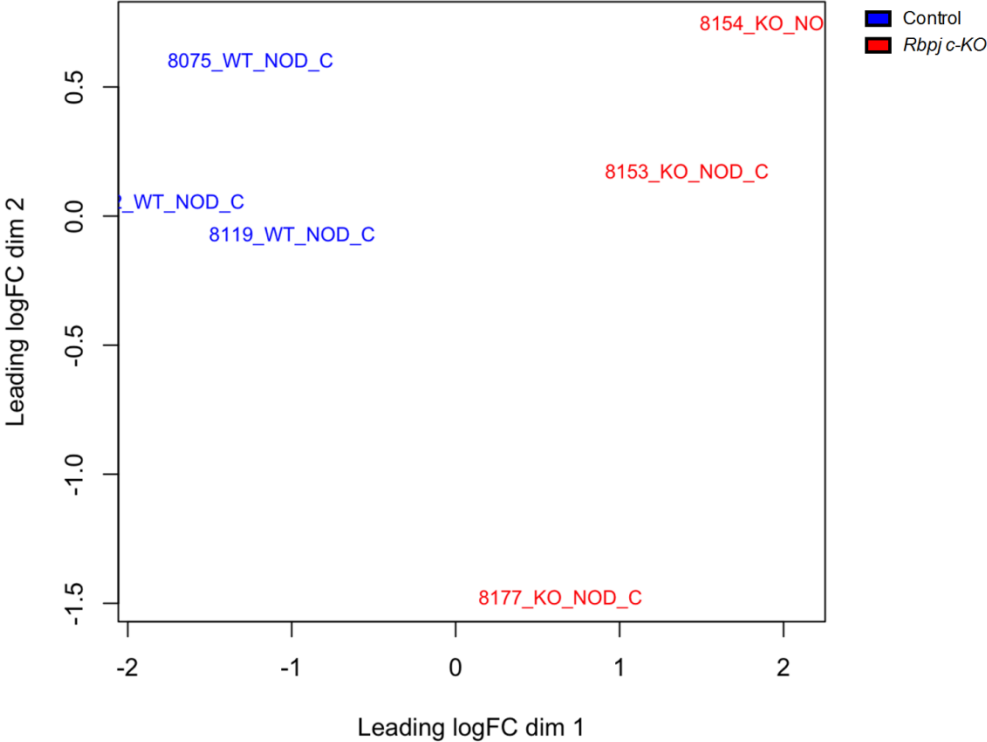


Figure S2-4. Principal Component Analysis (PCA) from PPD 3 RNA-Sequencing.

Process	P-value (FDR)	# Genes
Chemotaxis	5.093E-30	66
Cell adhesion_Leucocyte chemotaxis	6.631E-22	71
Proliferation_Lymphocyte proliferation	1.647E-21	71
Inflammation_Interferon signaling	1.227E-20	49
Immune response_Antigen presentation	5.684E-17	62
Cell adhesion_Platelet-endothelium-leucocyte interactions	3.600E-15	55
Inflammation_Jak-STAT Pathway	1.615E-14	56
Inflammation_Complement system	2.406E-14	33
Inflammation_NK cell cytotoxicity	1.239E-12	49
Immune response_TCR signaling	3.353E-12	50
Inflammation_Innate inflammatory response	1.624E-11	50
Immune response_T helper cell differentiation	5.233E-11	42
Inflammation_Neutrophil activation	1.197E-09	52
Inflammation_IFN-gamma signaling	5.305E-07	30
Inflammation_IL-10 anti-inflammatory response	5.305E-07	26
Inflammation_IL-4 signaling	1.453E-06	30
Immune response_Phagosome in antigen presentation	4.150E-06	48
Apoptosis_Death Domain receptors & caspases in apoptosis	1.645E-04	27
Proteolysis_Connective tissue degradation	1.460E-03	24
Proteolysis_ECM remodeling	1.541E-03	19

Table S2-1. Significantly affected pathways by Process Network Enrichment of PPD3 RNA-seq up regulated genes

Process	P-value (FDR)	# Genes
Muscle contraction	3.110E-10	30
Development_Neurogenesis_Synaptogenesis	2.446E-09	29
Development_Skeletal muscle development	5.627E-06	21
Development_Hedgehog signaling	3.170E-03	23
Development_Neurogenesis in general	3.322E-03	19
Cytoskeleton_Actin filaments	7.409E-03	17
Development_Neurogenesis_Axonal guidance	8.373E-03	20
Transport_Synaptic vesicle exocytosis	1.452E-02	16
Cardiac development_Wnt_beta-catenin, Notch, VEGF, IP3 and integrin signaling	4.756E-02	13
Development_Regulation of angiogenesis	4.814E-02	17

Table S2-2. Significantly affected pathways by Process Network Enrichment of PPD3 RNA-seq down regulated genes

Antibody	Company	Catalog #	Host Species	Method	Dilution
Anti-CD68	Santa Cruz	sc-5474	Goat	IF	1:500
Rbpj	Santa Cruz	sc-28713	Rabbit	IHC	1:1000
CC-3	Cell Signaling	cs-9661	Rabbit	ICH/IF	1:500
Ki-67	BD Pharmingen	550609	Mouse	IHC	1:250
Cytokeratin	Sigma	C2562	Mouse	IF	1:1000
Vimentin	Santa Cruz	sc-7557	Goat	IF	1:500
Ly6G	BD Pharmingen	551459	Rat	IHC	1:200
CD3	Abcam	5690	Rabbit	IHC	1:500
C3	Santa Cruz	sc-14612	Goat	IF	1:250
IFNγ	Bioss	bs-0480R	Rabbit	IF	1:250

Table S2-3. Antibodies used in the study

Gene Symbol	Application	Accession ID	Species	Forward	Reverse
<i>Rpl19</i>	Taqman	NM_001159483	Mouse	Mm01606037_g1	
<i>Rbpj</i>	Taqman	NM_001080927	Mouse	Mm01217627_g1	
<i>Bmp2</i>	SYBR Green	NM_007553	Mouse	CGCAGCTTCCATCACGAA	GCTTCCTGTATCTGTTCCCG
<i>Wnt4</i>	SYBR Green	NM_009523	Mouse	AGTGCCAATACCAGTTCCG	CACACTTCTCCAGTTCTCCAC
<i>Csf1</i>	SYBR Green	NM_007778	Mouse	TCGAAACCCTCAGACATTGG	AGGAAGATGGTAGGAGAGGG
<i>Cxcl12</i>	SYBR Green	NM_021704.3	Mouse	CCACATCGCCAGAGCCAAC	TGGGCTGTTGTGCTTACTTGT
<i>Cxcr4</i>	SYBR Green	NM_009911.3	Mouse	GCAGTGAACCTCTGAGCG	GTCTCCAGAACCCTTCTTCCAG
<i>IL6</i>	SYBR Green	NM031168	Mouse	CTCTGGGAAATCGTGGAAATG	AAGTGCATCATCGTTGTTCATACA
<i>Cox2</i>	SYBR Green	NM_011198	Mouse	CCAGCACTTCACCCATCAG	GTCCAGAGTTTACCATAAATGTG
<i>Esr1</i>	SYBR Green	NM_007956	Mouse	AACCGCCCATGATCTATTCTG	AGATTCAAGTCCCAAAGCC
<i>Muc1</i>	SYBR Green	NM_013605	Mouse	TTCCAACCCAGGACACCTAC	ATTACCTGCCGAAACCTCT
<i>Muc4</i>	SYBR Green	NM_080457	Mouse	AATGTTCTGCCTATACTGCC	TTGTATGGTTCCTGGGTCAC
<i>Emr1</i>	SYBR Green	NM_010130	Mouse	CTTTGGCTATGGGCTCCAGTC	GCAAGGAGGACAGAGTTTATCGTG
<i>Ifng</i>	SYBR Green	NM_008337	Mouse	TCAAGTGGCATAGATGTGGAAGAA	TGGCTCTGCAGGATTTTCATG
<i>Nos2</i>	SYBR Green	NM_010927	Mouse	GCAAACATCACATTCAGATCCC	TCAGCCTCATGGTAAACACG
<i>Arg1</i>	SYBR Green	NM_007482	Mouse	AAGAATGGAAGAGTCAGTGTGG	GGGAGTGTGATGTCAGTGTG
<i>Tnfa</i>	SYBR Green	NM_000594	Mouse	CCAGACCCTCAGACTCAGATC	CAC TTGGTGGTTTGCTACGAC

Table S2-4. Primer sequences used for core pathways tested for the study

Gene Symbol	Application	Accession ID	Species	Forward	Reverse
Inflammation: Complement System					
<i>C5aR1</i>	SYBR Green	NM_007577	Mouse	CATACCTGCGGATGGCATTCA	GGAACACACAGTAGATGAT
<i>Cfp</i>	SYBR Green	NM_008023	Mouse	TTCCACCCATTGAGGAGTCC	GCTGACATTGTGGAGACT
<i>Cfi</i>	SYBR Green	NM_007686	Mouse	CTTGGCTCTCCACTTGATTC	GGAGCGATGCGTGTATTCTG
<i>C4b</i>	SYBR Green	NM_009780	Mouse	ACTTCAGCAGCTTAGTCAGGG	GTCCCTTTTTCAGGGGACAG
<i>C2</i>	SYBR Green	NM_013484	Mouse	CGGTGTAATTTACCCTCAG	GGTGTAGTGTGAGCTAGACCT
<i>Cr2</i>	SYBR Green	NM_007758	Mouse	AACACATGGTTACCAGGTGTACC	CGTGCCTCCAGCATAAG
<i>ITGB2</i>	SYBR Green	NM_008404	Mouse	CAGGAATGCACCAAGTACAAAGT	CCTGTGCTCAGTGAAGTCCAGC
<i>C3</i>	SYBR Green	NM_009778	Mouse	AGACTGCCTGACCTTCAAG	CATCCCATCTGCTCTCTGCT
<i>Clu</i>	SYBR Green	NM_013492	Mouse	AGCAGGAGTCTCTGACAATG	GGCTTCTCTAAACTGTGGAGC
<i>Itgax</i>	SYBR Green	NM_021334	Mouse	CTGGTAGCCTTCTCTGCTG	GCACACTGTCTCCGAAGTCA
Inflammation: Neutrophil Activation					
<i>Nox1</i>	SYBR Green	NM_172203	Mouse	GGTTGGGGCTGAACATTTTTC	TCGACACACAGGAATCAGGAT
		NM_0010829			
<i>ITGAM</i>	SYBR Green	60	Mouse	CCATGACCTTCCAGAGAGATGC	ACCGGCTTGTGCTGTGAT
<i>Ncf2</i>	SYBR Green	NM_010877	Mouse	GCTGCTGAACACTATCTCTGG	AGGTGCTACTTCTCCATCTGTGA
<i>Mapk13</i>	SYBR Green	NM_011950	Mouse	ATGAGCTCCTCAGGAAAGG	GCATGTGCTTCCAGAGCAGAA
<i>CCL2</i>	SYBR Green	NM_011333	Mouse	TTAAAACCTGGATCGGAACCAA	GCATTAGCTCAGATTACGGGT
<i>Selp1g</i>	SYBR Green	NM_009151	Mouse	GAAAGGGCTGATTGTGACCCC	AGTAGTTCGCACTGGGTACA
<i>Rac2</i>	SYBR Green	NM_009008	Mouse	GACAGTAAGCCGGTGAACCTG	CTGACTAGCGAGAAGCAGATG
<i>Cxcl2</i>	SYBR Green		Mouse	CCAAACACACAGGCTACAGG	GCCTCACACTCAAGCTCTG
<i>Cyba</i>	SYBR Green	NM_007806	Mouse	TGCCAGTGTGATCTATCTGCT	TCGGCTTCTTTCGGACCTCT
<i>Cybb</i>	SYBR Green	NM_007807	Mouse	TGTGGTTGGGGCTGAATGCT	CTGAAAGGAGGAGCAGATTCTG
Proliferation: Lymphocyte Proliferation					
<i>Grap2</i>	SYBR Green	NM_010815	Mouse	AGGACGACGTTACGACTTTC	TGTCGGTAGTAGTCCACCAG
<i>Picg2</i>	SYBR Green	NM_172285	Mouse	GTGGACACCCTCCAGAATATG	ACCTGCCGAGTCTCCATATG
<i>Xccl13</i>	SYBR Green	NM_018866	Mouse	GGCCACGGTATTCTGGAAGC	GGCGGTAACTTGAATCCGATCTA
		NM_0011624			
<i>Lck</i>	SYBR Green	33	Mouse	TGGAGAATTGACGTGTGTG	ATCCCTCATAGGTGACCACTG
<i>Il2ra</i>	SYBR Green	NM_008367	Mouse	AACCATAGTACCCAGTGTCCG	TCCTAAGCAACGCATATAGACCA
<i>Ccl7</i>	SYBR Green	NM_013654	Mouse	GCTGCTTTCAGCATCCAAAGT	CCAGGGACACCGACTACTG
<i>Cd2</i>	SYBR Green	NM_013486	Mouse	TTCTGGTAGTCTTCTTCTGC	TTGGGGATGTTCAAGGGTATG
		NM_0011903			
<i>Ccr6</i>	SYBR Green	33	Mouse	ATGCGGTCAACTTTAACTGTGG	CCCAGAAAGATTGTTGTGCT
		NM_0012538			
<i>Itgal</i>	SYBR Green	74	Mouse	CCAGACTTTTGTACTGAGGAC	GCTTGTCCGGCAGTATAGAG
<i>Bst2</i>	SYBR Green	NM_198095	Mouse	TGTTCCGGGTATCTTAGTCA	GCAGGAGTTTGCCTGTGTCT
Inflammation: Interferon Signaling					
<i>Irf1</i>	SYBR Green	NM_001159396	Mouse	ATGCCAATCACTGAATGGG	TTGTATCGGCTGTGTGAATG
<i>Il18rap</i>	SYBR Green	NM_010553	Mouse	AGACTACTTCTGAGCACAAGA	TGTCCTTACC AATGGTCTCACT
<i>Ccl5</i>	SYBR Green	NM_013653	Mouse	GGTGTCTTGCCTACTCTTCC	TCGAGTGACAACACAGACTGC
<i>Isp15</i>	SYBR Green	NM_015783	Mouse	GGTGTCTGCTGACTAAGCTCC	TGGAAGAGTAAAGCCTGCTCT
<i>Il21r</i>	SYBR Green	NM_021887	Mouse	GGCTGCTTACTCTCTGCTG	TCATCTTGCAGAGTGAAGCTG
<i>Tnfrsf10</i>	SYBR Green	NM_009425	Mouse	ATGGTATTGTCATAGTCTCC	GCAAGCAGGGTCTTCCAGA
<i>Mefv</i>	SYBR Green	NM_001161790	Mouse	TCATCTGCTAAACACCCTGGA	GGGATCTTAGAGTGCCCTTTC
<i>Gbp2</i>	SYBR Green	NM_010260	Mouse	CTGCACATGTGACGGAGCTA	CGGAATCGTCACTCCCACTC
<i>Cd86</i>	SYBR Green	NM_019388	Mouse	TCAATGGGACTGCATATCTGCC	GCCAAAATCACTACAGCTCACT
<i>Stat1</i>	SYBR Green	NM_001205314	Mouse	TCACAGTGGTTCGAGCTTCCAG	CGAGCATCATAGGACGCGTG
Apoptosis: Death Domain Receptors & Caspases in Apoptosis					
<i>Birc3</i>	SYBR Green	NM_007464	Mouse	ACGACAGCAATCGTCAATTTTG	CCTATAACGAGGCTACTGACGG
<i>Card9</i>	SYBR Green	NM_001037747	Mouse	ACTATGAGAATGACGACGAGTGC	GATCCGGGAGGGGTCAATG
<i>Nlrp1a</i>	SYBR Green	NM_001004142	Mouse	GGACCTCATGGTGTACTTTC	TCCCAGGGGCCGTAACCT
<i>Fasr</i>	SYBR Green	NM_001146708	Mouse	GCGGGTTCGTGAAACTGATAA	GCAAAATGGGCCCTCTTGATA
<i>Nlrp12</i>	SYBR Green	NM_001033431	Mouse	GGATGGCTCTATCGACTGTC	CCTCTGCAATCCCAGGAATAA
<i>Tnfrsf14</i>	SYBR Green	NM_019418	Mouse	GTTCCTCTGAGACTGCATCAA	TGGCTCTGTAAAGTGTGCTG
<i>Lta</i>	SYBR Green	NM_010735	Mouse	CCACCTCTTGGAGGTGCTTG	CATGTCCGAGAAAGCAGAT
<i>Casp4</i>	SYBR Green	NM_007609	Mouse	ACAACACCTGACAACACAC	CACCTGCTCAGCATTGTTAA
<i>Tnfrsf8</i>	SYBR Green	NM_009403	Mouse	GCAGTACTTCTACTCAGCA	GCCATCTCTGTTCCATGACAGT
<i>Nod2</i>	SYBR Green	NM_145857	Mouse	CAGGTCTCCGAGAGGTAAGT	GCTACGGATGAGCCAAATGAA
Proteolysis: Connective Tissue Degradation					
<i>Adam8</i>	SYBR Green	NM_007403	Mouse	GCAGGACCACTGCCTCTACC	TGGACCAACTCGGAAAGAGC
<i>Tinag</i>	SYBR Green	NM_012033	Mouse	ACAGACATCTGCAGTGAAGCT	CTTTTGTGCGAGAACTTCA
<i>Serpina3n</i>	SYBR Green	NM_009252	Mouse	GCTCTGCTAGCCCAAAAG	TGAAGCTGTCAAGAGGCTCA
<i>Mmp10</i>	SYBR Green	NM_019471	Mouse	GAGCCACTAGCATCTCTGG	CTGAGCAAGTCCATGCTTGG
<i>Fcst1g</i>	SYBR Green	NM_010185	Mouse	ATCTCAGCCGTGATCTTGTCT	ACCATACAAAACAGGACAGCAT
<i>Adam28</i>	SYBR Green	NM_183366	Mouse	GCAATGGAGTCTTCTGGTATG	ACGCAATGGATGAAGTCTTATGG
<i>Mmp25</i>	SYBR Green	NM_001033339	Mouse	CTCCTGCCGTCTACTACC	GACCTTCCGATCGGGATTCTG
<i>Mmp12</i>	SYBR Green	NM_008605	Mouse	CTGCTCCATGAATGACAGTG	AGTTGCTTCTAGCCCAAGAAC
<i>Mmp3</i>	SYBR Green	NM_010809	Mouse	GGCTTGAACAGTCTTGGC	TGCTCATCGTTCCATCTGCTCA
<i>Tmprss6</i>	SYBR Green	NM_027902	Mouse	ATGCCGAGATGTTTCCAGTCT	GGGCTTGAACCTTCCCTCTG
Cytoskeleton: Actin Filaments					
<i>Tagln</i>	SYBR Green	NM_011526	Mouse	CAACAAGGGTCTATCTACGG	ATCTGGCCGCCTACATCA
<i>Myl9</i>	SYBR Green	NM_172118	Mouse	AGAGGGCTACTGCTCAATGCT	CTCCAGATACTGCTGTGGG
<i>Tln2</i>	SYBR Green	NM_001081242	Mouse	GCCACTGCAATGTGGTGAAG	TCTCCCTAATGACTGCACAGC
<i>Tnnt2</i>	SYBR Green	NM_001130181	Mouse	CAGAGGGGCCAACGTAGAAG	CTCCATCGGGGATCTTGGGT
<i>Tpm2</i>	SYBR Green	NM_009416	Mouse	GTGGCTGAGAGTAAATGTGGG	TTGGTGAATACTTGTCCGCT
<i>Tpm1</i>	SYBR Green	NM_001164252	Mouse	AACGGTGACGAACAATTGAA	GGAAGTATATCTGTGAGAGCG
<i>Sptbn4</i>	SYBR Green	NM_001199235	Mouse	CGGACACAGTGTGACAGAG	CACCGGGGTCTACGCTTGT
<i>Acta1</i>	SYBR Green	NM_009606	Mouse	CCCAAAGCTAACCGGGAGAAG	GACAGCACCGCTGGATAG
<i>Cnn1</i>	SYBR Green	NM_009922	Mouse	TCTGCACATTTAACCGAGGTC	GCCAGCTTGTCTTACTTCAGC
<i>Myh11</i>	SYBR Green	NM_013607	Mouse	ATGAGTGGTCTGTGAGTTG	GCCTGAGAAATGCTGCTCC
Cardiac Development: Wnt/ Beta-Catenin, Notch, VEGF, IP3 and Integrin Signaling					
<i>Adra1a</i>	SYBR Green	NM_013461	Mouse	CTAAGGCCATTCTACTTGGGGT	CGAGTGCAGATGCCGATGA
<i>Hey2</i>	SYBR Green	NM_013904	Mouse	CGCCCTTGTGAGGAAACGA	CCCAGGGTAATTGTTCTGCT
<i>Acta2</i>	SYBR Green	NM_007392	Mouse	CCAGACATGAGGGAGTATGG	TCTATCGATACTACAGCTCA
<i>Tbx2</i>	SYBR Green	NM_009324	Mouse	CGACCCGAGATGCTAAAC	GAATCCGGCTGCTTACACT
<i>Calca</i>	SYBR Green	NM_007587	Mouse	CAGTGCCTTTGAGTCAATCT	CCAGCAGGGCAACTTCTTCT
<i>Myocd</i>	SYBR Green	NM_146386	Mouse	AGGAAGTCCGATCAGTCTTACA	GGTATTAGCCCTTGGTAGCCAG
<i>Pln</i>	SYBR Green	NM_001141927	Mouse	AAAGTCAATACCTCACTCCG	GGCATTTC AATAGTGAGGCTC
<i>Lef1</i>	SYBR Green	NM_010703	Mouse	GCCACGATGAGATGATGCC	TTGATGCTGGCTAAGTCCGC
<i>Kcnd2</i>	SYBR Green	NM_019697	Mouse	TCCAGGACGCTGATGATGCT	TCTGGTATCTGTTCCAGGGTG

Table S2-5. Primer sequences used for Process Network Enrichment validation from PPD3 RNA-seq results

CONCLUSIONS AND FUTURE DIRECTIONS

SECTION 1: RBPJ and Decidualization

The evolutionarily conserved Notch signaling pathway is ubiquitously expressed in cells of many different tissues and is essential for their function and ability to react to their environment^{96,99}. Notch-regulated processes which are specifically important in the context of the current studies include cellular differentiation and survival¹⁰⁸. Based on the induction of NOTCH1 expression in response to the embryonic signal hCG in the non-human primate and during embryo implantation in the mouse, we hypothesized that Notch signaling plays a crucial role during embryo implantation^{112,114}. Generation of a *Notch1* c-KO mouse and *NOTCH1* siRNA knockdown in HuF cells demonstrated that Notch signaling is critical for decidualization by promoting stromal cell survival and aversion of apoptosis^{112,114}. However, embryo implantation was unaffected in *Notch1* c-KO mice since these mice were fertile following a slightly reduced first litter size¹¹⁴. Fecundity and rescue of subsequent litter sizes with *Notch1* loss indicated the potential for compensation by other Notch receptors, which have been described in the context of reproduction, including decidualization^{114,123}. Therefore, I sought to disrupt all Notch receptor (1-4) signaling in order to determine the role of the Notch pathway during the establishment of pregnancy. I hypothesized that selective uterine ablation of the Notch family transcription factor, *Rbpj*, would result in implantation failure and infertility in *Rbpj* c-KO mice.

As expected, loss of *Rbpj* significantly impaired decidualization in mice and resulting initially in subfertility followed by complete infertility. During implantation, failed

decidualization in *Rbpj* c-KO mice was associated with down regulation of Pgr and progesterone target gene expression and the up regulation of Esr1 signaling. During the period of uterine receptivity, Pgr promotes stromal proliferation and ultimately differentiation, while suppressing epithelial proliferation by down regulating Esr1 expression to allow for the embryo to invade through to the underlying stroma⁵³. Similar to *Notch1* c-KO mice, loss of *Rbpj* resulted in down regulation of *Cdk6*, a downstream mediator of Pgr signaling responsible for cell cycle progression during decidualization^{37,39}. Next, I confirmed the translational importance of *RBPJ* expression in HuF cells during *in vitro* decidualization. Consistent with the *in vivo* artificial decidualization study in *Rbpj* c-KO mice, siRNA knockdown of *RBPJ* reduced expression of decidual markers along with *PGR*. However, *ESR1* expression was not affected, suggesting that epithelial Esr1 expression contributes to the up regulated Esr1 signaling in *Rbpj* c-KO mice, since HuF cells represent only isolated stromal cells.

In the initial studies published on the *Rbpj* c-KO mouse, the level of Esr1 was not changed on 4.5 dpc, rather Esr1 phosphorylation was enhanced coupled with increased target gene expression¹²⁴. *Rbpj* was found to interact with Esr1 in both 4.5 dpc mouse uterine protein isolates along with Ishikawa cells to suppress Esr1 phosphorylation¹²⁴. However, our work in *Rbpj* c-KO mice on AD5 mimics the decidual response at 9.5 dpc, which also corresponds to the time point of embryo loss. Therefore, persistence of Esr1 and epithelial proliferation beyond 4.5 dpc may contribute to the reported implantation failure along with a reduction in the decidualization response found in my current study. Our current work in NICD overexpressing mice identifies an additional role for activation of epithelial Esr1 signaling by the Notch pathway, where *Rbpj* likely acts to suppress

Esr1 phosphorylation basally and Notch binding results in activation²⁶⁴. Further, loss of Rbpj partially restores Esr1 signaling with Notch over activation, suggesting a dual role for Rbpj in activating and suppressing Esr1 signaling depending on the state of Notch activation. Our work has shown that balanced Notch signaling is clearly an essential component for normal uterine physiological functioning during implantation.

Cellular survival, proliferation, and differentiation during decidualization depends on the energy status of the cell, and glucose transport plays an important role in these processes⁶⁹⁻⁷¹. Notch signaling through Rbpj is critical for the survival and proliferation of CD4+ memory T cells¹²², which suggested these mechanisms may be conserved within endometrial stromal cells during decidualization. Impaired decidualization was associated with decreased expression of Slc2a1 in Rbpj c-KO mice. Expression of Slc2a1 was more concentrated in the secondary decidual zone, consistent with Rbpj expression during early pregnancy on 8.5 dpc as previously reported¹²⁴. These findings indicate that similar to Notch1, Rbpj is spatially expressed and drives glucose transporter expression for the initiation of decidualization, which subsequently decreases upon completion of decidualization¹¹². I confirmed my findings in HuF cells during *in vitro* decidualization in the presence or absence of *RBPJ*. *SLC2A1* was decreased with *RBPJ* knockdown during decidualization.

In the work performed in mice with *Rbpj*-deficient CD4+ memory T cells, administration of pyruvate was able to bypass the effect of reduced glucose transporter expression to rescue cell survival¹²². I hypothesized that supplementation of supraphysiologic levels of glucose or pyruvate would rescue the decidualization impairment. First, I performed preliminary dose response experiments to determine

whether glucose or pyruvate alone can improve decidualization response and which doses would be considered cytotoxic. Eventually, 8 mM glucose and 16 mM pyruvate (pyruvate doses chosen based on the assumption that 1 mol of glucose is converted to 2 mol of pyruvate) were selected due to minimal osmotic effects without any visual evidence for cell swelling. For comparison, the selected dose of glucose is slightly less than twice the physiologic serum level of 5.56 mM²⁸³. Pyruvate supplementation restored mRNA expression levels of decidual marker *PRL* and *PGR* in *RBPJ* knockdown HuF cells. Therefore, decidual impairments associated with loss of *RBPJ* and glucose transporter expression can be partially overcome through providing exogenous pyruvate.

Future studies need to be performed in order to determine the functional impact of reduced glucose transporter expression due to loss of *RBPJ* during decidualization. This would be accomplished through measurement of uptake of the fluorescently tagged glucose analog 2-NBDG in response to EPC treatment, which has been used in many other studies¹²². Another important question to answer would be whether decidualization in the *Rbpj* c-KO mouse could be rescued through supplementation of glucose or pyruvate, similar to the case in HuF cells. There are multiple approaches that could address this question. However, the most technically feasible, would be to supplement dietary glucose or pyruvate through oral gavage during the period leading up to and after the mechanical scratch. Preliminary studies in order to determine the pharmacokinetics of glucose and/or pyruvate administration would need to be performed. Specifically, bioavailability of these two molecules would be calculated through serum measurements after administration. It may be necessary to determine

tissue distribution to the uterus to ensure a pharmacological effect, although due to the physiological requirement of glucose it could be assumed that serum levels of glucose are distributed evenly to most organs. Additionally, *in vivo* experiments to determine the functional impact of reduced glucose transporter expression in the *Rbpj* c-KO mice could be performed using intravenous 2-NBDG administrations.

Lastly, potential mechanisms contributing to decreased glucose transporter expression with loss of *RBPJ* would need to be elucidated. In CD4⁺ memory T cells, *Rbpj* mediated Akt phosphorylation, and the phenotype of *Rbpj* loss was restored upon viral transduction with constitutively active Akt¹²². Based on previous studies, Akt phosphorylation is induced in the decidua during pregnancy *in vivo*; conversely, its expression is reduced over time during decidualization *in vitro*, suggesting additional factors contribute to maintenance of its expression *in vivo*²⁸⁴. Therefore, it would be useful to assess the expression of Akt phosphorylation in the setting of *RBPJ* loss and determine potential differences in the *Rbpj* c-KO mouse versus decidualizing *RBPJ* knockdown HuF cells. Altogether, these studies have shown a crucial role for Notch signaling through *RBPJ* for both ovarian steroid receptor and glucose transporter expression during decidualization, and the dysregulation of these processes likely contributes to embryo implantation failure.

SECTION 2: RBPJ and Postpartum Repair

During characterization of the fertility phenotype in the *Rbpj* c-KO mouse, the most unanticipated and surprising finding I discovered was the profound effect that *Rbpj* loss had on the postpartum repair process. Based on our previous work in the *Notch1* c-

KO mice, I expected that disrupting all Notch pathway signaling through *Rbpj* would result in decidualization failure, which we hypothesize contributes in part to the initial subfertility in *Rbpj* c-KO mice. However, upon closer scrutiny of the 6-month fertility test data, I observed declining fertility where *Rbpj* c-KO developed complete infertility approximately mid-way through the breeding protocol. In order to determine the cause of infertility, I confirmed that ovulation and fertilization were normal in the infertile *Rbpj* c-KO mice and artificial decidualization response was still reduced similarly to the nulliparous mice. However, the visible, brown uterine banding pattern and large accumulations of nodule cells indicated dysfunctional postpartum repair. Further, immune chemoattractant expression was increased in the decidualized horn of the infertile *Rbpj* c-KO mice, likely contributing to the infertility.

A carefully dissected time course of postpartum repair from PPD 1 to PPD 10 was performed in *Rbpj* c-KO and control mice. Dysfunctional postpartum repair was clearly evident as a consequence of delayed reformation of the mesometrial LE and myometrial isolation of the postpartum nodule. However, during the earliest stages of repair, LE proliferation was increased with associated abnormal hyperplasia forming a “sawtooth” pattern. Additionally, apoptosis was reduced within the LE on PPD1 in *Rbpj* c-KO mice. Initially, enhanced epithelial proliferation on PPD 1 and decreased apoptosis seemed to contradict the delayed postpartum repair phenotype in *Rbpj* c-KO mice. However, staining for epithelial and mesenchymal markers (pan-cytokeratin and vimentin, respectively) revealed accumulations of dual-staining cells present within the LE of *Rbpj* c-KO mice. Dual staining cells were present to a lesser extent in the control mice on PPD1, and triple staining with CC-3 revealed apoptosis of both epithelial cells

and the double-positive cells in these mice. The dual-positive staining epithelial cells persisted in *Rbpj* c-KO mice to PPD3 and were essentially absent at that point in control mice. Mounting evidence supports a role for mesenchymal progenitor cells repopulating the endometrial epithelium following parturition and menstruation, and my work supports these previous studies^{177,178}. Additionally, *Rbpj* may mediate the transformation of stromal cells towards their epithelial phenotype during MET during re-epithelialization after parturition. The inability of these cells to differentiate seems to result in continued proliferation and failure to undergo apoptosis following transformation.

Repair of intestinal wounds, which represent a mucosal surface similar to the endometrium, is dependent on the presence of a layer of dying cells mixed with mucus and fibrin¹⁷²⁻¹⁷⁴. Therefore, the dead epithelial cells may secrete specific signals, which promote mesenchymal progenitors to transform into epithelial cells. Future studies are warranted to understand whether injury to epithelial cells promotes transformation of endometrial stromal cells. To test this hypothesis, cultured immortalized endometrial epithelial cells (EECs)²⁸⁵ would be injured through mechanical scratching of the plate or exposure to ischemia/reperfusion conditions through oxygen starvation. Next, culture media from the injured EECs would be filtered to remove all cellular debris and then added to GFP-labeled immortalized HESCs²⁸⁶. Immunofluorescent staining for pan-cytokeratin would identify any HESCs that transformed to epithelial cells and overlay with GFP would confirm that these cells are derived from stromal cell origin. Additionally, this experiment would identify that secreted factors from injured epithelial cells promote MET.

Based on the histological assessment of morphology and the abnormal

proliferation pattern during postpartum repair in *Rbpj* c-KO mice, I performed RNA-seq on the uterine repair sites on PPD 3. Based on pathway enrichment analysis, failed postpartum repair in *Rbpj* c-KO mice was associated with up regulation of immune signaling and inflammation, including the complement system, neutrophil activation, lymphocyte proliferation and interferon signaling. I randomly selected genes from these enriched pathways to validate by qPCR and confirmed the presence of increased numbers of neutrophils, CD3+ T cells, and macrophages in *Rbpj* c-KO mice by immunostaining. Cell-specific localization of innate immune signaling activator, Complement C3, and M1-macrophage inducer, IFN γ , were determined through dual staining immunofluorescence. Endometrial epithelial and stromal cells of *Rbpj* c-KO mice were responsible for producing high levels of these immune activators. Additionally, M1 macrophage marker, *Nos2*, and secreted factor, *Tnfa*, were increased in *Rbpj* c-KO mice. Increased cytotoxic M1 populations during repair occur through suppression of tissue IFN γ production, where continued expression of IFN γ or presence of M1 macrophages inhibits repair^{157,166}. Initially after parturition, neutrophils are recruited to the endometrium in response to complement activation and products of platelet breakdown¹⁴⁰. However, wound healing will not occur until the immune cell population shifts from an acute pro-inflammatory neutrophil-dominant phenotype towards an anti-inflammatory M2-macrophage-driven response¹⁶⁴. Further, continued secretion of IFN γ and M1-macrophage predominance inhibits wound healing likely due to the production of molecules, like TNF α ^{157,166}.

I have developed potential theories for how disruption of *Rbpj* results in enhanced IFN γ production in *Rbpj* c-KO mice during postpartum repair. Since no *Rbpj*

binding sites are identifiable on the IFN γ promoter, it is unlikely that Rbpj directly regulates IFN γ expression. However, others have described a role for RBPJ expression in basally suppressing IFN γ secretion, in the absence of Notch activation^{278,279}. Since we did not see a postpartum repair phenotype in *Notch1* c-KO mice, this supports a Notch activation-independent function for Rbpj. GATA3, a transcriptional target of Rbpj²⁸⁷, increases IFN γ , and Rbpj may suppress its expression during repair^{246,247}. Inhibition of Notch receptor activation, which subsequently enhances Rbpj repression of target genes, results in reduced IFN γ production^{246,247}. Interestingly, known roles for IFN γ include priming of macrophages for recognition of abnormal cells or viral infected cells for destruction along with enhancing apoptosis and reducing proliferation²⁸⁸. Therefore, it is possible that increased production of IFN γ may occur in a response to abnormal epithelial cell transformation during MET in *Rbpj* c-KO mice to reduce proliferation of abnormal mesenchymal-derived progenitors. A final theory, which may explain why enhanced immune signaling occurs during the postpartum period and persists for months after, includes abnormal vasculature regeneration following parturition. Rbpj has been implicated to promote transformation of endothelial progenitor cells during repair of liver injury, while its absence results in veno-occlusive disease and failed liver regeneration^{227,289}. Additionally, veno-occlusive disease is associated with chronic extravasation of blood into the tissue parenchyma with recruitment of macrophages to phagocytize blood cells, and this predisposes macrophages to iron overload with polarization towards an M1 phenotype^{145,166,167}. This seems particularly relevant in the setting of Rbpj loss, where hemosiderin-laden macrophages are associated with developed infertility. Future studies will need to be performed to determine whether vascular permeability resulting from abnormal postpartum vasculogenesis contributes to

failed postpartum repair and cytotoxic immune recruitment in *Rbpj* c-KO mice.

I have shown that RBPJ is reduced in women with RPL and many phenotypical features of *Rbpj* c-KO mice resemble clinical aspects of RPL. Specifically, *Rbpj* c-KO mice initially display subfertility with mid-gestation fetal loss followed by complete infertility. Developed infertility in *Rbpj* c-KO mice results from failed postpartum repair, which was clearly evidenced by implantation failure following embryo transfer. Similar to *Rbpj* c-KO mice, RPL patients display up regulation of pathways related to regulation of the immune response, such as complement and interferon signaling, along with markers of proteolysis, like matrix metalloproteinases^{257,258}.

Endometrial repair processes are required on a monthly basis in the human endometrium following menstruation. Menstruation and subsequent endometrial repair are hypothesized to precondition the uterus for future pregnancy¹³⁰. Repeated embryo loss and endometrial repair are particularly relevant in the setting of RPL. Therefore, if these repair processes are disrupted similarly to *Rbpj* c-KO mice in women with RPL, then aberrant repair with each cycle or pregnancy loss likely reduces the chances of becoming pregnant. One particularly interesting aim for future work in RPL patients would be to determine whether women with RPL display alterations in mesenchymal stem cell populations and their ability to repopulate the endometrium during the menstrual cycle, which may contribute to dysfunctional repair similar to *Rbpj* c-KO mice.

Overall, I have shown that transformation of endometrial stromal cells during decidualization and postpartum repair are essential for pregnancy and that Notch signaling through *Rbpj* regulates both processes (**Fig 3**). Additionally, I have generated a mouse model for studying RPL, which shares many features with the clinical disease.

Critical Role of RBPJ During Pregnancy and Postpartum Repair

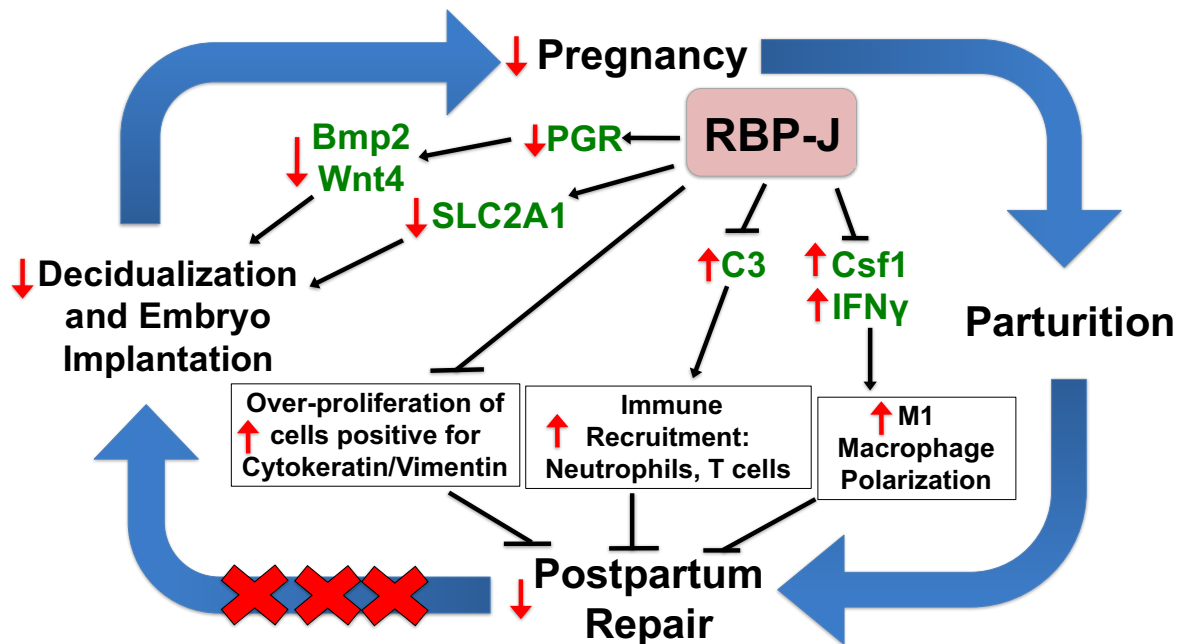


Figure 3. Summary of the role of RBPJ during the establishment of pregnancy and during postpartum repair. As described in this dissertation, the events leading up to pregnancy and postpartum uterine repair are a cycle, where RBPJ plays a central role in regulating many key events. First, RBPJ is critical during decidualization (**Chapter 1**), which occurs through steroid hormone PGR and glucose transporter, SLC2A1 signaling. Loss of *Rbpj* results in initially subfertility in the *Rbpj* c-KO mouse followed by infertility due to failed postpartum repair. Mechanisms by which *Rbpj* promotes postpartum repair is through 1) control of over-proliferation of dual positive cyokeratin/vimentin epithelial cells, 2) suppression of neutrophil and lymphocyte recruitment, and 3) macrophage recruitment and M1 polarization. Ultimately, failed postpartum repair has the potential to disrupt future fertility potential. Red items (arrows, X marks) indicate phenotype associated with RBPJ loss.

The work presented here will have a significant impact on how clinicians and scientists treat RPL. Notch signaling serves as a novel pathway for identifying biomarkers, developing therapeutics and stratifying response to assisted reproductive technologies.

REFERENCES

REFERENCES

1. Cha, J., Sun, X. & Dey, S.K. Mechanisms of implantation: strategies for successful pregnancy. *Nat Med* 18, 1754-1767 (2012). **PMID:23223073**
2. Wang, H. & Dey, S.K. Roadmap to embryo implantation: clues from mouse models. *Nat Rev Genet* 7, 185-199 (2006). **PMID:16485018**
3. Fazleabas, A.T., Donnelly, K.M., Srinivasan, S., Fortman, J.D. & Miller, J.B. Modulation of the baboon (*Papio anubis*) uterine endometrium by chorionic gonadotrophin during the period of uterine receptivity. *Proc Natl Acad Sci U S A* 96, 2543-2548 (1999). **PMID:10051679**
4. Fazleabas, A.T., Kim, J.J. & Strakova, Z. Implantation: embryonic signals and the modulation of the uterine environment--a review. *Placenta* 25 Suppl A, S26-31 (2004). **PMID:15033303**
5. Banerjee, P. & Fazleabas, A.T. Endometrial responses to embryonic signals in the primate. *Int J Dev Biol* 54, 295-302 (2010). **PMID:19876822**
6. Finn, C.A. The biology of decidual cells. *Adv Reprod Physiol* 5, 1-26 (1971). **PMID:4949999**
7. Jayatilak, P.G., Glaser, L.A., Warshaw, M.L., Herz, Z., Gruber, J.R. & Gibori, G. Relationship between luteinizing hormone and decidual luteotropin in the maintenance of luteal steroidogenesis. *Biol Reprod* 31, 556-564 (1984). **PMID:6487695**
8. Lala, P.K. & Graham, C.H. Mechanisms of trophoblast invasiveness and their control: the role of proteases and protease inhibitors. *Cancer Metastasis Rev* 9, 369-379 (1990). **PMID:2097085**
9. Gellersen, B. & Brosens, J.J. Cyclic decidualization of the human endometrium in reproductive health and failure. *Endocr Rev* 35, 851-905 (2014). **PMID:25141152**
10. Weimar, C.H., Macklon, N.S., Post Uiterweer, E.D., Brosens, J.J. & Gellersen, B. The motile and invasive capacity of human endometrial stromal cells:

- implications for normal and impaired reproductive function. *Hum Reprod Update* 19, 542-557 (2013). **PMID:**23827985
11. Anacker, J., Segerer, S.E., Hagemann, C., Feix, S., Kapp, M., Bausch, R. & Kammerer, U. Human decidua and invasive trophoblasts are rich sources of nearly all human matrix metalloproteinases. *Mol Hum Reprod* 17, 637-652 (2011). **PMID:**21565864
 12. Grewal, S., Carver, J., Ridley, A.J. & Mardon, H.J. Human endometrial stromal cell rho GTPases have opposing roles in regulating focal adhesion turnover and embryo invasion in vitro. *Biol Reprod* 83, 75-82 (2010). **PMID:**20357266
 13. Nancy, P., Tagliani, E., Tay, C.S., Asp, P., Levy, D.E. & Erlebacher, A. Chemokine gene silencing in decidual stromal cells limits T cell access to the maternal-fetal interface. *Science* 336, 1317-1321 (2012). **PMID:**22679098
 14. Erlebacher, A. Immunology of the maternal-fetal interface. *Annu Rev Immunol* 31, 387-411 (2013). **PMID:**23298207
 15. Goddard, L.M., Murphy, T.J., Org, T., Enciso, J.M., Hashimoto-Partyka, M.K., Warren, C.M., Domigan, C.K., McDonald, A.I., He, H., Sanchez, L.A., Allen, N.C., Orsenigo, F., Chao, L.C., Dejana, E., Tontonoz, P., Mikkola, H.K. & Iruela-Arispe, M.L. Progesterone receptor in the vascular endothelium triggers physiological uterine permeability preimplantation. *Cell* 156, 549-562 (2014). **PMID:**24485460
 16. Lim, H., Paria, B.C., Das, S.K., Dinchuk, J.E., Langenbach, R., Trzaskos, J.M. & Dey, S.K. Multiple female reproductive failures in cyclooxygenase 2-deficient mice. *Cell* 91, 197-208 (1997). **PMID:**9346237
 17. Salker, M., Teklenburg, G., Molokhia, M., Lavery, S., Trew, G., Aojanpong, T., Mardon, H.J., Lokugamage, A.U., Rai, R., Landles, C., Roelen, B.A., Quenby, S., Kuijk, E.W., Kavelaars, A., Heijnen, C.J., Regan, L., Macklon, N.S. & Brosens, J.J. Natural selection of human embryos: impaired decidualization of endometrium disables embryo-maternal interactions and causes recurrent pregnancy loss. *PLoS One* 5, e10287 (2010). **PMID:**20422017
 18. Plaks, V., Rinkenberger, J., Dai, J., Flannery, M., Sund, M., Kanasaki, K., Ni, W., Kalluri, R. & Werb, Z. Matrix metalloproteinase-9 deficiency phenocopies features of preeclampsia and intrauterine growth restriction. *Proceedings of the National Academy of Sciences of the United States of America* 110, 11109-11114 (2013). **PMID:**23776237

19. Su, R.W., Strug, M.R., Joshi, N.R., Jeong, J.W., Miele, L., Lessey, B.A., Young, S.L. & Fazleabas, A.T. Decreased Notch pathway signaling in the endometrium of women with endometriosis impairs decidualization. *J Clin Endocrinol Metab* 100, E433-442 (2015). **PMID:25546156**
20. TH, H. *A Manual of the Anatomy of Vertebrate Animals*, (D. Appleton, New York, 1898).
21. Enders, A.C. & Carter, A.M. Review: The evolving placenta: different developmental paths to a hemochorial relationship. *Placenta* 33 Suppl, S92-98 (2012). **PMID:22061678**
22. Rock, J. & Bartlett, M.K. Biopsy studies of human endometrium: criteria of dating and information about amenorrhea, menorrhagia, and time of ovulation. *J Am Med Assoc* 108, 2022-2028 (1937). **PMID:12255649**
23. Johansson, E.D. & Wide, L. Periovulatory levels of plasma progesterone and luteinizing hormone in women. *Acta Endocrinol (Copenh)* 62, 82-88 (1969). **PMID:5394291**
24. Tang, B. & Gurside, E. Direct effect of gonadotropins on decidualization of human endometrial stroma cells. *J Steroid Biochem Mol Biol* 47, 115-121 (1993). **PMID:8274425**
25. Han, S.W., Lei, Z.M. & Rao, C.V. Treatment of human endometrial stromal cells with chorionic gonadotropin promotes their morphological and functional differentiation into decidua. *Mol Cell Endocrinol* 147, 7-16 (1999). **PMID:10195687**
26. Kasahara, K., Takakura, K., Takebayashi, K., Kimura, F., Nakanishi, K. & Noda, Y. The role of human chorionic gonadotropin on decidualization of endometrial stromal cells in vitro. *J Clin Endocrinol Metab* 86, 1281-1286 (2001). **PMID:11238521**
27. Tang, B., Guller, S. & Gurside, E. Cyclic adenosine 3',5'-monophosphate induces prolactin expression in stromal cells isolated from human proliferative endometrium. *Endocrinology* 133, 2197-2203 (1993). **PMID:8404671**

28. Kim, J.J., Jaffe, R.C. & Fazleabas, A.T. Comparative studies on the in vitro decidualization process in the baboon (*Papio anubis*) and human. *Biol Reprod* 59, 160-168 (1998). **PMID:**9675007
29. Tseng, L., Gao, J.G., Chen, R., Zhu, H.H., Mazella, J. & Powell, D.R. Effect of progestin, antiprogestin, and relaxin on the accumulation of prolactin and insulin-like growth factor-binding protein-1 messenger ribonucleic acid in human endometrial stromal cells. *Biol Reprod* 47, 441-450 (1992). **PMID:**1380842
30. Frank, G.R., Brar, A.K., Cedars, M.I. & Handwerger, S. Prostaglandin E2 enhances human endometrial stromal cell differentiation. *Endocrinology* 134, 258-263 (1994). **PMID:**7506205
31. Dimitriadis, E., Stoikos, C., Baca, M., Fairlie, W.D., McCoubrie, J.E. & Salamonsen, L.A. Relaxin and prostaglandin E(2) regulate interleukin 11 during human endometrial stromal cell decidualization. *J Clin Endocrinol Metab* 90, 3458-3465 (2005). **PMID:**15784719
32. Karpovich, N., Klemmt, P., Hwang, J.H., McVeigh, J.E., Heath, J.K., Barlow, D.H. & Mardon, H.J. The production of interleukin-11 and decidualization are compromised in endometrial stromal cells derived from patients with infertility. *J Clin Endocrinol Metab* 90, 1607-1612 (2005). **PMID:**15613426
33. Strakova, Z., Mavrogianis, P., Meng, X., Hastings, J.M., Jackson, K.S., Cameo, P., Brudney, A., Knight, O. & Fazleabas, A.T. In vivo infusion of interleukin-1beta and chorionic gonadotropin induces endometrial changes that mimic early pregnancy events in the baboon. *Endocrinology* 146, 4097-4104 (2005). **PMID:**15932926
34. Geisert, R., Fazleabas, A., Lucy, M. & Mathew, D. Interaction of the conceptus and endometrium to establish pregnancy in mammals: role of interleukin 1beta. *Cell Tissue Res* 349, 825-838 (2012). **PMID:**22382391
35. Maslar, I.A. & Riddick, D.H. Prolactin production by human endometrium during the normal menstrual cycle. *Am J Obstet Gynecol* 135, 751-754 (1979). **PMID:**495675
36. Daly, D.C., Maslar, I.A. & Riddick, D.H. Prolactin production during in vitro decidualization of proliferative endometrium. *Am J Obstet Gynecol* 145, 672-678 (1983). **PMID:**6829654

37. Stefanoska, I., Jovanovic Krivokuca, M., Vasilijic, S., Cujic, D. & Vicovac, L. Prolactin stimulates cell migration and invasion by human trophoblast in vitro. *Placenta* 34, 775-783 (2013). **PMID:**23849393
38. Corbacho, A.M., Martinez De La Escalera, G. & Clapp, C. Roles of prolactin and related members of the prolactin/growth hormone/placental lactogen family in angiogenesis. *J Endocrinol* 173, 219-238 (2002). **PMID:**12010630
39. Jabbour, H.N. & Critchley, H.O. Potential roles of decidual prolactin in early pregnancy. *Reproduction* 121, 197-205 (2001). **PMID:**11226044
40. Gleeson, L.M., Chakraborty, C., McKinnon, T. & Lala, P.K. Insulin-like growth factor-binding protein 1 stimulates human trophoblast migration by signaling through alpha 5 beta 1 integrin via mitogen-activated protein Kinase pathway. *J Clin Endocrinol Metab* 86, 2484-2493 (2001). **PMID:**11397844
41. Brosens, J.J., Hayashi, N. & White, J.O. Progesterone receptor regulates decidual prolactin expression in differentiating human endometrial stromal cells. *Endocrinology* 140, 4809-4820 (1999). **PMID:**10499541
42. Ramathal, C.Y., Bagchi, I.C., Taylor, R.N. & Bagchi, M.K. Endometrial decidualization: of mice and men. *Semin Reprod Med* 28, 17-26 (2010). **PMID:**20104425
43. Cochrane, R.L. & Meyer, R.K. Delayed nidation in the rat induced by progesterone. *Proc Soc Exp Biol Med* 96, 155-159 (1957). **PMID:**13485043
44. Glasser SR, M.J., Mani SK, Julian J, Munir MI, Lampelo S, Soares MJ. Blastocyst-endometrial relationships: Reciprocal interactions between uterine epithelial and stromal cells and blastocysts. *Trophoblast Research* 5, 229-280 (1991).
45. Lee, K.Y. & DeMayo, F.J. Animal models of implantation. *Reproduction* 128, 679-695 (2004). **PMID:**15579585
46. Branda, C.S. & Dymecki, S.M. Talking about a revolution: The impact of site-specific recombinases on genetic analyses in mice. *Dev Cell* 6, 7-28 (2004). **PMID:**14723844

47. Mukherjee, A., Amato, P., Allred, D.C., Fernandez-Valdivia, R., Nguyen, J., O'Malley, B.W., DeMayo, F.J. & Lydon, J.P. Steroid receptor coactivator 2 is essential for progesterone-dependent uterine function and mammary morphogenesis: insights from the mouse--implications for the human. *J Steroid Biochem Mol Biol* 102, 22-31 (2006). **PMID:17045797**
48. Lee, K., Jeong, J., Tsai, M.J., Tsai, S., Lydon, J.P. & DeMayo, F.J. Molecular mechanisms involved in progesterone receptor regulation of uterine function. *J Steroid Biochem Mol Biol* 102, 41-50 (2006). **PMID:17067792**
49. Lee, K., Jeong, J., Kwak, I., Yu, C.T., Lanske, B., Soegiarto, D.W., Toftgard, R., Tsai, M.J., Tsai, S., Lydon, J.P. & DeMayo, F.J. Indian hedgehog is a major mediator of progesterone signaling in the mouse uterus. *Nat Genet* 38, 1204-1209 (2006). **PMID:16951680**
50. Soyol, S.M., Mukherjee, A., Lee, K.Y., Li, J., Li, H., DeMayo, F.J. & Lydon, J.P. Cre-mediated recombination in cell lineages that express the progesterone receptor. *Genesis* 41, 58-66 (2005). **PMID:15682389**
51. Schust, D.J., Anderson, D.J. & Hill, J.A. Progesterone-induced immunosuppression is not mediated through the progesterone receptor. *Hum Reprod* 11, 980-985 (1996). **PMID:8671374**
52. Mansour, I., Reznikoff-Etievant, M.F. & Netter, A. No evidence for the expression of the progesterone receptor on peripheral blood lymphocytes during pregnancy. *Hum Reprod* 9, 1546-1549 (1994). **PMID:7989520**
53. Large, M.J. & DeMayo, F.J. The regulation of embryo implantation and endometrial decidualization by progesterone receptor signaling. *Mol Cell Endocrinol* 358, 155-165 (2012). **PMID:21821095**
54. Lydon, J.P., DeMayo, F.J., Funk, C.R., Mani, S.K., Hughes, A.R., Montgomery, C.A., Jr., Shyamala, G., Conneely, O.M. & O'Malley, B.W. Mice lacking progesterone receptor exhibit pleiotropic reproductive abnormalities. *Genes Dev* 9, 2266-2278 (1995). **PMID:7557380**
55. Franco, H.L., Rubel, C.A., Large, M.J., Wetendorf, M., Fernandez-Valdivia, R., Jeong, J.W., Spencer, T.E., Behringer, R.R., Lydon, J.P. & Demayo, F.J. Epithelial progesterone receptor exhibits pleiotropic roles in uterine development and function. *FASEB J* 26, 1218-1227 (2012). **PMID:22155565**

56. Lim, H., Ma, L., Ma, W.G., Maas, R.L. & Dey, S.K. Hoxa-10 regulates uterine stromal cell responsiveness to progesterone during implantation and decidualization in the mouse. *Molecular endocrinology* 13, 1005-1017 (1999). **PMID:**10379898
57. Kurihara, I., Lee, D.K., Petit, F.G., Jeong, J., Lee, K., Lydon, J.P., DeMayo, F.J., Tsai, M.J. & Tsai, S.Y. COUP-TFII mediates progesterone regulation of uterine implantation by controlling ER activity. *PLoS Genet* 3, e102 (2007). **PMID:**17590085
58. Lee, K.Y., Jeong, J.W., Wang, J., Ma, L., Martin, J.F., Tsai, S.Y., Lydon, J.P. & DeMayo, F.J. Bmp2 is critical for the murine uterine decidual response. *Mol Cell Biol* 27, 5468-5478 (2007). **PMID:**17515606
59. Li, Q., Kannan, A., Wang, W., Demayo, F.J., Taylor, R.N., Bagchi, M.K. & Bagchi, I.C. Bone morphogenetic protein 2 functions via a conserved signaling pathway involving Wnt4 to regulate uterine decidualization in the mouse and the human. *J Biol Chem* 282, 31725-31732 (2007). **PMID:**17711857
60. Franco, H.L., Dai, D., Lee, K.Y., Rubel, C.A., Roop, D., Boerboom, D., Jeong, J.W., Lydon, J.P., Bagchi, I.C., Bagchi, M.K. & DeMayo, F.J. WNT4 is a key regulator of normal postnatal uterine development and progesterone signaling during embryo implantation and decidualization in the mouse. *FASEB J* 25, 1176-1187 (2011). **PMID:**21163860
61. Li, Q., Kannan, A., Das, A., Demayo, F.J., Hornsby, P.J., Young, S.L., Taylor, R.N., Bagchi, M.K. & Bagchi, I.C. WNT4 acts downstream of BMP2 and functions via beta-catenin signaling pathway to regulate human endometrial stromal cell differentiation. *Endocrinology* 154, 446-457 (2013). **PMID:**23142810
62. Rahman, M.A., Li, M., Li, P., Wang, H., Dey, S.K. & Das, S.K. Hoxa-10 deficiency alters region-specific gene expression and perturbs differentiation of natural killer cells during decidualization. *Dev Biol* 290, 105-117 (2006). **PMID:**16337623
63. Chakraborty, I., Das, S.K., Wang, J. & Dey, S.K. Developmental expression of the cyclo-oxygenase-1 and cyclo-oxygenase-2 genes in the peri-implantation mouse uterus and their differential regulation by the blastocyst and ovarian steroids. *Journal of molecular endocrinology* 16, 107-122 (1996). **PMID:**9156514
64. von Bubnoff, A. & Cho, K.W. Intracellular BMP signaling regulation in vertebrates: pathway or network? *Dev Biol* 239, 1-14 (2001). **PMID:**11784015

65. Whitman, M. Smads and early developmental signaling by the TGFbeta superfamily. *Genes Dev* 12, 2445-2462 (1998). **PMID:9716398**
66. Massague, J. & Chen, Y.G. Controlling TGF-beta signaling. *Genes Dev* 14, 627-644 (2000). **PMID:10733523**
67. Wrana, J.L., Attisano, L., Wieser, R., Ventura, F. & Massague, J. Mechanism of activation of the TGF-beta receptor. *Nature* 370, 341-347 (1994). **PMID:8047140**
68. MacDonald, B.T., Tamai, K. & He, X. Wnt/beta-catenin signaling: components, mechanisms, and diseases. *Dev Cell* 17, 9-26 (2009). **PMID:19619488**
69. Frolova, A.I. & Moley, K.H. Glucose transporters in the uterus: an analysis of tissue distribution and proposed physiological roles. *Reproduction* 142, 211-220 (2011). **PMID:21642384**
70. von Wolff, M., Ursel, S., Hahn, U., Steldinger, R. & Strowitzki, T. Glucose transporter proteins (GLUT) in human endometrium: expression, regulation, and function throughout the menstrual cycle and in early pregnancy. *J Clin Endocrinol Metab* 88, 3885-3892 (2003). **PMID:12915684**
71. Frolova, A., Flessner, L., Chi, M., Kim, S.T., Foyouzi-Yousefi, N. & Moley, K.H. Facilitative glucose transporter type 1 is differentially regulated by progesterone and estrogen in murine and human endometrial stromal cells. *Endocrinology* 150, 1512-1520 (2009). **PMID:18948400**
72. Kim, S.T. & Moley, K.H. Regulation of facilitative glucose transporters and AKT/MAPK/PRKAA signaling via estradiol and progesterone in the mouse uterine epithelium. *Biol Reprod* 81, 188-198 (2009). **PMID:19208550**
73. Frolova, A.I. & Moley, K.H. Quantitative analysis of glucose transporter mRNAs in endometrial stromal cells reveals critical role of GLUT1 in uterine receptivity. *Endocrinology* 152, 2123-2128 (2011). **PMID:21343253**
74. Augustin, R. The protein family of glucose transport facilitators: It's not only about glucose after all. *IUBMB Life* 62, 315-333 (2010). **PMID:20209635**

75. Yamaguchi, M., Sakata, M., Ogura, K. & Miyake, A. Gestational changes of glucose transporter gene expression in the mouse placenta and decidua. *J Endocrinol Invest* 19, 567-569 (1996). **PMID:**8905482
76. Smith, S.D., Dunk, C.E., Aplin, J.D., Harris, L.K. & Jones, R.L. Evidence for immune cell involvement in decidual spiral arteriole remodeling in early human pregnancy. *Am J Pathol* 174, 1959-1971 (2009). **PMID:**19349361
77. Lidstrom, C., Matthiesen, L., Berg, G., Sharma, S., Ernerudh, J. & Ekerfelt, C. Cytokine secretion patterns of NK cells and macrophages in early human pregnancy decidua and blood: implications for suppressor macrophages in decidua. *Am J Reprod Immunol* 50, 444-452 (2003). **PMID:**14750551
78. Salker, M.S., Nautiyal, J., Steel, J.H., Webster, Z., Sucurovic, S., Nicou, M., Singh, Y., Lucas, E.S., Murakami, K., Chan, Y.W., James, S., Abdallah, Y., Christian, M., Croy, B.A., Mulac-Jericevic, B., Quenby, S. & Brosens, J.J. Disordered IL-33/ST2 activation in decidualizing stromal cells prolongs uterine receptivity in women with recurrent pregnancy loss. *PLoS One* 7, e52252 (2012). **PMID:**23300625
79. Bulmer, J.N., Morrison, L., Longfellow, M., Ritson, A. & Pace, D. Granulated lymphocytes in human endometrium: histochemical and immunohistochemical studies. *Human reproduction* 6, 791-798 (1991). **PMID:**1757516
80. Tabibzadeh, S.S., X.Z.; Kong, Q.F.; Kasnic, G.; Miller, J.; Satyaswaroop, P.G. Induction of a polarized micro-environment by human T cells and interferon-gamma in three-dimensional spheroid cultures of human endometrial epithelial cells. *Hum Reprod* 8, 182-192 (1992).
81. Stewart, C.J., Farquharson, M.A. & Foulis, A.K. The distribution and possible function of gamma interferon-immunoreactive cells in normal endometrium and myometrium. *Virchows Arch A Pathol Anat Histopathol* 420, 419-424 (1992). **PMID:**1375796
82. Christian, M., Marangos, P., Mak, I., McVey, J., Barker, F., White, J. & Brosens, J.J. Interferon-gamma modulates prolactin and tissue factor expression in differentiating human endometrial stromal cells. *Endocrinology* 142, 3142-3151 (2001). **PMID:**11416037
83. Inoue, T., Kanzaki, H., Iwai, M., Imai, K., Narukawa, S., Higuchi, T., Katsuragawa, H. & Mori, T. Tumour necrosis factor alpha inhibits in-vitro

- decidualization of human endometrial stromal cells. *Hum Reprod* 9, 2411-2417 (1994). **PMID:7714166**
84. Spratte, J., Oemus, A., Zygmunt, M. & Fluhr, H. Interferon-gamma differentially modulates the impact of tumor necrosis factor-alpha on human endometrial stromal cells. *Reprod Biol* 15, 146-153 (2015). **PMID:26370457**
 85. Todt, J.C., Yang, Y., Lei, J., Lauria, M.R., Sorokin, Y., Cotton, D.B. & Yelian, F.D. Effects of tumor necrosis factor-alpha on human trophoblast cell adhesion and motility. *Am J Reprod Immunol* 36, 65-71 (1996). **PMID:8862248**
 86. Pollard, J.W., Hunt, J.S., Wiktor-Jedrzejczak, W. & Stanley, E.R. A pregnancy defect in the osteopetrotic (op/op) mouse demonstrates the requirement for CSF-1 in female fertility. *Dev Biol* 148, 273-283 (1991). **PMID:1834496**
 87. Stewart, I.J. & Mitchell, B.S. The distribution of uterine macrophages in virgin and early pregnant mice. *J Anat* 179, 183-196 (1991). **PMID:1817136**
 88. Brandon, J.M. Macrophage distribution in decidual tissue from early implantation to the periparturient period in mice as defined by the macrophage differentiation antigens F4/80, macrosialin and the type 3 complement receptor. *J Reprod Fertil* 103, 9-16 (1995). **PMID:7707305**
 89. Tagliani, E., Shi, C., Nancy, P., Tay, C.S., Pamer, E.G. & Erlebacher, A. Coordinate regulation of tissue macrophage and dendritic cell population dynamics by CSF-1. *J Exp Med* 208, 1901-1916 (2011). **PMID:21825019**
 90. Heikkinen, J., Mottonen, M., Komi, J., Alanen, A. & Lassila, O. Phenotypic characterization of human decidual macrophages. *Clin Exp Immunol* 131, 498-505 (2003). **PMID:12605704**
 91. Gustafsson, C., Mjosberg, J., Matussek, A., Geffers, R., Matthiesen, L., Berg, G., Sharma, S., Buer, J. & Ernerudh, J. Gene expression profiling of human decidual macrophages: evidence for immunosuppressive phenotype. *PLoS One* 3, e2078 (2008). **PMID:18446208**
 92. Cupurdija, K., Azzola, D., Hainz, U., Gratchev, A., Heitger, A., Takikawa, O., Goerdt, S., Wintersteiger, R., Dohr, G. & Sedlmayr, P. Macrophages of human first trimester decidua express markers associated to alternative activation. *Am J Reprod Immunol* 51, 117-122 (2004). **PMID:14748837**

93. Dexter, J.S. The analysis of a case of continuous variation in *Drosophila* by a study of its linkage relationships. *Am Nat* 48, 712-758 (1914).
94. Kidd, S., Kelley, M.R. & Young, M.W. Sequence of the notch locus of *Drosophila melanogaster*: relationship of the encoded protein to mammalian clotting and growth factors. *Mol Cell Biol* 6, 3094-3108 (1986). **PMID:3097517**
95. Wharton, K.A., Johansen, K.M., Xu, T. & Artavanis-Tsakonas, S. Nucleotide sequence from the neurogenic locus notch implies a gene product that shares homology with proteins containing EGF-like repeats. *Cell* 43, 567-581 (1985). **PMID:3935325**
96. Artavanis-Tsakonas, S., Rand, M.D. & Lake, R.J. Notch signaling: cell fate control and signal integration in development. *Science* 284, 770-776 (1999). **PMID:10221902**
97. Borggreffe, T. & Oswald, F. The Notch signaling pathway: transcriptional regulation at Notch target genes. *Cell Mol Life Sci* 66, 1631-1646 (2009). **PMID:19165418**
98. Bray, S.J. Notch signalling: a simple pathway becomes complex. *Nat Rev Mol Cell Biol* 7, 678-689 (2006). **PMID:16921404**
99. D'Souza, B., Meloty-Kapella, L. & Weinmaster, G. Canonical and non-canonical Notch ligands. *Curr Top Dev Biol* 92, 73-129 (2010). **PMID:20816393**
100. Tamura, K., Taniguchi, Y., Minoguchi, S., Sakai, T., Tun, T., Furukawa, T. & Honjo, T. Physical interaction between a novel domain of the receptor Notch and the transcription factor RBP-J kappa/Su(H). *Curr Biol* 5, 1416-1423 (1995). **PMID:8749394**
101. Kageyama, R. & Ohtsuka, T. The Notch-Hes pathway in mammalian neural development. *Cell Res* 9, 179-188 (1999). **PMID:10520600**
102. Iso, T., Kedes, L. & Hamamori, Y. HES and HERP families: multiple effectors of the Notch signaling pathway. *J Cell Physiol* 194, 237-255 (2003). **PMID:12548545**

103. Kopan, R. & Ilagan, M.X. The canonical Notch signaling pathway: unfolding the activation mechanism. *Cell* 137, 216-233 (2009). **PMID:**19379690
104. Tun, T., Hamaguchi, Y., Matsunami, N., Furukawa, T., Honjo, T. & Kawaichi, M. Recognition sequence of a highly conserved DNA binding protein RBP-J kappa. *Nucleic Acids Res* 22, 965-971 (1994). **PMID:**8152928
105. Castel, D., Mourikis, P., Bartels, S.J., Brinkman, A.B., Tajbakhsh, S. & Stunnenberg, H.G. Dynamic binding of RBPJ is determined by Notch signaling status. *Genes Dev* 27, 1059-1071 (2013). **PMID:**23651858
106. Radtke, F., Wilson, A., Stark, G., Bauer, M., van Meerwijk, J., MacDonald, H.R. & Aguet, M. Deficient T cell fate specification in mice with an induced inactivation of Notch1. *Immunity* 10, 547-558 (1999). **PMID:**10367900
107. Santos, M.A., Sarmiento, L.M., Rebelo, M., Doce, A.A., Maillard, I., Dumortier, A., Neves, H., Radtke, F., Pear, W.S., Parreira, L. & Demengeot, J. Notch1 engagement by Delta-like-1 promotes differentiation of B lymphocytes to antibody-secreting cells. *Proc Natl Acad Sci U S A* 104, 15454-15459 (2007). **PMID:**17878313
108. Miele, L. & Osborne, B. Arbiter of differentiation and death: Notch signaling meets apoptosis. *J Cell Physiol* 181, 393-409 (1999). **PMID:**10528225
109. Miele, L. Notch signaling. *Clin Cancer Res* 12, 1074-1079 (2006). **PMID:**16489059
110. Kim, J.J., Jaffe, R.C. & Fazleabas, A.T. Insulin-like growth factor binding protein-1 expression in baboon endometrial stromal cells: regulation by filamentous actin and requirement for de novo protein synthesis. *Endocrinology* 140, 997-1004 (1999). **PMID:**9927334
111. Jasinska, A., Strakova, Z., Szmidt, M. & Fazleabas, A.T. Human chorionic gonadotropin and decidualization in vitro inhibits cytochalasin-D-induced apoptosis in cultured endometrial stromal fibroblasts. *Endocrinology* 147, 4112-4121 (2006). **PMID:**16740972
112. Afshar, Y., Miele, L. & Fazleabas, A.T. Notch1 is regulated by chorionic gonadotropin and progesterone in endometrial stromal cells and modulates

- decidualization in primates. *Endocrinology* 153, 2884-2896 (2012). **PMID:22535768**
113. Strug, M.R., Su, R., Young, J.E., Dodds, W.G., Shavell, V.I., Diaz-Gimeno, P., Ruiz-Alonso, M., Simon, C., Lessey, B.A., Leach, R.E. & Fazleabas, A.T. Intrauterine human chorionic gonadotropin infusion in oocyte donors promotes endometrial synchrony and induction of early decidual markers for stromal survival: a randomized clinical trial. *Hum Reprod* (2016). **PMID:27122490**
 114. Afshar, Y., Jeong, J.W., Roqueiro, D., DeMayo, F., Lydon, J., Radtke, F., Radnor, R., Miele, L. & Fazleabas, A. Notch1 mediates uterine stromal differentiation and is critical for complete decidualization in the mouse. *FASEB J* 26, 282-294 (2012). **PMID:21990372**
 115. Limbourg, F.P., Takeshita, K., Radtke, F., Bronson, R.T., Chin, M.T. & Liao, J.K. Essential role of endothelial Notch1 in angiogenesis. *Circulation* 111, 1826-1832 (2005). **PMID:15809373**
 116. Swiatek, P.J., Lindsell, C.E., del Amo, F.F., Weinmaster, G. & Gridley, T. Notch1 is essential for postimplantation development in mice. *Genes Dev* 8, 707-719 (1994). **PMID:7926761**
 117. Finn, C.A. & Martin, L. Endocrine control of the timing of endometrial sensitivity to a decidual stimulus. *Biol Reprod* 7, 82-86 (1972). **PMID:5050152**
 118. Manaster, I., Gazit, R., Goldman-Wohl, D., Stern-Ginossar, N., Mizrahi, S., Yagel, S. & Mandelboim, O. Notch activation enhances IFN γ secretion by human peripheral blood and decidual NK cells. *J Reprod Immunol* 84, 1-7 (2010). **PMID:20004979**
 119. Ashkar, A.A., Di Santo, J.P. & Croy, B.A. Interferon gamma contributes to initiation of uterine vascular modification, decidual integrity, and uterine natural killer cell maturation during normal murine pregnancy. *J Exp Med* 192, 259-270 (2000). **PMID:10899912**
 120. Aluvihare, V.R., Kallikourdis, M. & Betz, A.G. Regulatory T cells mediate maternal tolerance to the fetus. *Nat Immunol* 5, 266-271 (2004). **PMID:14758358**
 121. Fu, T., Zhang, P., Feng, L., Ji, G., Wang, X.H., Zheng, M.H., Qin, H.Y., Chen, D.L., Wang, W.Z. & Han, H. Accelerated acute allograft rejection accompanied

- by enhanced T-cell proliferation and attenuated Treg function in RBP-J deficient mice. *Mol Immunol* 48, 751-759 (2011). **PMID:**21168915
122. Maekawa, Y., Ishifune, C., Tsukumo, S., Hozumi, K., Yagita, H. & Yasutomo, K. Notch controls the survival of memory CD4⁺ T cells by regulating glucose uptake. *Nat Med* 21, 55-61 (2015). **PMID:**25501905
 123. Otti, G.R., Saleh, L., Velicky, P., Fiala, C., Pollheimer, J. & Knofler, M. Notch2 controls prolactin and insulin-like growth factor binding protein-1 expression in decidualizing human stromal cells of early pregnancy. *PLoS One* 9, e112723 (2014). **PMID:**25397403
 124. Zhang, S., *et al.* Uterine Rbpj is required for embryonic-uterine orientation and decidual remodeling via Notch pathway-independent and -dependent mechanisms. *Cell Res* 24, 925-942 (2014). **PMID:**24971735
 125. Oka, C., Nakano, T., Wakeham, A., de la Pompa, J.L., Mori, C., Sakai, T., Okazaki, S., Kawaichi, M., Shiota, K., Mak, T.W. & Honjo, T. Disruption of the mouse RBP-J kappa gene results in early embryonic death. *Development* 121, 3291-3301 (1995). **PMID:**7588063
 126. Han, H., Tanigaki, K., Yamamoto, N., Kuroda, K., Yoshimoto, M., Nakahata, T., Ikuta, K. & Honjo, T. Inducible gene knockout of transcription factor recombination signal binding protein-J reveals its essential role in T versus B lineage decision. *Int Immunol* 14, 637-645 (2002). **PMID:**12039915
 127. Salamonsen, L.A. Tissue injury and repair in the female human reproductive tract. *Reproduction* 125, 301-311 (2003). **PMID:**12611594
 128. Evans, J., Kaitu'u-Lino, T. & Salamonsen, L.A. Extracellular matrix dynamics in scar-free endometrial repair: perspectives from mouse in vivo and human in vitro studies. *Biol Reprod* 85, 511-523 (2011). **PMID:**21613633
 129. Emera, D., Romero, R. & Wagner, G. The evolution of menstruation: a new model for genetic assimilation: explaining molecular origins of maternal responses to fetal invasiveness. *Bioessays* 34, 26-35 (2012). **PMID:**22057551
 130. Brosens, J.J., Parker, M.G., McIndoe, A., Pijnenborg, R. & Brosens, I.A. A role for menstruation in preconditioning the uterus for successful pregnancy. *Am J Obstet Gynecol* 200, 615 e611-616 (2009). **PMID:**19136085

131. Finn, C.A. & Martin, L. Patterns of cell division in the mouse uterus during early pregnancy. *J Endocrinol* 39, 593-597 (1967). **PMID:**6075199
132. Pollard, J.W., Pacey, J., Cheng, S.V. & Jordan, E.G. Estrogens and cell death in murine uterine luminal epithelium. *Cell Tissue Res* 249, 533-540 (1987). **PMID:**3664603
133. Finn, C.A. & Pope, M. Vascular and cellular changes in the decidualized endometrium of the ovariectomized mouse following cessation of hormone treatment: a possible model for menstruation. *J Endocrinol* 100, 295-300 (1984). **PMID:**6699534
134. Xu, X.B., He, B. & Wang, J.D. Menstrual-like changes in mice are provoked through the pharmacologic withdrawal of progesterone using mifepristone following induction of decidualization. *Hum Reprod* 22, 3184-3191 (2007). **PMID:**17921135
135. Kaitu'u-Lino, T.J., Ye, L. & Gargett, C.E. Reepithelialization of the uterine surface arises from endometrial glands: evidence from a functional mouse model of breakdown and repair. *Endocrinology* 151, 3386-3395 (2010). **PMID:**20444944
136. Rudolph, M., Docke, W.D., Muller, A., Menning, A., Rose, L., Zollner, T.M. & Gashaw, I. Induction of overt menstruation in intact mice. *PLoS One* 7, e32922 (2012). **PMID:**22412950
137. Cha, J., Bartos, A., Egashira, M., Haraguchi, H., Saito-Fujita, T., Leishman, E., Bradshaw, H., Dey, S.K. & Hirota, Y. Combinatory approaches prevent preterm birth profoundly exacerbated by gene-environment interactions. *J Clin Invest* 123, 4063-4075 (2013). **PMID:**23979163
138. Brown, A.G., Leite, R.S. & Strauss, J.F., 3rd. Mechanisms underlying "functional" progesterone withdrawal at parturition. *Ann N Y Acad Sci* 1034, 36-49 (2004). **PMID:**15731298
139. Gurtner, G.C., Werner, S., Barrandon, Y. & Longaker, M.T. Wound repair and regeneration. *Nature* 453, 314-321 (2008). **PMID:**18480812
140. Shynlova, O., Nedd-Roderique, T., Li, Y., Dorogin, A., Nguyen, T. & Lye, S.J. Infiltration of myeloid cells into decidua is a critical early event in the labour

- cascade and post-partum uterine remodelling. *J Cell Mol Med* 17, 311-324 (2013). **PMID:**23379349
141. Kulidjian, A.A., Inman, R. & Issekutz, T.B. Rodent models of lymphocyte migration. *Semin Immunol* 11, 85-93 (1999). **PMID:**10329495
142. Engelhardt, E., Toksoy, A., Goebeler, M., Debus, S., Brocker, E.B. & Gillitzer, R. Chemokines IL-8, GROalpha, MCP-1, IP-10, and Mig are sequentially and differentially expressed during phase-specific infiltration of leukocyte subsets in human wound healing. *Am J Pathol* 153, 1849-1860 (1998). **PMID:**9846975
143. Weiss, S.J. Tissue destruction by neutrophils. *N Engl J Med* 320, 365-376 (1989). **PMID:**2536474
144. Peters, T., Sindrilaru, A., Hinz, B., Hinrichs, R., Menke, A., Al-Azzeh, E.A., Holzwarth, K., Oreshkova, T., Wang, H., Kess, D., Walzog, B., Sulyok, S., Sunderkotter, C., Friedrich, W., Wlaschek, M., Krieg, T. & Scharffetter-Kochanek, K. Wound-healing defect of CD18(-/-) mice due to a decrease in TGF-beta1 and myofibroblast differentiation. *EMBO J* 24, 3400-3410 (2005). **PMID:**16148944
145. Brandon, J.M. Distribution of macrophages in the mouse uterus from one day to three months after parturition, as defined by the immunohistochemical localization of the macrophage-restricted antigens F4/80 and macrosialin. *Anat Rec* 240, 233-242 (1994). **PMID:**7992889
146. Deno, R. Uterine macrophages in the mouse and their relation to involution. *Amer J Anat* 60, 433-471 (1937).
147. Eming, S.A., Krieg, T. & Davidson, J.M. Inflammation in wound repair: molecular and cellular mechanisms. *J Invest Dermatol* 127, 514-525 (2007). **PMID:**17299434
148. DiPietro, L.A., Burdick, M., Low, Q.E., Kunkel, S.L. & Strieter, R.M. MIP-1alpha as a critical macrophage chemoattractant in murine wound repair. *J Clin Invest* 101, 1693-1698 (1998). **PMID:**9541500
149. Wetzler, C., Kampfer, H., Stallmeyer, B., Pfeilschifter, J. & Frank, S. Large and sustained induction of chemokines during impaired wound healing in the genetically diabetic mouse: prolonged persistence of neutrophils and

- macrophages during the late phase of repair. *J Invest Dermatol* 115, 245-253 (2000). **PMID:**10951242
150. Werner, S. & Grose, R. Regulation of wound healing by growth factors and cytokines. *Physiol Rev* 83, 835-870 (2003). **PMID:**12843410
 151. Zhang, M.Z., Yao, B., Yang, S., Jiang, L., Wang, S., Fan, X., Yin, H., Wong, K., Miyazawa, T., Chen, J., Chang, I., Singh, A. & Harris, R.C. CSF-1 signaling mediates recovery from acute kidney injury. *J Clin Invest* 122, 4519-4532 (2012). **PMID:**23143303
 152. Weber, C. Liver: Macrophage-stimulating CSF1 is important in liver injury. *Nat Rev Gastroenterol Hepatol* (2015). **PMID:**26392068
 153. Stutchfield, B.M., *et al.* CSF1 Restores Innate Immunity Following Liver Injury in Mice and Serum Levels Indicate Outcomes of Patients With Acute Liver Failure. *Gastroenterology* (2015). **PMID:**26344055
 154. MacDonald, K.P., Palmer, J.S., Cronau, S., Seppanen, E., Olver, S., Raffelt, N.C., Kuns, R., Pettit, A.R., Clouston, A., Wainwright, B., Branstetter, D., Smith, J., Paxton, R.J., Cerretti, D.P., Bonham, L., Hill, G.R. & Hume, D.A. An antibody against the colony-stimulating factor 1 receptor depletes the resident subset of monocytes and tissue- and tumor-associated macrophages but does not inhibit inflammation. *Blood* 116, 3955-3963 (2010). **PMID:**20682855
 155. Wiktor-Jedrzejczak, W., Bartocci, A., Ferrante, A.W., Jr., Ahmed-Ansari, A., Sell, K.W., Pollard, J.W. & Stanley, E.R. Total absence of colony-stimulating factor 1 in the macrophage-deficient osteopetrotic (op/op) mouse. *Proc Natl Acad Sci U S A* 87, 4828-4832 (1990). **PMID:**2191302
 156. Amemiya, H., Kono, H. & Fujii, H. Liver regeneration is impaired in macrophage colony stimulating factor deficient mice after partial hepatectomy: the role of M-CSF-induced macrophages. *J Surg Res* 165, 59-67 (2011). **PMID:**20031174
 157. Luster, A.D., Cardiff, R.D., MacLean, J.A., Crowe, K. & Granstein, R.D. Delayed wound healing and disorganized neovascularization in transgenic mice expressing the IP-10 chemokine. *Proc Assoc Am Physicians* 110, 183-196 (1998). **PMID:**9625525

158. Ishida, Y., Kondo, T., Takayasu, T., Iwakura, Y. & Mukaida, N. The essential involvement of cross-talk between IFN-gamma and TGF-beta in the skin wound-healing process. *J Immunol* 172, 1848-1855 (2004). **PMID:**14734769
159. Sica, A. & Mantovani, A. Macrophage plasticity and polarization: in vivo veritas. *J Clin Invest* 122, 787-795 (2012). **PMID:**22378047
160. Krausgruber, T., Blazek, K., Smallie, T., Alzabin, S., Lockstone, H., Sahgal, N., Hussell, T., Feldmann, M. & Udalova, I.A. IRF5 promotes inflammatory macrophage polarization and TH1-TH17 responses. *Nat Immunol* 12, 231-238 (2011). **PMID:**21240265
161. Gordon, S. & Martinez, F.O. Alternative activation of macrophages: mechanism and functions. *Immunity* 32, 593-604 (2010). **PMID:**20510870
162. Lang, R., Patel, D., Morris, J.J., Rutschman, R.L. & Murray, P.J. Shaping gene expression in activated and resting primary macrophages by IL-10. *J Immunol* 169, 2253-2263 (2002). **PMID:**12193690
163. Junttila, I.S., Mizukami, K., Dickensheets, H., Meier-Schellersheim, M., Yamane, H., Donnelly, R.P. & Paul, W.E. Tuning sensitivity to IL-4 and IL-13: differential expression of IL-4Ralpha, IL-13Ralpha1, and gammac regulates relative cytokine sensitivity. *J Exp Med* 205, 2595-2608 (2008). **PMID:**18852293
164. Lucas, T., Waisman, A., Ranjan, R., Roes, J., Krieg, T., Muller, W., Roers, A. & Eming, S.A. Differential roles of macrophages in diverse phases of skin repair. *J Immunol* 184, 3964-3977 (2010). **PMID:**20176743
165. Yoshii, A., Kitahara, S., Ueta, H., Matsuno, K. & Ezaki, T. Role of uterine contraction in regeneration of the murine postpartum endometrium. *Biol Reprod* 91, 32 (2014). **PMID:**24966392
166. Sindrilaru, A., Peters, T., Wieschalka, S., Baican, C., Baican, A., Peter, H., Hainzl, A., Schatz, S., Qi, Y., Schlecht, A., Weiss, J.M., Wlaschek, M., Sunderkotter, C. & Scharffetter-Kochanek, K. An unrestrained proinflammatory M1 macrophage population induced by iron impairs wound healing in humans and mice. *J Clin Invest* 121, 985-997 (2011). **PMID:**21317534

167. Cairo, G., Recalcati, S., Mantovani, A. & Locati, M. Iron trafficking and metabolism in macrophages: contribution to the polarized phenotype. *Trends Immunol* 32, 241-247 (2011). **PMID:**21514223
168. Winter, W.E., Bazydlo, L.A. & Harris, N.S. The molecular biology of human iron metabolism. *Lab Med* 45, 92-102 (2014). **PMID:**24868988
169. Lederer, H., Muggli, B., Speich, R., Treder, U., Stricker, H., Goede, J., Ulrich, S., Stampfli, S.F. & Breitenstein, A. Haemosiderin-laden sputum macrophages for diagnosis in pulmonary veno-occlusive disease. *PLoS One* 9, e115219 (2014). **PMID:**25501010
170. Momberg, H.a.C., C. The distribution of placental scars of the first and second pregnancy in the rat. *J Embryol Exp Morphol* 4, 376-384 (1956).
171. Brandon, J.M. Decidualization in the post-partum uterus of the mouse. *J Reprod Fertil* 88, 151-158 (1990). **PMID:**2313633
172. Wilson, A.J. & Gibson, P.R. Epithelial migration in the colon: filling in the gaps. *Clin Sci (Lond)* 93, 97-108 (1997). **PMID:**9301423
173. Basson, M.D. In vitro evidence for matrix regulation of intestinal epithelial biology during mucosal healing. *Life Sci* 69, 3005-3018 (2001). **PMID:**11758827
174. Wallace, J.L. & Whittle, B.J. The role of extracellular mucus as a protective cap over gastric mucosal damage. *Scand J Gastroenterol Suppl* 125, 79-85 (1986). **PMID:**3469742
175. Ferenczy, A. Studies on the cytodynamics of human endometrial regeneration. I. Scanning electron microscopy. *Am J Obstet Gynecol* 124, 64-74 (1976). **PMID:**1244749
176. Ludwig, H. & Spornitz, U.M. Microarchitecture of the human endometrium by scanning electron microscopy: menstrual desquamation and remodeling. *Ann N Y Acad Sci* 622, 28-46 (1991). **PMID:**2064187
177. Huang, C.C., Orvis, G.D., Wang, Y. & Behringer, R.R. Stromal-to-epithelial transition during postpartum endometrial regeneration. *PLoS One* 7, e44285 (2012). **PMID:**22970108

178. Patterson, A.L., Zhang, L., Arango, N.A., Teixeira, J. & Pru, J.K. Mesenchymal-to-epithelial transition contributes to endometrial regeneration following natural and artificial decidualization. *Stem Cells Dev* 22, 964-974 (2013). **PMID:23216285**
179. Ferenczy, A., Bertrand, G. & Gelfand, M.M. Studies on the cytodynamics of human endometrial regeneration. III. In vitro short-term incubation autoradiography. *Am J Obstet Gynecol* 134, 297-304 (1979). **PMID:453263**
180. Okulicz, W.C., Ace, C.I. & Scarrell, R. Zonal changes in proliferation in the rhesus endometrium during the late secretory phase and menses. *Proc Soc Exp Biol Med* 214, 132-138 (1997). **PMID:9034130**
181. Prianishnikov, V.A. On the concept of stem cell and a model of functional-morphological structure of the endometrium. *Contraception* 18, 213-223 (1978). **PMID:569035**
182. Gargett, C.E. Uterine stem cells: what is the evidence? *Hum Reprod Update* 13, 87-101 (2007). **PMID:16960017**
183. Padykula, H.A. Regeneration in the primate uterus: the role of stem cells. *Ann N Y Acad Sci* 622, 47-56 (1991). **PMID:2064204**
184. Chan, R.W., Schwab, K.E. & Gargett, C.E. Clonogenicity of human endometrial epithelial and stromal cells. *Biol Reprod* 70, 1738-1750 (2004). **PMID:14766732**
185. Schwab, K.E., Chan, R.W. & Gargett, C.E. Putative stem cell activity of human endometrial epithelial and stromal cells during the menstrual cycle. *Fertil Steril* 84 Suppl 2, 1124-1130 (2005). **PMID:16210003**
186. Gargett, C.E., Schwab, K.E., Zillwood, R.M., Nguyen, H.P. & Wu, D. Isolation and culture of epithelial progenitors and mesenchymal stem cells from human endometrium. *Biol Reprod* 80, 1136-1145 (2009). **PMID:19228591**
187. Taylor, H.S. Endometrial cells derived from donor stem cells in bone marrow transplant recipients. *JAMA* 292, 81-85 (2004). **PMID:15238594**
188. Bratincsak, A., Brownstein, M.J., Cassiani-Ingoni, R., Pastorino, S., Szalayova, I., Toth, Z.E., Key, S., Nemeth, K., Pickel, J. & Mezey, E. CD45-positive blood cells

- give rise to uterine epithelial cells in mice. *Stem Cells* 25, 2820-2826 (2007). **PMID:**17656643
189. Du, H. & Taylor, H.S. Contribution of bone marrow-derived stem cells to endometrium and endometriosis. *Stem Cells* 25, 2082-2086 (2007). **PMID:**17464086
190. Mints, M., Jansson, M., Sadeghi, B., Westgren, M., Uzunel, M., Hassan, M. & Palmblad, J. Endometrial endothelial cells are derived from donor stem cells in a bone marrow transplant recipient. *Hum Reprod* 23, 139-143 (2008). **PMID:**17981818
191. Ikoma, T., Kyo, S., Maida, Y., Ozaki, S., Takakura, M., Nakao, S. & Inoue, M. Bone marrow-derived cells from male donors can compose endometrial glands in female transplant recipients. *Am J Obstet Gynecol* 201, 608 e601-608 (2009). **PMID:**19800602
192. Cervello, I., Gil-Sanchis, C., Mas, A., Faus, A., Sanz, J., Moscardo, F., Higuera, G., Sanz, M.A., Pellicer, A. & Simon, C. Bone marrow-derived cells from male donors do not contribute to the endometrial side population of the recipient. *PLoS One* 7, e30260 (2012). **PMID:**22276168
193. Morelli, S.S., Rameshwar, P. & Goldsmith, L.T. Experimental evidence for bone marrow as a source of nonhematopoietic endometrial stromal and epithelial compartment cells in a murine model. *Biol Reprod* 89, 7 (2013). **PMID:**23699390
194. Du, H., Naqvi, H. & Taylor, H.S. Ischemia/reperfusion injury promotes and granulocyte-colony stimulating factor inhibits migration of bone marrow-derived stem cells to endometrium. *Stem Cells Dev* 21, 3324-3331 (2012). **PMID:**22897736
195. Okulicz, W.C. & Scarrell, R. Estrogen receptor alpha and progesterone receptor in the rhesus endometrium during the late secretory phase and menses. *Proc Soc Exp Biol Med* 218, 316-321 (1998). **PMID:**9714074
196. Winuthayanon, W., Hewitt, S.C., Orvis, G.D., Behringer, R.R. & Korach, K.S. Uterine epithelial estrogen receptor alpha is dispensable for proliferation but essential for complete biological and biochemical responses. *Proc Natl Acad Sci U S A* 107, 19272-19277 (2010). **PMID:**20974921

197. Medh, R.D. & Thompson, E.B. Hormonal regulation of physiological cell turnover and apoptosis. *Cell Tissue Res* 301, 101-124 (2000). **PMID:**10928284
198. Osteen, K.G., Bruner-Tran, K.L., Keller, N.R. & Eisenberg, E. Progesterone-mediated endometrial maturation limits matrix metalloproteinase (MMP) expression in an inflammatory-like environment: a regulatory system altered in endometriosis. *Ann N Y Acad Sci* 955, 37-47; discussion 86-38, 396-406 (2002). **PMID:**11949963
199. King, A., Gardner, L. & Loke, Y.W. Evaluation of oestrogen and progesterone receptor expression in uterine mucosal lymphocytes. *Hum Reprod* 11, 1079-1082 (1996). **PMID:**8671394
200. Salamonsen, L.A., Zhang, J. & Brasted, M. Leukocyte networks and human endometrial remodelling. *J Reprod Immunol* 57, 95-108 (2002). **PMID:**12385836
201. Stygar, D., Masironi, B., Eriksson, H. & Sahlin, L. Studies on estrogen receptor (ER) alpha and beta responses on gene regulation in peripheral blood leukocytes in vivo using selective ER agonists. *J Endocrinol* 194, 101-119 (2007). **PMID:**17592025
202. Molero, L., Garcia-Duran, M., Diaz-Recasens, J., Rico, L., Casado, S. & Lopez-Farre, A. Expression of estrogen receptor subtypes and neuronal nitric oxide synthase in neutrophils from women and men: regulation by estrogen. *Cardiovasc Res* 56, 43-51 (2002). **PMID:**12237165
203. Dosiou, C., Hamilton, A.E., Pang, Y., Overgaard, M.T., Tulac, S., Dong, J., Thomas, P. & Giudice, L.C. Expression of membrane progesterone receptors on human T lymphocytes and Jurkat cells and activation of G-proteins by progesterone. *J Endocrinol* 196, 67-77 (2008). **PMID:**18180318
204. Kramer, P.R., Winger, V. & Kramer, S.F. 17beta-Estradiol utilizes the estrogen receptor to regulate CD16 expression in monocytes. *Mol Cell Endocrinol* 279, 16-25 (2007). **PMID:**17923257
205. Srivastava, M.D. & Anderson, D.J. Progesterone receptor expression by human leukocyte cell lines: molecular mechanisms of cytokine suppression. *Clin Exp Obstet Gynecol* 34, 14-24 (2007). **PMID:**17447631

206. Pierdominici, M., Maselli, A., Colasanti, T., Giammarioli, A.M., Delunardo, F., Vacirca, D., Sanchez, M., Giovannetti, A., Malorni, W. & Ortona, E. Estrogen receptor profiles in human peripheral blood lymphocytes. *Immunol Lett* 132, 79-85 (2010). **PMID:**20542061
207. Kelly, R.W., Illingworth, P., Baldie, G., Leask, R., Brouwer, S. & Calder, A.A. Progesterone control of interleukin-8 production in endometrium and chorio-decidual cells underlines the role of the neutrophil in menstruation and parturition. *Hum Reprod* 9, 253-258 (1994). **PMID:**8027281
208. Wira, C.R., Rodriguez-Garcia, M. & Patel, M.V. The role of sex hormones in immune protection of the female reproductive tract. *Nat Rev Immunol* 15, 217-230 (2015). **PMID:**25743222
209. Wira, C.R., Fahey, J.V., Rodriguez-Garcia, M., Shen, Z. & Patel, M.V. Regulation of mucosal immunity in the female reproductive tract: the role of sex hormones in immune protection against sexually transmitted pathogens. *Am J Reprod Immunol* 72, 236-258 (2014). **PMID:**24734774
210. Cindrova-Davies, T., Yung, H.W., Johns, J., Spasic-Boskovic, O., Korolchuk, S., Jauniaux, E., Burton, G.J. & Charnock-Jones, D.S. Oxidative stress, gene expression, and protein changes induced in the human placenta during labor. *Am J Pathol* 171, 1168-1179 (2007). **PMID:**17823277
211. Eltzschig, H.K. & Eckle, T. Ischemia and reperfusion--from mechanism to translation. *Nat Med* 17, 1391-1401 (2011). **PMID:**22064429
212. Frangogiannis, N.G. The immune system and the remodeling infarcted heart: cell biological insights and therapeutic opportunities. *J Cardiovasc Pharmacol* 63, 185-195 (2014). **PMID:**24072174
213. Hausenloy, D.J. & Yellon, D.M. Myocardial ischemia-reperfusion injury: a neglected therapeutic target. *J Clin Invest* 123, 92-100 (2013). **PMID:**23281415
214. Seropian, I.M., Toldo, S., Van Tassell, B.W. & Abbate, A. Anti-inflammatory strategies for ventricular remodeling following ST-segment elevation acute myocardial infarction. *J Am Coll Cardiol* 63, 1593-1603 (2014). **PMID:**24530674

215. Kalogeris, T., Baines, C.P., Krenz, M. & Korthuis, R.J. Cell biology of ischemia/reperfusion injury. *Int Rev Cell Mol Biol* 298, 229-317 (2012). **PMID:22878108**
216. Guruharsha, K.G., Kankel, M.W. & Artavanis-Tsakonas, S. The Notch signalling system: recent insights into the complexity of a conserved pathway. *Nat Rev Genet* 13, 654-666 (2012). **PMID:22868267**
217. Bergmann, A. & Steller, H. Apoptosis, stem cells, and tissue regeneration. *Sci Signal* 3, re8 (2010). **PMID:20978240**
218. Li, F., Huang, Q., Chen, J., Peng, Y., Roop, D.R., Bedford, J.S. & Li, C.Y. Apoptotic cells activate the "phoenix rising" pathway to promote wound healing and tissue regeneration. *Sci Signal* 3, ra13 (2010). **PMID:20179271**
219. Tseng, A.S., Adams, D.S., Qiu, D., Koustubhan, P. & Levin, M. Apoptosis is required during early stages of tail regeneration in *Xenopus laevis*. *Dev Biol* 301, 62-69 (2007). **PMID:17150209**
220. Zeng, C., Xing, R., Liu, J. & Xing, F. Role of CSL-dependent and independent Notch signaling pathways in cell apoptosis. *Apoptosis* (2015). **PMID:26496776**
221. Liu, J., Sato, C., Cerletti, M. & Wagers, A. Notch signaling in the regulation of stem cell self-renewal and differentiation. *Curr Top Dev Biol* 92, 367-409 (2010). **PMID:20816402**
222. Mazzone, M., Selfors, L.M., Albeck, J., Overholtzer, M., Sale, S., Carroll, D.L., Pandya, D., Lu, Y., Mills, G.B., Aster, J.C., Artavanis-Tsakonas, S. & Brugge, J.S. Dose-dependent induction of distinct phenotypic responses to Notch pathway activation in mammary epithelial cells. *Proc Natl Acad Sci U S A* 107, 5012-5017 (2010). **PMID:20194747**
223. Kulic, I., *et al.* Loss of the Notch effector RBPJ promotes tumorigenesis. *J Exp Med* 212, 37-52 (2015). **PMID:25512468**
224. MacKenzie, F., Duriez, P., Wong, F., Nosedà, M. & Karsan, A. Notch4 inhibits endothelial apoptosis via RBP-J κ -dependent and -independent pathways. *J Biol Chem* 279, 11657-11663 (2004). **PMID:14701863**

225. Gude, N. & Sussman, M. Notch signaling and cardiac repair. *J Mol Cell Cardiol* 52, 1226-1232 (2012). **PMID:**22465038
226. Boni, A., Urbanek, K., Nascimbene, A., Hosoda, T., Zheng, H., Delucchi, F., Amano, K., Gonzalez, A., Vitale, S., Ojaimi, C., Rizzi, R., Bolli, R., Yutzey, K.E., Rota, M., Kajstura, J., Anversa, P. & Leri, A. Notch1 regulates the fate of cardiac progenitor cells. *Proceedings of the National Academy of Sciences of the United States of America* 105, 15529-15534 (2008). **PMID:**18832173
227. Wang, L., Wang, C.M., Hou, L.H., Dou, G.R., Wang, Y.C., Hu, X.B., He, F., Feng, F., Zhang, H.W., Liang, Y.M., Dou, K.F. & Han, H. Disruption of the transcription factor recombination signal-binding protein-Jkappa (RBP-J) leads to veno-occlusive disease and interfered liver regeneration in mice. *Hepatology* 49, 268-277 (2009). **PMID:**19065680
228. Yu, H.C., Qin, H.Y., He, F., Wang, L., Fu, W., Liu, D., Guo, F.C., Liang, L., Dou, K.F. & Han, H. Canonical notch pathway protects hepatocytes from ischemia/reperfusion injury in mice by repressing reactive oxygen species production through JAK2/STAT3 signaling. *Hepatology* 54, 979-988 (2011). **PMID:**21633967
229. Radtke, F., MacDonald, H.R. & Tacchini-Cottier, F. Regulation of innate and adaptive immunity by Notch. *Nat Rev Immunol* 13, 427-437 (2013). **PMID:**23665520
230. Pui, J.C., Allman, D., Xu, L., DeRocco, S., Karnell, F.G., Bakkour, S., Lee, J.Y., Kadesch, T., Hardy, R.R., Aster, J.C. & Pear, W.S. Notch1 expression in early lymphopoiesis influences B versus T lineage determination. *Immunity* 11, 299-308 (1999). **PMID:**10514008
231. Amsen, D., Antov, A. & Flavell, R.A. The different faces of Notch in T-helper-cell differentiation. *Nat Rev Immunol* 9, 116-124 (2009). **PMID:**19165228
232. Asano, N., Watanabe, T., Kitani, A., Fuss, I.J. & Strober, W. Notch1 signaling and regulatory T cell function. *J Immunol* 180, 2796-2804 (2008). **PMID:**18292500
233. Samon, J.B., Champhekar, A., Minter, L.M., Telfer, J.C., Miele, L., Fauq, A., Das, P., Golde, T.E. & Osborne, B.A. Notch1 and TGFbeta1 cooperatively regulate Foxp3 expression and the maintenance of peripheral regulatory T cells. *Blood* 112, 1813-1821 (2008). **PMID:**18550850

234. Wang, Y.C., He, F., Feng, F., Liu, X.W., Dong, G.Y., Qin, H.Y., Hu, X.B., Zheng, M.H., Liang, L., Feng, L., Liang, Y.M. & Han, H. Notch signaling determines the M1 versus M2 polarization of macrophages in antitumor immune responses. *Cancer research* 70, 4840-4849 (2010). **PMID:**20501839
235. Wang, Y.C., Wang, S.H., Wei, Y.N., Du, D.W., Xu, H., Gao, C.C., Zheng, M.H., Xie, J., Li, J.C., Dong, G.Y., Li, L., Xiao, Y. & Han, H. Notch-RBP-J signaling is required by bone marrow stromal cells for the treatment of acute graft versus host disease. *Stem Cell Res* 11, 721-735 (2013). **PMID:**23735298
236. Gallucci, R.M., Simeonova, P.P., Matheson, J.M., Kommineni, C., Guriel, J.L., Sugawara, T. & Luster, M.I. Impaired cutaneous wound healing in interleukin-6-deficient and immunosuppressed mice. *FASEB J* 14, 2525-2531 (2000). **PMID:**11099471
237. Hurst, S.M., Wilkinson, T.S., McLoughlin, R.M., Jones, S., Horiuchi, S., Yamamoto, N., Rose-John, S., Fuller, G.M., Topley, N. & Jones, S.A. Il-6 and its soluble receptor orchestrate a temporal switch in the pattern of leukocyte recruitment seen during acute inflammation. *Immunity* 14, 705-714 (2001). **PMID:**11420041
238. Robertson SA, O.C.A., and Ramsey A. The effect of interleukin-6 deficiency on implantation, fetal development and parturition in mice. in *31st Annual Conference of the Australian Society for Reproductive Biology*, Vol. 31 97 (Canberra, Australia, 2000).
239. Robertson, S.A., Christiaens, I., Dorian, C.L., Zaragoza, D.B., Care, A.S., Banks, A.M. & Olson, D.M. Interleukin-6 is an essential determinant of on-time parturition in the mouse. *Endocrinology* 151, 3996-4006 (2010). **PMID:**20610570
240. Jasper, M.J., Tremellen, K.P. & Robertson, S.A. Reduced expression of IL-6 and IL-1alpha mRNAs in secretory phase endometrium of women with recurrent miscarriage. *Journal of reproductive immunology* 73, 74-84 (2007). **PMID:**17034864
241. Wongchana, W. & Palaga, T. Direct regulation of interleukin-6 expression by Notch signaling in macrophages. *Cellular & molecular immunology* 9, 155-162 (2012). **PMID:**21983868
242. Diehl, S. & Rincon, M. The two faces of IL-6 on Th1/Th2 differentiation. *Molecular immunology* 39, 531-536 (2002). **PMID:**12431386

243. Cheng, J.G. & Stewart, C.L. Loss of cyclooxygenase-2 retards decidual growth but does not inhibit embryo implantation or development to term. *Biology of reproduction* 68, 401-404 (2003). **PMID:**12533402
244. Kelly, R.W., King, A.E. & Critchley, H.O. Cytokine control in human endometrium. *Reproduction* 121, 3-19 (2001). **PMID:**11226025
245. Yeh, T.S., Wu, C.W., Hsu, K.W., Liao, W.J., Yang, M.C., Li, A.F., Wang, A.M., Kuo, M.L. & Chi, C.W. The activated Notch1 signal pathway is associated with gastric cancer progression through cyclooxygenase-2. *Cancer research* 69, 5039-5048 (2009). **PMID:**19491270
246. Sawamiphak, S., Kontarakis, Z. & Stainier, D.Y. Interferon gamma signaling positively regulates hematopoietic stem cell emergence. *Dev Cell* 31, 640-653 (2014). **PMID:**25490269
247. Jaiswal, M.K., Agrawal, V., Pamarthy, S., Katara, G.K., Kulshrestha, A., Gilman-Sachs, A., Beaman, K.D. & Hirsch, E. Notch Signaling in Inflammation-Induced Preterm Labor. *Sci Rep* 5, 15221 (2015). **PMID:**26472156
248. Samson, S.I., Richard, O., Tavian, M., Ranson, T., Vosshenrich, C.A., Colucci, F., Buer, J., Grosveld, F., Godin, I. & Di Santo, J.P. GATA-3 promotes maturation, IFN-gamma production, and liver-specific homing of NK cells. *Immunity* 19, 701-711 (2003). **PMID:**14614857
249. Amsen, D., Antov, A., Jankovic, D., Sher, A., Radtke, F., Souabni, A., Busslinger, M., McCright, B., Gridley, T. & Flavell, R.A. Direct regulation of Gata3 expression determines the T helper differentiation potential of Notch. *Immunity* 27, 89-99 (2007). **PMID:**17658279
250. Lu, Y., Bocca, S., Anderson, S., Wang, H., Manhua, C., Beydoun, H. & Oehninger, S. Modulation of the expression of the transcription factors T-bet and GATA-3 in immortalized human endometrial stromal cells (HESCs) by sex steroid hormones and cAMP. *Reprod Sci* 20, 699-709 (2013). **PMID:**23308012
251. Practice Committee of American Society for Reproductive, M. Definitions of infertility and recurrent pregnancy loss: a committee opinion. *Fertil Steril* 99, 63 (2013). **PMID:**23095139

252. Rai, R. & Regan, L. Recurrent miscarriage. *Lancet* 368, 601-611 (2006). **PMID:**16905025
253. Practice Committee of the American Society for Reproductive, M. Evaluation and treatment of recurrent pregnancy loss: a committee opinion. *Fertil Steril* 98, 1103-1111 (2012). **PMID:**22835448
254. Branch, D.W., Gibson, M. & Silver, R.M. Clinical practice. Recurrent miscarriage. *N Engl J Med* 363, 1740-1747 (2010). **PMID:**20979474
255. Kwak-Kim, J.Y., Chung-Bang, H.S., Ng, S.C., Ntrivalas, E.I., Mangubat, C.P., Beaman, K.D., Beer, A.E. & Gilman-Sachs, A. Increased T helper 1 cytokine responses by circulating T cells are present in women with recurrent pregnancy losses and in infertile women with multiple implantation failures after IVF. *Hum Reprod* 18, 767-773 (2003). **PMID:**12660269
256. Raghupathy, R., Makhseed, M., Azizieh, F., Hassan, N., Al-Azemi, M. & Al-Shamali, E. Maternal Th1- and Th2-type reactivity to placental antigens in normal human pregnancy and unexplained recurrent spontaneous abortions. *Cell Immunol* 196, 122-130 (1999). **PMID:**10527564
257. Krieg, S.A., Fan, X., Hong, Y., Sang, Q.X., Giaccia, A., Westphal, L.M., Lathi, R.B., Krieg, A.J. & Nayak, N.R. Global alteration in gene expression profiles of deciduas from women with idiopathic recurrent pregnancy loss. *Mol Hum Reprod* 18, 442-450 (2012). **PMID:**22505054
258. Comba, C., Bastu, E., Dural, O., Yasa, C., Keskin, G., Ozsurmeli, M., Buyru, F. & Serdaroglu, H. Role of inflammatory mediators in patients with recurrent pregnancy loss. *Fertil Steril* (2015). **PMID:**26368793
259. Liang, P.Y., Diao, L.H., Huang, C.Y., Lian, R.C., Chen, X., Li, G.G., Zhao, J., Li, Y.Y., He, X.B. & Zeng, Y. The pro-inflammatory and anti-inflammatory cytokine profile in peripheral blood of women with recurrent implantation failure. *Reprod Biomed Online* (2015). **PMID:**26371706
260. Weimar, C.H., Kavelaars, A., Brosens, J.J., Gellersen, B., de Vreeden-Elbertse, J.M., Heijnen, C.J. & Macklon, N.S. Endometrial stromal cells of women with recurrent miscarriage fail to discriminate between high- and low-quality human embryos. *PLoS One* 7, e41424 (2012). **PMID:**22848492

261. Korgun, E.T., Demir, R., Hammer, A., Dohr, G., Desoye, G., Skofitsch, G. & Hahn, T. Glucose transporter expression in rat embryo and uterus during decidualization, implantation, and early postimplantation. *Biol Reprod* 65, 1364-1370 (2001). **PMID:**11673251
262. Strakova, Z., Srisuparp, S. & Fazleabas, A.T. Interleukin-1beta induces the expression of insulin-like growth factor binding protein-1 during decidualization in the primate. *Endocrinology* 141, 4664-4670 (2000). **PMID:**11108281
263. Pawar, S., Laws, M.J., Bagchi, I.C. & Bagchi, M.K. Uterine Epithelial Estrogen Receptor-alpha Controls Decidualization via a Paracrine Mechanism. *Mol Endocrinol* 29, 1362-1374 (2015). **PMID:**26241389
264. Su, R.W., Strug, M.R., Jeong, J.W., Miele, L. & Fazleabas, A.T. Aberrant activation of canonical Notch1 signaling in the mouse uterus decreases progesterone receptor by hypermethylation and leads to infertility. *Proc Natl Acad Sci U S A* 113, 2300-2305 (2016). **PMID:**26858409
265. Tan, J., Raja, S., Davis, M.K., Tawfik, O., Dey, S.K. & Das, S.K. Evidence for coordinated interaction of cyclin D3 with p21 and cdk6 in directing the development of uterine stromal cell decidualization and polyploidy during implantation. *Mech Dev* 111, 99-113 (2002). **PMID:**11804782
266. Hantak, A.M., Bagchi, I.C. & Bagchi, M.K. Role of uterine stromal-epithelial crosstalk in embryo implantation. *Int J Dev Biol* 58, 139-146 (2014). **PMID:**25023679
267. Hao, L., Rizzo, P., Osipo, C., Pannuti, A., Wyatt, D., Cheung, L.W., Sonenshein, G., Osborne, B.A. & Miele, L. Notch-1 activates estrogen receptor-alpha-dependent transcription via IKKalpha in breast cancer cells. *Oncogene* 29, 201-213 (2010). **PMID:**19838210
268. Conaghan, J., Handyside, A.H., Winston, R.M. & Leese, H.J. Effects of pyruvate and glucose on the development of human preimplantation embryos in vitro. *J Reprod Fertil* 99, 87-95 (1993). **PMID:**8283458
269. Fuhrich, D.G., Lessey, B.A. & Savaris, R.F. Comparison of HSCORE assessment of endometrial beta3 integrin subunit expression with digital HSCORE using computerized image analysis (ImageJ). *Anal Quant Cytopathol Histopathol* 35, 210-216 (2013). **PMID:**24341124

270. Surveyor, G.A., Gendler, S.J., Pemberton, L., Das, S.K., Chakraborty, I., Julian, J., Pimental, R.A., Wegner, C.C., Dey, S.K. & Carson, D.D. Expression and steroid hormonal control of Muc-1 in the mouse uterus. *Endocrinology* 136, 3639-3647 (1995). **PMID:**7628404
271. Nosedá, M., Fu, Y., Niessen, K., Wong, F., Chang, L., McLean, G. & Karsan, A. Smooth Muscle alpha-actin is a direct target of Notch/CSL. *Circ Res* 98, 1468-1470 (2006). **PMID:**16741155
272. Sundstrom, S.A., Komm, B.S., Ponce-de-Leon, H., Yi, Z., Teuscher, C. & Lyttle, C.R. Estrogen regulation of tissue-specific expression of complement C3. *J Biol Chem* 264, 16941-16947 (1989). **PMID:**2674144
273. Mao, D., Wu, X., Deppong, C., Friend, L.D., Dolecki, G., Nelson, D.M. & Molina, H. Negligible role of antibodies and C5 in pregnancy loss associated exclusively with C3-dependent mechanisms through complement alternative pathway. *Immunity* 19, 813-822 (2003). **PMID:**14670299
274. Girardi, G., Berman, J., Redecha, P., Spruce, L., Thurman, J.M., Kraus, D., Hollmann, T.J., Casali, P., Carroll, M.C., Wetsel, R.A., Lambris, J.D., Holers, V.M. & Salmon, J.E. Complement C5a receptors and neutrophils mediate fetal injury in the antiphospholipid syndrome. *J Clin Invest* 112, 1644-1654 (2003). **PMID:**14660741
275. Lamouille, S., Xu, J. & Derynck, R. Molecular mechanisms of epithelial-mesenchymal transition. *Nat Rev Mol Cell Biol* 15, 178-196 (2014). **PMID:**24556840
276. Espinoza, I. & Miele, L. Deadly crosstalk: Notch signaling at the intersection of EMT and cancer stem cells. *Cancer Lett* 341, 41-45 (2013). **PMID:**23973264
277. Xie, J., Wang, W., Si, J.W., Miao, X.Y., Li, J.C., Wang, Y.C., Wang, Z.R., Ma, J., Zhao, X.C., Li, Z., Yi, H. & Han, H. Notch signaling regulates CXCR4 expression and the migration of mesenchymal stem cells. *Cell Immunol* 281, 68-75 (2013). **PMID:**23474530
278. Orent, W., McHenry, A.R., Rao, D.A., White, C., Klein, H.U., Bassil, R., Srivastava, G., Replogle, J.M., Raj, T., Frangieh, M., Cimpean, M., Cuerdon, N., Chibnik, L., Khoury, S.J., Karlson, E.W., Brenner, M.B., De Jager, P., Bradshaw, E.M. & Elyaman, W. Rheumatoid Arthritis-Associated RBPJ Polymorphism Alters Memory CD4+ T Cells. *Hum Mol Genet* (2015). **PMID:**26604133

279. Palaga, T., Miele, L., Golde, T.E. & Osborne, B.A. TCR-mediated Notch signaling regulates proliferation and IFN-gamma production in peripheral T cells. *J Immunol* 171, 3019-3024 (2003). **PMID:12960327**
280. Kosova, G., Stephenson, M.D., Lynch, V.J. & Ober, C. Evolutionary forward genomics reveals novel insights into the genes and pathways dysregulated in recurrent early pregnancy loss. *Hum Reprod* 30, 519-529 (2015). **PMID:25586782**
281. Liao, Y., Smyth, G.K. & Shi, W. The Subread aligner: fast, accurate and scalable read mapping by seed-and-vote. *Nucleic Acids Res* 41, e108 (2013). **PMID:23558742**
282. Liao, Y., Smyth, G.K. & Shi, W. featureCounts: an efficient general purpose program for assigning sequence reads to genomic features. *Bioinformatics* 30, 923-930 (2014). **PMID:24227677**
283. Fraser, R.B., Waite, S.L., Wood, K.A. & Martin, K.L. Impact of hyperglycemia on early embryo development and embryopathy: in vitro experiments using a mouse model. *Hum Reprod* 22, 3059-3068 (2007). **PMID:17933753**
284. Toyofuku, A., Hara, T., Taguchi, T., Katsura, Y., Ohama, K. & Kudo, Y. Cyclic and characteristic expression of phosphorylated Akt in human endometrium and decidual cells in vivo and in vitro. *Hum Reprod* 21, 1122-1128 (2006). **PMID:16373405**
285. Hombach-Klonisch, S., Kehlen, A., Fowler, P.A., Huppertz, B., Jugert, J.F., Bischoff, G., Schluter, E., Buchmann, J. & Klonisch, T. Regulation of functional steroid receptors and ligand-induced responses in telomerase-immortalized human endometrial epithelial cells. *J Mol Endocrinol* 34, 517-534 (2005). **PMID:15821114**
286. Krikun, G., Mor, G., Alvero, A., Guller, S., Schatz, F., Sapi, E., Rahman, M., Caze, R., Qumsiyeh, M. & Lockwood, C.J. A novel immortalized human endometrial stromal cell line with normal progesterational response. *Endocrinology* 145, 2291-2296 (2004). **PMID:14726435**
287. Amsen, D., Blander, J.M., Lee, G.R., Tanigaki, K., Honjo, T. & Flavell, R.A. Instruction of distinct CD4 T helper cell fates by different notch ligands on antigen-presenting cells. *Cell* 117, 515-526 (2004). **PMID:15137944**

288. Schroder, K., Hertzog, P.J., Ravasi, T. & Hume, D.A. Interferon-gamma: an overview of signals, mechanisms and functions. *J Leukoc Biol* 75, 163-189 (2004). **PMID:**14525967
289. Wang, L., Wang, Y.C., Hu, X.B., Zhang, B.F., Dou, G.R., He, F., Gao, F., Feng, F., Liang, Y.M., Dou, K.F. & Han, H. Notch-RBP-J signaling regulates the mobilization and function of endothelial progenitor cells by dynamic modulation of CXCR4 expression in mice. *PLoS One* 4, e7572 (2009). **PMID:**19859544